nature biotechnology

SUPPLEMENTARY INFORMATION

https://doi.org/10.1038/s41587-019-0242-8

In the format provided by the authors and unedited.

Multi-input chemical control of protein dimerization for programming graded cellular responses

Glenna Wink Foight[1,2,8], Zhizhi Wang[2,3,8], Cindy T. Wei[1], Per Jr Greisen[2,4,6], Katrina M. Warner[1], Daniel Cunningham-Bryant[1], Keunwan Park[2,4,7], T. J. Brunette[2,4], William Sheffler[2,4], David Baker[2,4,5] and Dustin J. Maly[1,4]*

[1]Department of Chemistry, University of Washington, Seattle, WA, USA. [2]Institute for Protein Design, University of Washington, Seattle, WA, USA. [3]Department of Biological Structure, University of Washington, Seattle, WA, USA. [4]Department of Biochemistry, University of Washington, Seattle, WA, USA. [5]Howard Hughes Medical Institute, University of Washington, Seattle, WA, USA. [6]Present address: Global Research, Novo Nordisk A/S, Måløv, Denmark. [7]Present address: Systems Biotechnology Research Center, Korea Institute of Science and Technology, Gangneung, Republic of Korea. [8]These authors contributed equally: Glenna Wink Foight, Zhizhi Wang. *e-mail: djmaly@uw.edu

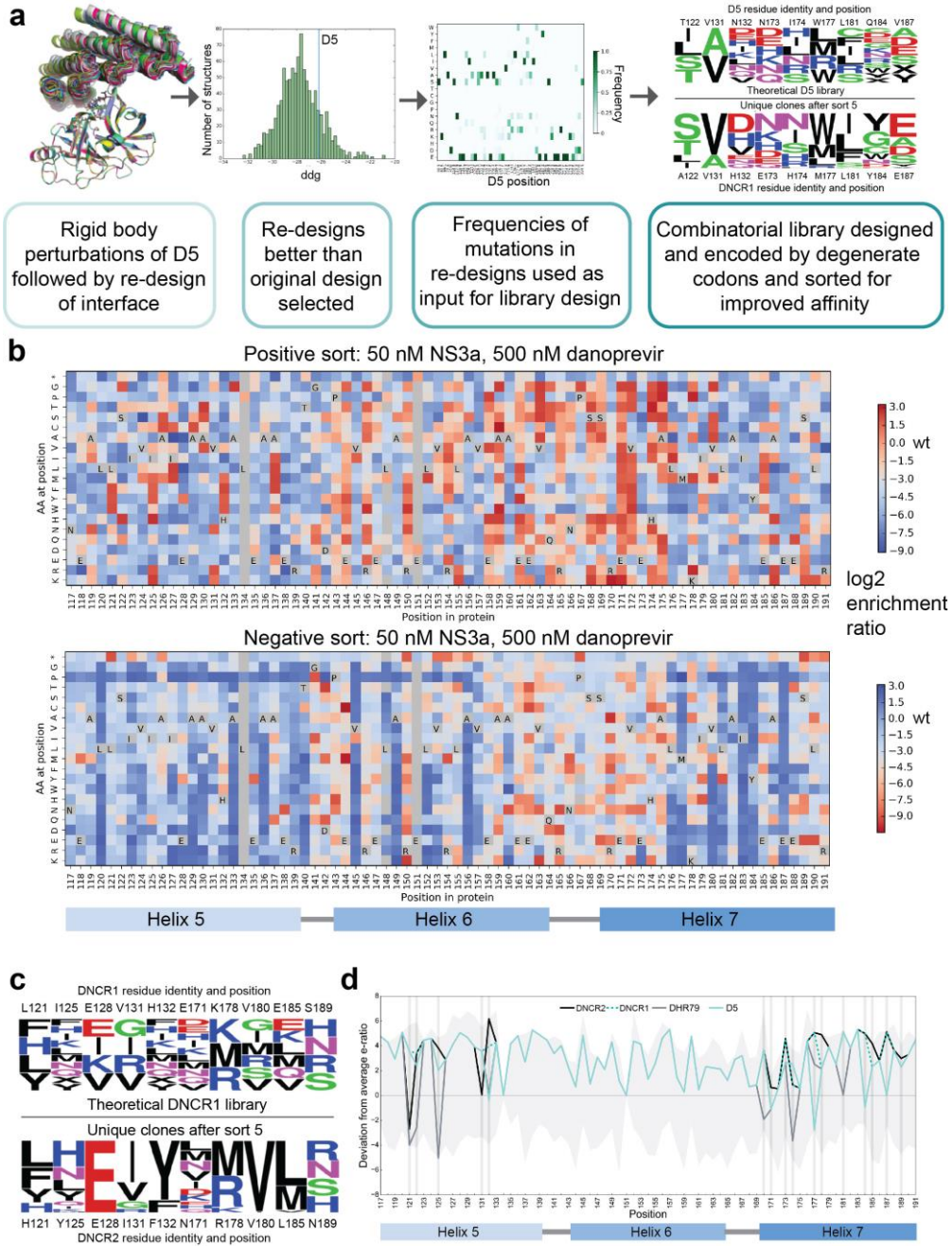

Supplementary Figure 1

Design and characterization of danoprevir:NS3a complex reader libraries.

a, Process of Rosetta re-design-informed design of a combinatorial D5 interface library. **b**, Enrichment ratios of the DNCR1 site saturation mutagenesis (SSM) library sorted for (positive sort, top) or against (negative sort, bottom) binding to 50 nM NS3a in the presence of 500 nM danoprevir. The color scale has been flipped for the negative sort such that for both sorts, blue corresponds to predicted weaker binders, and red corresponds to predicted tighter binders. Gray boxes with letters are the wild-type residue and other gray boxes are positions with <15 counts in the naïve library sequencing results. **c**, Sequence logos of the theoretical library for the second combinatorial library varying the DNCR1 interface (top), and the mutations found in the final enriched clones (bottom). Residue identities at the varied positions are indicated for the starting DNCR1 and final DNCR2. **d**, Progression of binding improvement from DHR79 to D5 to DNCR1 to DNCR2 as measured by the deviation from average enrichment ratio of the DNCR1 SSM values at each position. Gray shaded region indicates the range of enrichment ratios of all amino acids at each position, and vertical gray bars indicate positions at the interface.

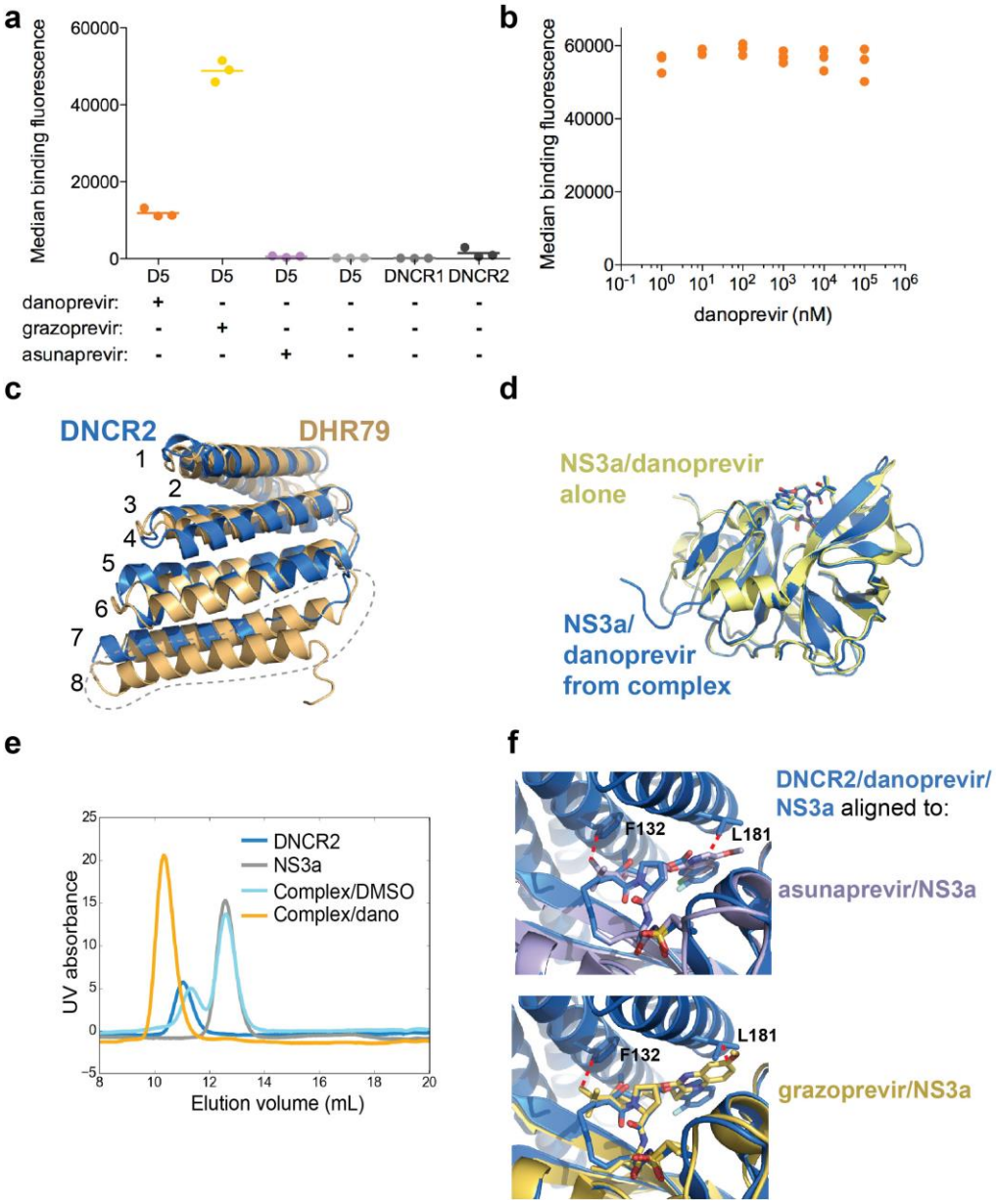

Supplementary Figure 2

Analysis of the DNCR2:danoprevir:NS3a complex crystal structure and the specificities of drug/NS3a complex reader proteins.

a, 1 µM NS3a with avidity binding to yeast-displayed D5, DNCR1, or DNCR2. Technical triplicates and their mean are shown. **b,** Binding of 1 nM NS3a to DNCR2 displayed on the surface of yeast in the presence of increasing concentrations of danoprevir. Technical triplicates are shown. **c**, An overlay of DNCR2 (blue) from the DNCR2:danoprevir:NS3a complex with the original DHR79 scaffold (orange) crystal structure (PDBID: 5CWP) (Nature 528, 580-584, 2015) . Regions where there are modest changes in the backbone conformation are circled with a dotted line, including missing density for helix 8 and an unraveled helix 7 N-terminus. **d**, NS3a:danoprevir (blue) from the DNCR2:danoprevir:NS3a complex aligns closely to a crystal structure of NS3a:danoprevir (yellow) alone (PDBID: 3M5L) (PNAS 107, 20986-20991, 2010). **e**, Size exclusion chromatograms of DNCR2, NS3a, or DNCR2:NS3a complexes in the presence or absence of danoprevir. Representative of three technical replicates. **f**, Crystal structure of DNCR2:danoprevir:NS3a (blue) aligned to structures of asunaprevir:NS3a (lavender, PDBID: 4WF8) or grazoprevir:NS3a (yellow, PDBID: 3SUD) with clashes (red) between residues of DNCR2 and asunaprevir and grazoprevir highlighted (PLoS Pathog 8, e1002832, 2012; ACS Chem Biol 9, 2485-2490, 2014).

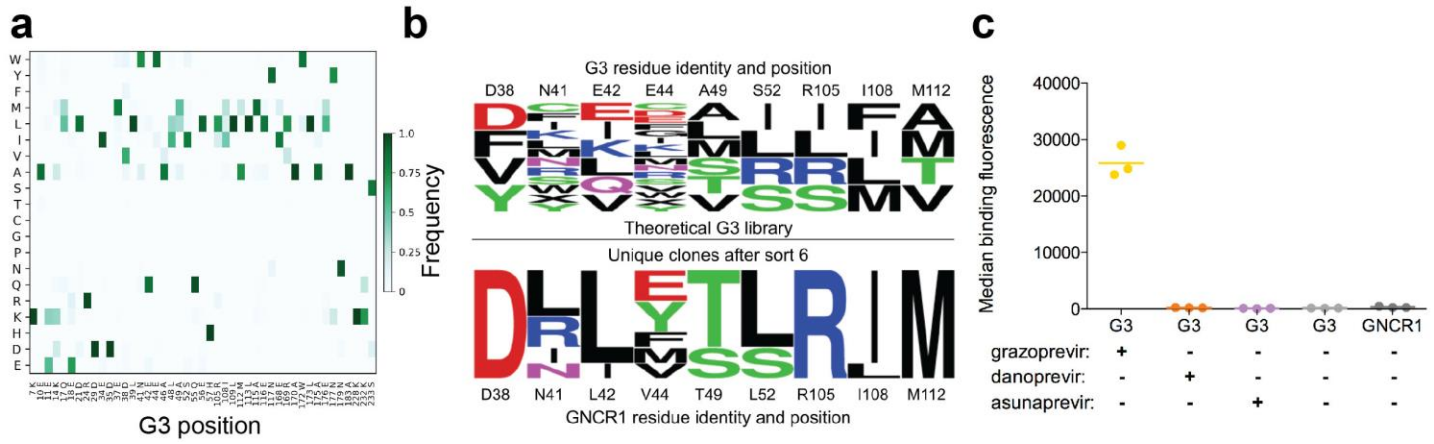

Supplementary Figure 3

Grazoprevir:NS3a complex reader binding and improvement.

a, Predicted mutational preferences of the G3 interface for binding to NS3a:grazoprevir, as defined by the frequencies of mutations found in Rosetta re-designs of the interface. **b**, Sequence logos of the theoretical library for the combinatorial library varying the G3 interface (top), and the mutations found in the final enriched library (bottom). Residue identities at the varied positions are indicated for the first-generation reader G3 and optimized reader GNCR1**. c**, Binding of 1 µM NS3a with avidity to yeast-displayed G3 or GNCR1 in the presence of grazoprevir, danoprevir, asunaprevir, or DMSO. Technical triplicates and their means are shown.

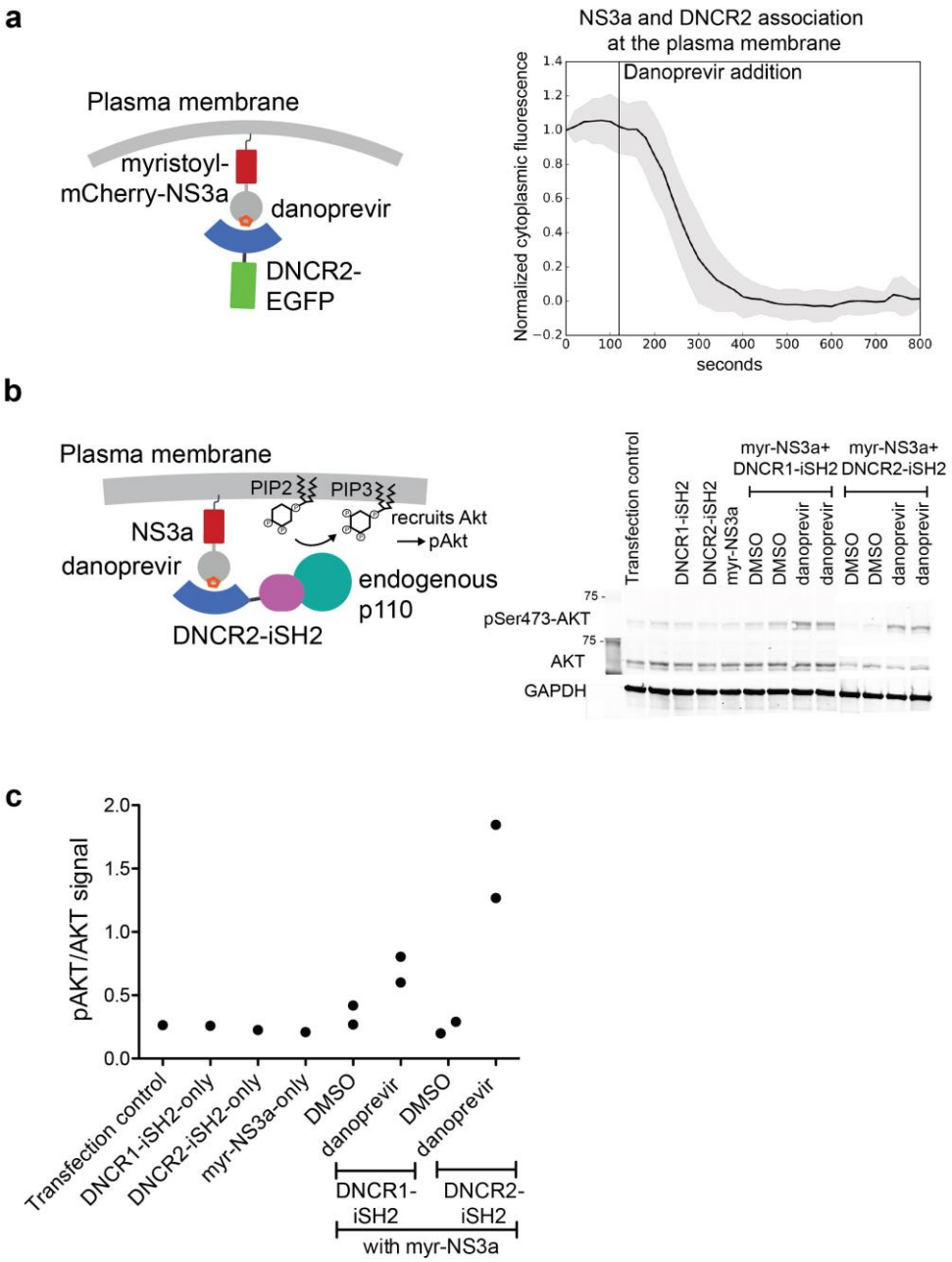

Supplementary Figure 4

Characterization of the kinetics and affinity of the DNCR2:danoprevir:NS3a complex in mammalian cells.

a, Kinetics of DNCR2-EGFP association with myristoylated NS3a-mCherry after adding 5 μM danoprevir (time of drug addition is denoted by the dark gray vertical line). Mean and standard deviation of the cytoplasmic EGFP fluorescence (normalized to first and last frame) of 18 NIH3T3 cells collected from 4 separate experiments. **b**, Schematic of danoprevir-mediated PI3K-Akt pathway activation through recruitment of an inter-Src homology 2 domain (iSH2) of the regulatory PI3K subunit p85/DNCR2 fusion (DNCR2-iSH2) to myristoylated NS3a-mCherry (left panel). Western blots of phospho-AKT (pSer473) and AKT performed in COS-7 cells transfected with control plasmid (GFP), DNCR1-iSH2-only, DNCR2-iSH2-only, myristoyl-NS3a-only, DNCR1-iSH2 or DNCR2-iSH2 co-transfected with myristoyl-NS3a treated with DMSO or 10 μM danoprevir from one experiment. See Supplementary Figure 15 for the full Western blots. **c**, Quantification of Western blot in (b) (singlicate for controls; two well replicates for DMSO and danoprevir conditions).

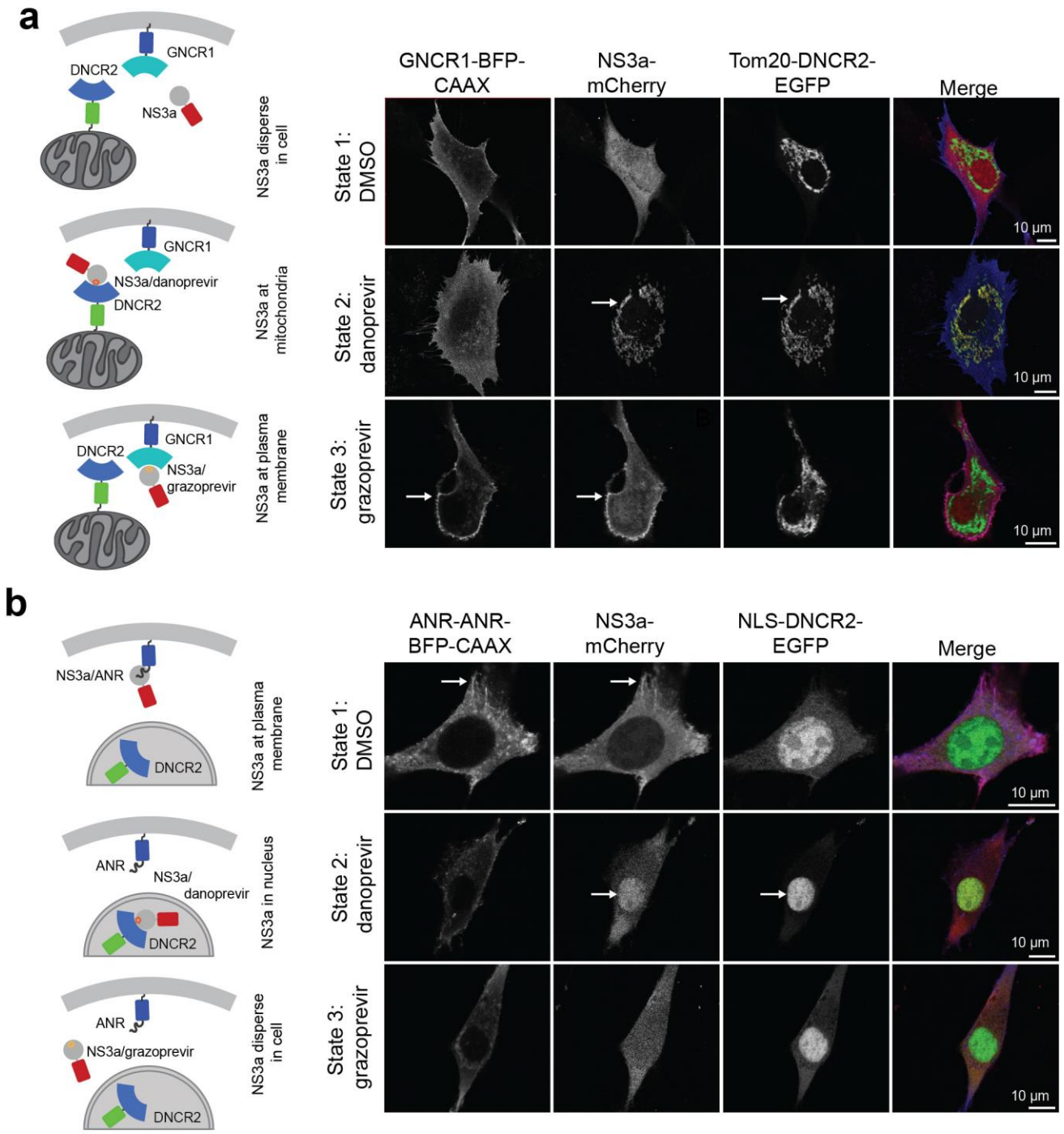

Supplementary Figure 5

Combination of reader pairs for inducible two-location and colocalization control with NS3a.

a, Colocalization of NS3a-mCherry with GNCR1-BFP-CAAX or Tom20-DNCR2-EGFP after treatment with danoprevir (5 μM), grazoprevir (5 μM), or DMSO. **b**, Colocalization of NS3a-mCherry with ANR-BFP-CAAX or NLS-DNCR2-EGFP after treatment with danoprevir (5 μM), grazoprevir (5 μM), or DMSO. See Fig. 2c,d for quantification of multiple cells and associated entry in Supplementary Table 3 for the number of cells and replicates of which these images are representative.

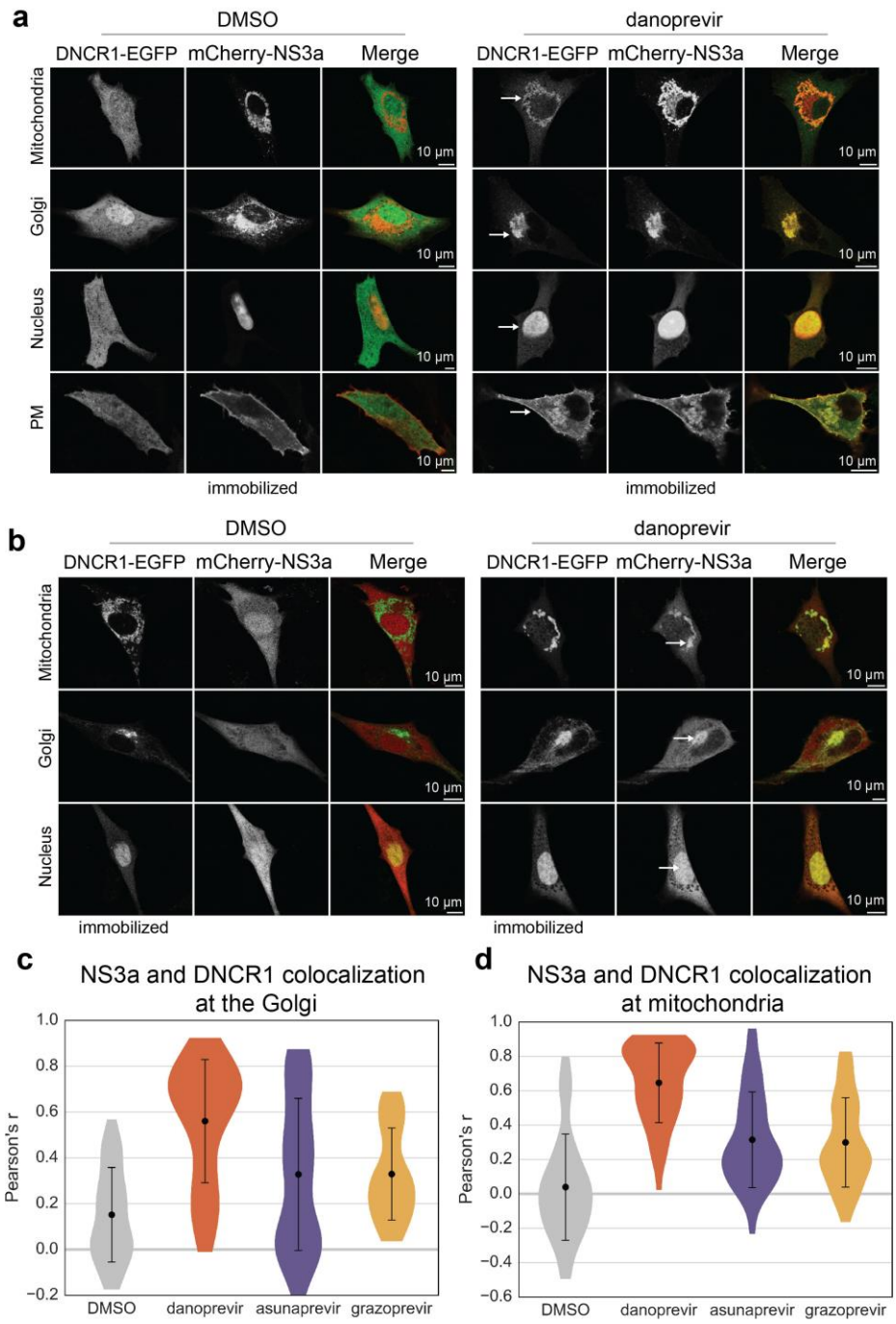

Supplementary Figure 6

Drug-regulated control of subcellular protein localization with intermediate-affinity danoprevir:NS3a reader DNCR1.

a, Colocalization of DNCR1-EGFP with mitochondria-, Golgi-, nuclear-, or plasma membrane-localized NS3a-mCherry under DMSO (left panel) or 10 µM danoprevir (right panel) treatment. **b**, Colocalization of mCherry-NS3a with mitochondria-, Golgi-, or nuclear-localized DNCR1-EGFP under DMSO (left panel) or 10 µM danoprevir (right panel) treatment. Each panel in (a,b) is representative of the majority population of n≥18 NIH3T3 cells from one well. Quantification of colocalization of mCherry-NS3a with **c,** Golgi- or **d**, mitochondrially-localized DNCR1-EGFP after treatment with grazoprevir (10 µM), danoprevir (10 µM), asunaprevir (10 µM), or DMSO. The mean and standard deviation of the Pearson's r of red/green pixel intensities is given for the number of cells stated in Supplementary Table 3 for each condition, along with the distributions for multiple NIH3T3 cells. See Supplementary Table 3 for sample sizes and P values.

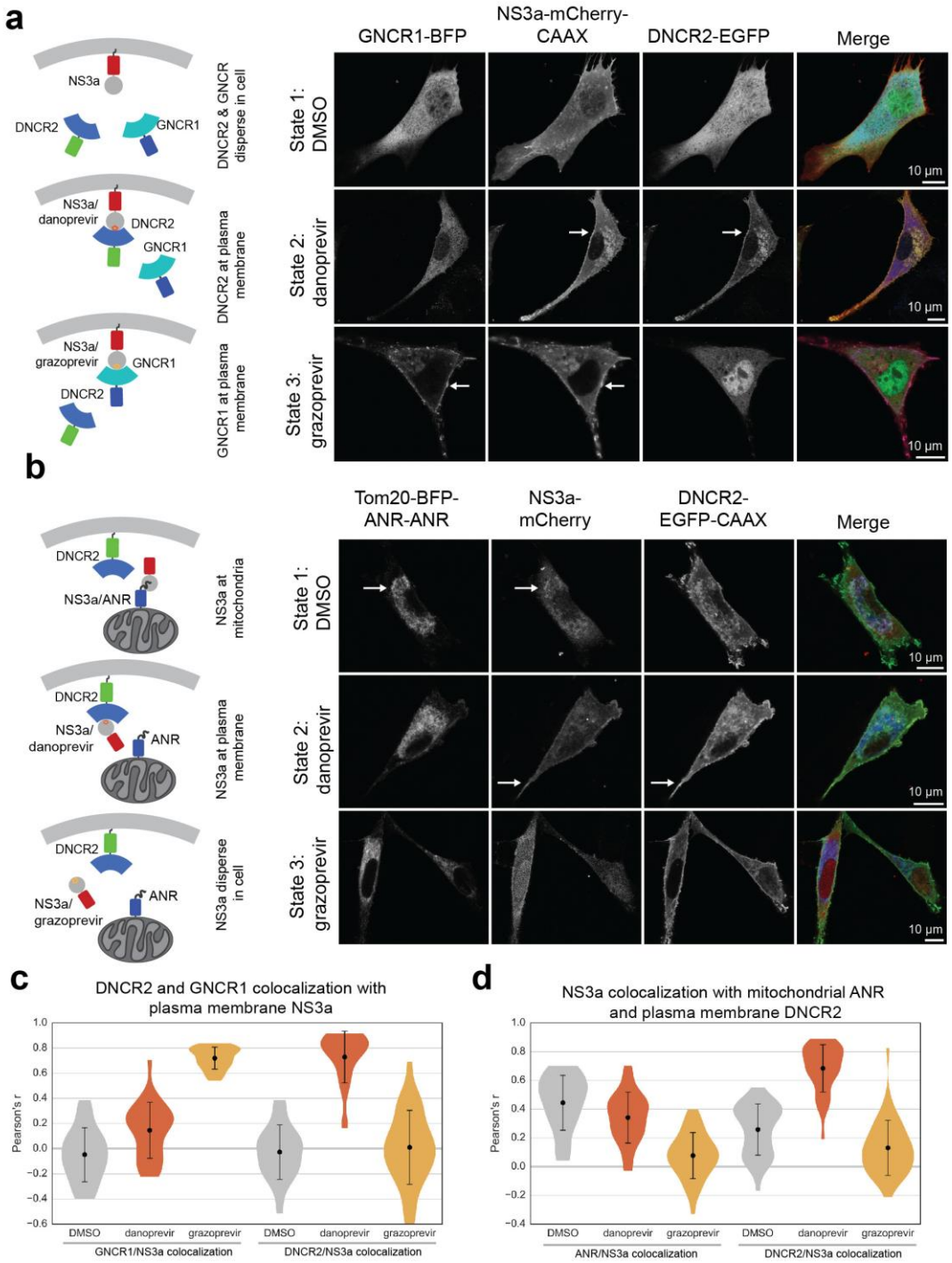

Supplementary Figure 7

Additional PROCISiR combinations for two-location control of NS3a.

a, Colocalization of GNCR1-BFP or DNCR2-EGFP with NS3a-mCherry-CAAX after treatment with danoprevir (5 µM), grazoprevir (5 µM), or DMSO. **b**, Colocalization of NS3a-mCherry with Tom20-BFP-ANR or DNCR2-EGFP-CAAX after treatment with danoprevir (5 µM), grazoprevir (5 µM), or DMSO. Images are representative of two separate wells and the number of cells given in Supplementary Table 3. **c,d**, The mean (marked by dot) and standard deviation (error bars) of the Pearson's r of red/blue or red/green pixel intensities for the number of cells stated in Supplementary Table 3 is given for each condition in (a,b), along with the distributions of Pearson's r.

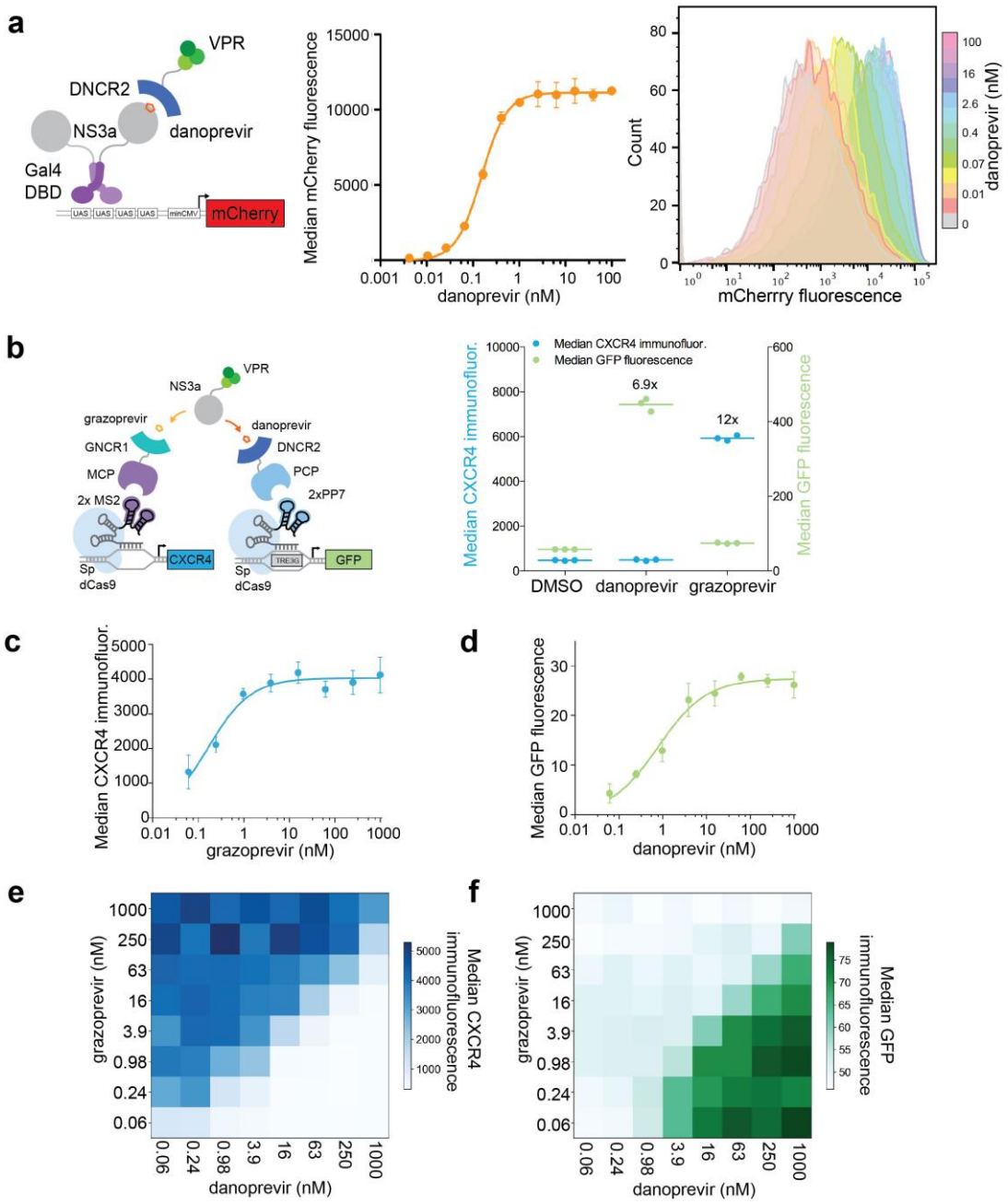

Supplementary Figure 8

Titration of gene expression with Gal4/UAS and a two-gene dCas9 system.

a, Titration of mCherry expression from a UAS-minCMV promoter using Gal4-NS3a and DNCR2-VPR (left). Median mCherry values are shown in the middle panel, with the histograms for one replicate shown on the right to illustrate that the full population shifts to intermediate levels of gene expression. **b**, Expression of CXCR4 and GFP in cells expressing an MS2 scRNA targeting CXCR4, a PP7 scRNA targeting a GFP reporter, GNCR1-MCP, DNCR2-PCP, and NS3a-VPR after treatment with DMSO, danoprevir, or grazoprevir. Fold changes relative to DMSO are given for each 10 μM drug response for three biological replicates from one experiment. See Supplementary Table 3 for P values. **c**, CXCR4 immunofluorescence from titration of grazoprevir alone in the same system as (b). **d**, GFP fluorescence from titration of danoprevir alone in the same system as (b). (a,c,d) are fit to a one-site, specific binding Hill equation, and each point shows the mean and standard deviation of 3 biological replicates from one experiment, with background fluorescence levels from a DMSO-only condition subtracted. **e**,**f**, Raw median fluorescence values for experiment shown in Fig. 3e and 3f (mean of two replicates, not DMSO-subtracted).

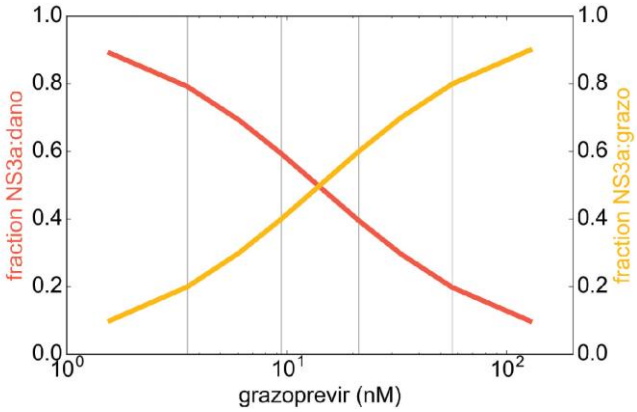

Supplementary Figure 9

Modeling of NS3a:danoprevir and NS3a:grazoprevir occupancies.

The fraction of NS3a bound to danoprevir (orange, left axis) and the fraction of NS3a bound to grazoprevir (yellow, right axis) was calculated for a constant concentration of 100 nM danoprevir, with increasing concentrations of grazoprevir. The vertical gray lines mark the grazoprevir concentrations used for the experiments in Fig. 4, Supplementary Fig. 11, and Supplementary Fig. 12.

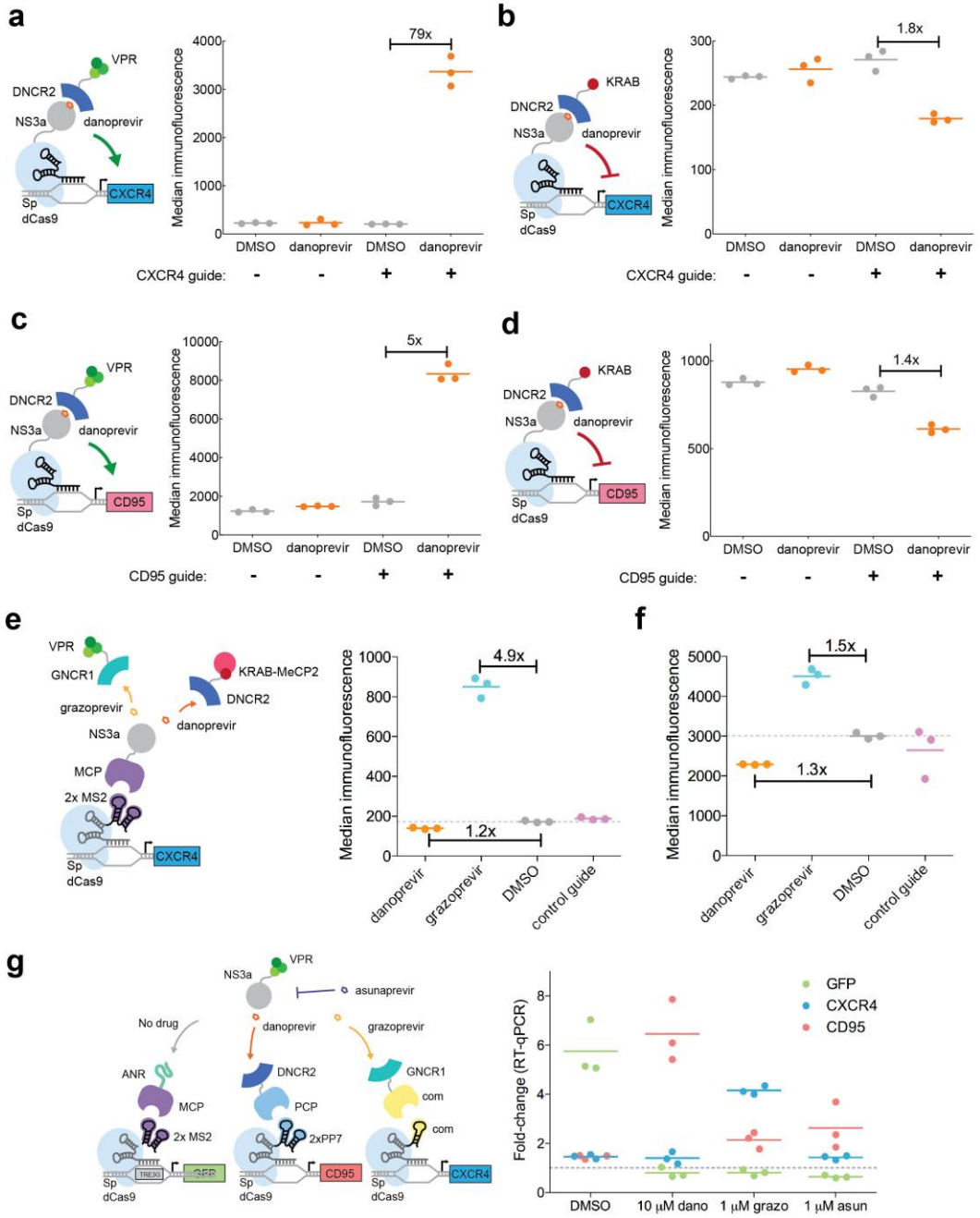

Supplementary Figure 10

Switchable repression, overexpression, and three-gene control.

Median immunofluorescence of CXCR4 (**a,b**) or CD95 (**c,d**) expression controlled by danoprevir-promoted recruitment of (a,c) DNCR2-VPR or (b,d) DNCR2-KRAB to NS3a-dCas9 in the absence or presence of guides targeting the CXCR4 (a,b) or CD95 (c,d) promoter region. Fold change (a,c) or inverse fold change (b,d) are given above each DMSO/danoprevir condition pair. **e**, Switching between repression and overexpression is achieved from endogenous promoters for CXCR4 and CD95 (**f**) using dCas9 with MCP-NS3a, GNCR1-VPR, and DNCR2-KRAB-MeCP2. Fold change or inverse fold change is shown for treatment with 100 nM grazoprevir or danoprevir, respectively. (a-f) The mean of the median immunofluorescence intensities are given in arbitrary units for data from 3 independent wells from one experiment. **g**, Expression of GFP, CD95, and CXCR4 using a MS2 scRNA targeting a GFP reporter, a PP7 scRNA targeting CD95, and a com scRNA targeting CXCR4 with MCP-ANR, PP7-DNCR2, and com-GNCR1, respectively. The mean of 3 independent wells from one experiment is given for each gene relative to untransfected cells. See Supplementary Table 3 for all P values.

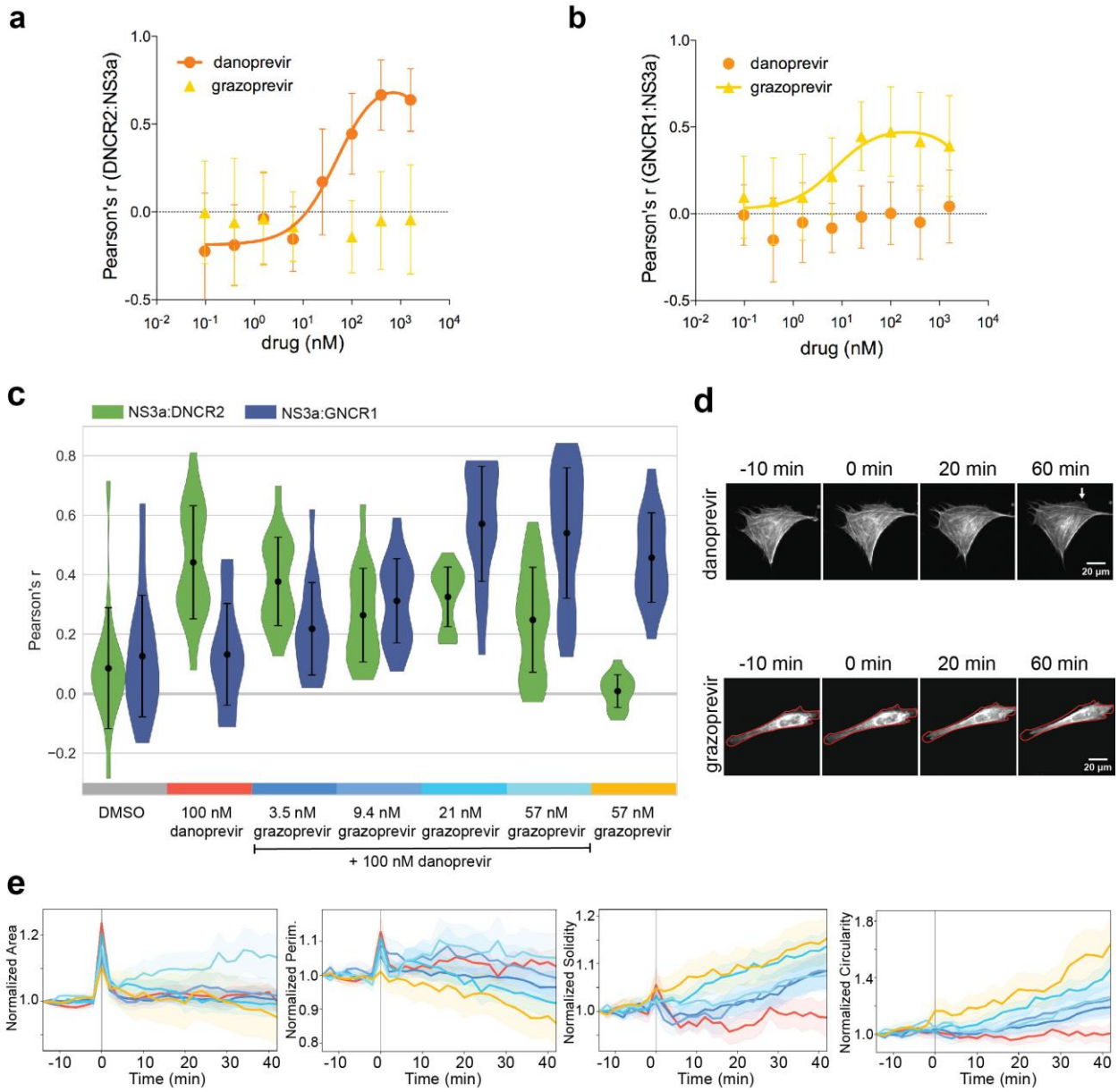

Supplementary Figure 11

Membrane localization control in Hela and NIH3T3 cells.

a,b, Confocal image quantification of EGFP-DNCR2 (a) or BFP-GNCR1 (b) colocalization with mCherry-NS3a-CAAX for single-drug titrations in HeLa cells. Mean and standard deviation of the number of cells per condition given in Supplementary Table 3 from one well. Curves are fit to a one-site, total binding equation. **c**, Confocal image quantification of EGFP-DNCR2 (green) and BFP-GNCR1 (blue) colocalization with mCherry-NS3a-CAAX for drug combinations shown in NIH3T3 cells. The mean (marked by dot) and standard deviation (error bars) of the Pearson's r of red/blue or red/green pixel intensities for the number of cells stated in Supplementary Table 3 is given for each condition along with the distributions of Pearson's r. **d**, Representative images from two experiments of NIH3T3 cells transiently co-expressing EGFP-DNCR2-TIAM, BFP-GNCR1-LARG, and NS3a-CAAX treated with danoprevir (top) or grazoprevir (bottom) for the times indicated (drug was added at t=0). Lifeact-mCherry was also co-expressed to allow visualization of F-actin. Danoprevir treatment led to membrane ruffling (arrow) and grazoprevir treatment led to cell contraction (a red outline illustrating the cell boundary at -10 min is overlaid to illustrate cell contraction). **e**, Cell morphology parameters (area, perimeter, solidity, and circularity) of NIH3T3 cells transiently co-expressing EGFP-DNCR2-TIAM, BFP-GNCR1-LARG, NS3a-CAAX, and Lifeact-mCherry that were treated with the drug combinations shown in (C) for the times indicated (drug was added at t=0). Mean and s.e.m. for the number of per condition given in Supplementary Table 3 normalized to first frame, from one well.

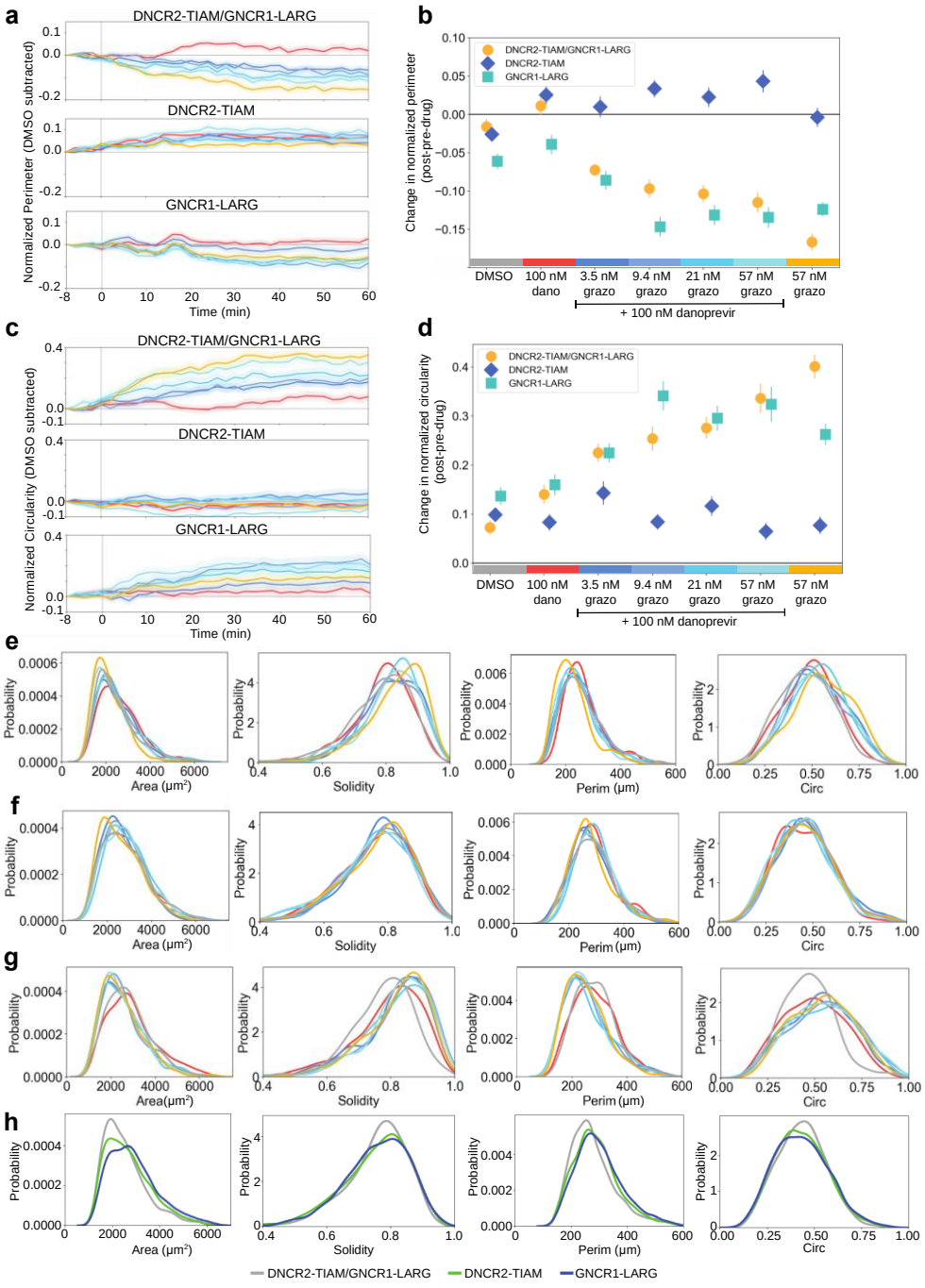

Supplementary Figure 12

Proportional control of RhoA and Rac1 activation in HeLa cells.

a,c, Change in normalized perimeter (a) or circularity (c) (DMSO baseline subtracted) over time (drug addition at 0 min) in HeLa cells expressing NS3a-CAAX with either DNCR2-TIAM and GNCR1-LARG, DNCR2-TIAM alone, or GNCR1-LARG alone. Lines are colored according to the drug conditions shown on the x-axis of the plot in (b). **b,d**, Change in normalized perimeter (b) or circularity (d) (average last 10 min-first 10 min). (a-d) Mean and s.e.m. of the number cells per condition listed in Supplementary Table 3 from four independent wells. **e-g**, Kernel density estimates of distributions of morphology statistics at 60 min post-drug addition in Hela cells expressing NS3a-CAAX with either (e) DNCR2-TIAM and GNCR1-LARG, (f) DNCR2-TIAM alone, or (g) GNCR1-LARG alone. **h**, Kernel density estimates of the distributions of morphology statistics at the first frame (before drug addition) for the three HeLa cell lines.

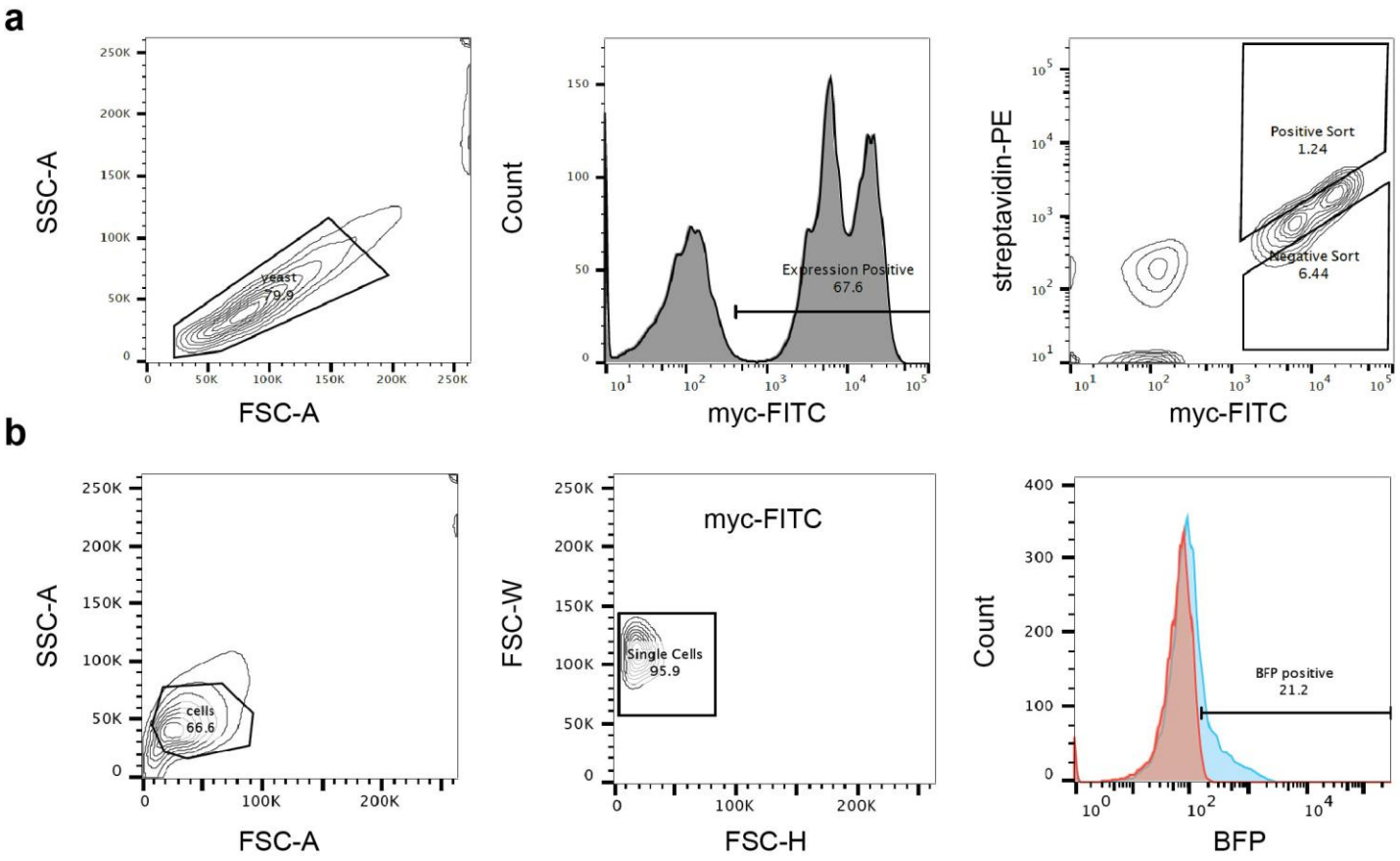

Supplementary Figure 13

Yeast and human cell FACS gating strategies.

a, Yeast gating for all events (left), expression positive events used to report median binding fluorescence values (middle), and example sorting gates (right). **b,** HEK293T gating for all events (left), followed by single cell gating (middle), and gating for transfection-positive cells (BFP positive, right). Untransfected cells (red), NS3aH1-BFP-dCas9-transfected cells (blue).

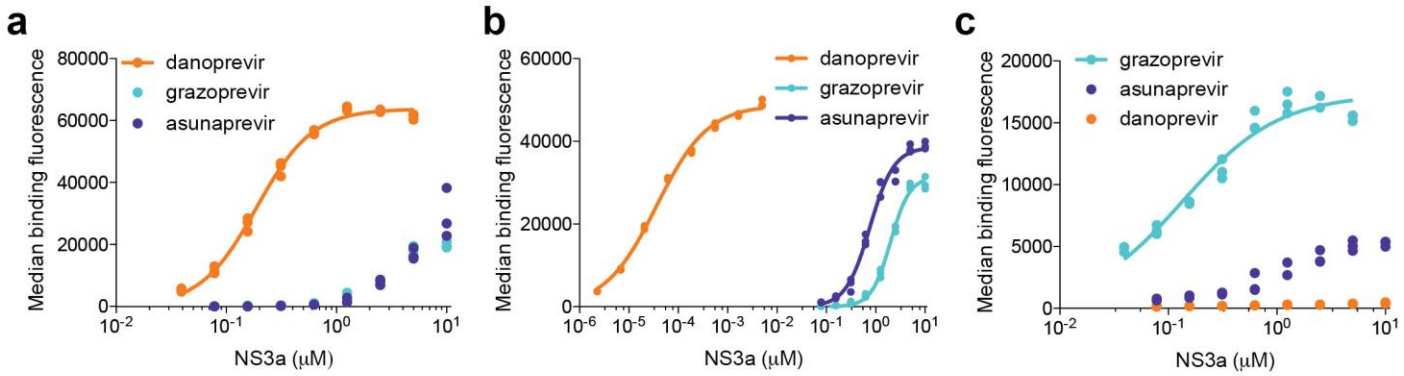

Supplementary Figure 14

Yeast-displayed design variants binding to NS3a:drug complexes.

Binding of NS3a:drug complexes (danoprevir, grazoprevir, asunaprevir) to yeast-displayed **a**, DNCR1, **b**, DNCR2, **c**, GNCR1. Shown are 3 technical replicates fit with the Hill equation for complete curves.

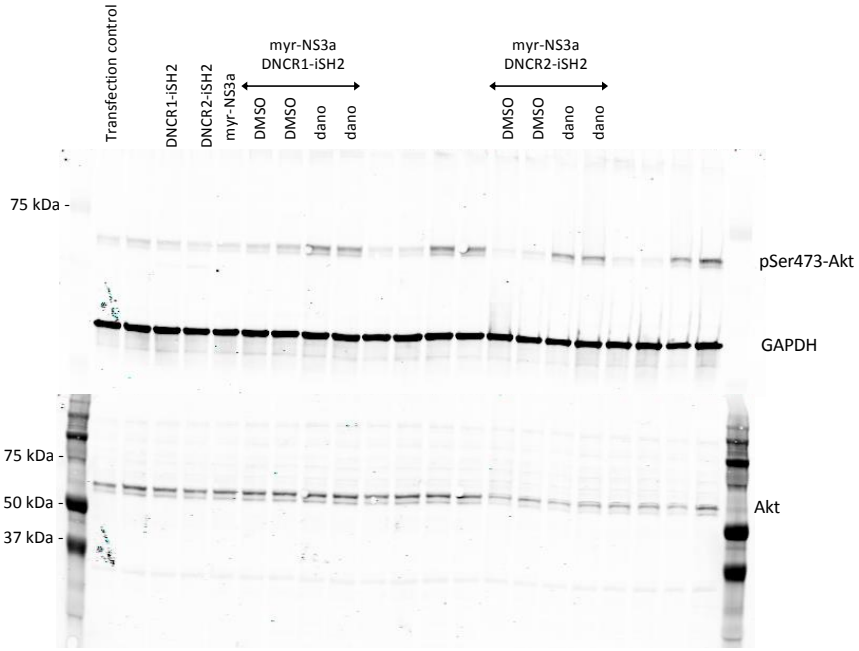

Supplementary Figure 15

Full western blots for Supplementary Figure 4b.

Full Western blots (top, anti-rabbit secondary with anti-pSer473-Akt and anti-GAPDH primaries; bottom, anti-mouse secondary with anti-Akt primary). Molecular weight markers are indicated on both blots.

Supplementary Notes

Protein engineering details and biochemical characterization of DNCR and GNCR

The danoprevir:NS3a complex reader design process started with docking a set of highly stable, de novo designed proteins on a danoprevir:NS3a structure using PatchDock: leucine-rich repeat proteins, designed helical repeat proteins (DHRs), ferredoxins, and helical bundles.[1-3] The scaffolds were docked over the danoprevir:NS3a binding surface by directing their docking in PatchDock to the danoprevir molecule. Rosetta design was used to optimize the residues on the scaffold that came in contact with danoprevir and NS3a, largely resulting in designs with a hydrophobic interface with danoprevir, as most danoprevir hydrophilic groups are inaccessible when it is bound to NS3a. One design, D5, based on a DHR, showed danoprevir-dependent binding to NS3a when assayed via yeast surface display.

To improve D5's affinity for the danoprevir:NS3a complex, we used two sequential yeast surface display libraries (Supplementary Fig. 1). First, a combinatorial library was designed based on the frequencies of mutations present in re-designs of the D5 interface (Supplementary Fig. 1a).[4,5] These Rosetta re-designs were obtained after small rigid-body perturbations of D5 relative to the danoprevir:NS3a complex. Sorting this library with increasingly stringent conditions led to a variant, danoprevir:NS3a complex reader 1 (DNCR1), that specifically bound the danoprevir:NS3a complex with high nanomolar affinity (Supplementary Table1). Next, we characterized a single-site saturation mutagenesis (SSM) library of DNCR1's two designed primary interface helices (5 and 7) and the non-interface helix 6. Enrichment ratios, calculated after sorting for both danoprevir:NS3a complex binders and non-binders, supported the overall designed binding mode (Supplementary Fig. 1b). Interestingly, the negative sort, which enriched for non-binders, gave us further structural insight into the binding mode of DNCR1. The surface

residues of helix 6, which faces away from the interface, were very permissive of substitution. Likewise, a region spanning the C-terminus of helix 6 to the N-terminus of helix 7 was permissive of mutation to nearly any residue, including proline. The helices in this region were found to be unfolded in the DNCR2:danoprevir:NS3a structure, and the shift of DNCR2 results in this region of the DHR not participating in the interface (Supplementary Fig. 2c). The trends seen in the negative sort SSM library enrichment ratios support the hypothesis that DNCR1 likely binds similarly to DNCR2. A second combinatorial library was designed based on the positive sort enrichment ratios, and enrichment of this library for danoprevir:NS3a binding resulted in multiple high affinity clones, of which one, DNCR2 (Supplementary Fig. 1c), was chosen for further characterization, based on its superior expression on the surface of yeast. The progression of improved binding from the original scaffold DHR79, to the design D5, and through two libraries resulting in DNCR1, and finally DNCR2, are illustrated by the DNCR1 SSM enrichment ratios in Supplementary Fig. 1d.

We performed a detailed biochemical analysis of the DNCR2:danoprevir:NS3a complex to confirm that it had the expected properties of a chemically-induced heterodimer. DNCR2 does not appear to bind substantially to danoprevir alone based on the inability of a high concentration (100 μM) of the free drug to disrupt the DNCR2:danoprevir:NS3a complex on yeast (Supplementary Fig. 2b). Size exclusion chromatography demonstrated that DNCR2 and NS3a behave as expected, forming a 1:1 complex only in the presence of danoprevir (Supplementary Fig. 2e). This behavior, along with the drug specificity described in the main text (Supplementary Fig. 2a,f), indicated that we had successfully designed and engineered a CID that was only inducible by danoprevir.

For our second drug:NS3a complex reader, we targeted the grazoprevir:NS3a complex. Grazoprevir is an FDA-approved drug with picomolar affinity to NS3a (K_i of 140 pM).[6] For this round of design, we exclusively used DHR scaffolds, as our first-generation design had indicated that they were more suitable scaffolds for our design goal. We assembled a DHR scaffold set of many curvatures and sizes from published DHR crystal structures, as well as an in-house set of models (available upon request). We used both PatchDock and a new rotamer interaction field docking protocol (RIFDock) to center the DHR scaffolds over grazoprevir, followed by the same design approach that was used for the danoprevir CID design.[7] We ordered and tested 29 designs by yeast surface display. Five designs based on DHR models showed very weak, but grazoprevir-dependent binding (data not shown). One design, G3, based on the crystal structure of DHR18, showed modest binding, similar to the first-generation danoprevir reader design, D5 (Supplementary Fig. 3c).

We computationally characterized the mutational preferences of the G3 interface via a similar Rosetta-based approach used to predict the mutational preferences of D5. The predicted mutational preferences at the G3 interface are shown in Supplementary Fig. 3a. These mutational frequencies were used to design a combinatorial library varying 9 positions of G3, which was sorted for sequences with increased affinity to grazoprevir:NS3a (Supplementary Fig. 3b). Both G3 and the final high-affinity clone, grazoprevir:NS3a complex reader 1 (GNCR1), showed high specificity for binding grazoprevir:NS3a over complexes of NS3a with danoprevir or asunaprevir, or apo NS3a (Supplementary Fig. 3c, Supplementary Table 1). GNCR1 had a similar affinity for the grazoprevir:NS3a complex as DNCR1 had for the danoprevir:NS3a complex (<200 nM). Because this affinity was found to be adequate for functioning as a chemically-inducible dimerizer in mammalian cells, we did not engineer GNCR1 further.

Further subcellular localization control with PROCISiR

As an assay for colocalization of NS3a and DNCR1, we used confocal fluorescence microscopy of NIH3T3 cells transiently transfected with pairs of NS3a-mCherry and DNCR1-EGFP constructs. NS3a was localized to different subcellular compartments via an N-terminal Tom20 tag (mitochondria), a nuclear localization signal (NLS, nucleus), an N-terminal myristoyl group (plasma membrane), or a C-terminal Giantin tag (Golgi). DNCR1-EGFP was diffuse throughout the cell under DMSO treatment (Supplementary Fig. 6a, left), and colocalized with NS3a-mCherry after treatment with 10 μM danoprevir (Supplementary Fig. 6a, right). The intermediate affinity reader also exhibited colocalization when the orientation was switched and DNCR1 was fused to the localization tags (Supplementary Fig. 6b), demonstrating that these components are interchangeable and modular. DNCR1 also demonstrated partial binding specificity for the danoprevir:NS3a complex over other drug:NS3a complexes, as quantification of EGFP/mCherry signal correlation for multiple cells showed lower (but non-zero) correlation in cells treated with 10 μM asunaprevir or grazoprevir (Supplementary Fig. 6c,d).

In addition to the GNCR1/DNCR2 and DNCR2/ANR combinations used for the control of NS3a's subcellular localization shown in Fig. 2c,d and Supplementary Fig. 5, we also tested two other PROCISiR combinations for localization control. Colocalization of untagged DNCR2-EGFP and GNCR1-BFP with NS3a-mCherry-CAAX clearly exhibited 3 states: no colocalization with no drug, DNCR2/NS3a colocalization with danoprevir, and GNCR1/NS3a colocalization with grazoprevir (Supplementary Fig. 7a,c). Likewise, NS3a-mCherry could be pre-localized to mitochondria with Tom20-BFP-ANR, and recruited to membrane-targeted DNCR2-EGFP-CAAX after treatment with danoprevir (Supplementary Fig. 7b,d). Thus, PROCISiR's readers

can be combined to specifically respond to different drug treatments and provide multiple localization state outputs.

Modeling of NS3a:drug complex binding

To predict drug concentration regimes that would yield intermediate levels of NS3a:DNCR2 and NS3a:GNCR1 complexes, we modeled the fraction of NS3a bound to danoprevir and grazoprevir. For this, we simply used NS3a:drug K_i values and the Cheng-Prussoff approximation for equilibrium drug:receptor binding in the presence of a competitive inhibitor:

$$f_{N_d} = \frac{D}{\left(1 + \frac{C}{K_{i,c}}\right) K_{i,d} + D}$$

$$f_{N_c} = \frac{C}{\left(1 + \frac{D}{K_{i,d}}\right) K_{i,c} + C}$$

where f_{Nd} is the fraction of NS3a bound to the target drug, and f_{Nc} is the fraction of NS3a bound to the competitor drug, D is the free concentration of target drug, C is the free concentration of competitor drug, $K_{i,d}$ is the NS3a K_i for the target drug, and $K_{i,c}$ is the NS3a K_i for the competitor drug.[8] The following NS3a:drug K_i values used are from published enzyme inhibition studies: danoprevir:NS3a = 1.0 nM, and grazoprevir:NS3a = 0.14 nM.[6] There are several assumptions made in applying these equations that are unlikely to be valid in all cellular conditions, including the direct inverse relationship between f_{Nd} and f_{Nc}, which is unlikely to be true when intracellular NS3a concentrations are high. Additionally, in applying these equations to model the fractions of NS3a:drug:reader complexes, we make the further approximation that all NS3a:drug complexes will be stoichiometrically bound to their corresponding reader. Despite these assumptions, we

see very good correspondence between our model and the experimental results in Fig. 3e. The predicted fraction of NS3a bound to danoprevir or grazoprevir at different drug concentrations closely matches transcriptional outputs resulting from NS3a:danoprevir:DNCR2 or NS3a:grazoprevir:GNCR1 complex formation. We also used the same equations to model the amount of DNCR2 and GNCR1 recruited to membrane-bound NS3a using different drug treatment regimes (Supplementary Fig. 9, Fig. 4b, Supplementary Fig. 12c). In both transcriptional and signaling output applications, we see that the relative EC50 values between DNCR2 and GNCR1 outputs match the ratio of their drug:NS3a K_i values. See discussion below.

Additional transcriptional control modes

In Supplementary Fig. 10a-d, we used a direct fusion of NS3a to dCas9 to recruit the transcriptional activator DNCR2-VPR or the transcriptional repressor DNCR2-KRAB to specific genomic loci.[9,10] We used this system to control the expression of two endogenous genes in HEK293 cells, CXCR4 and CD95. Detection of expression by immunofluorescence and FACS revealed expression induction of 79-fold (CXCR4) or 5-fold (CD95) over a DMSO-treated control for the DNCR2-VPR constructs, and repression induction of 1.8-fold (CXCR4) or 1.4-fold (CD95) for the DNCR2-KRAB constructs. Danoprevir had no effect on gene expression in the absence of the guide RNA. The gene induction for CXCR4 and CD95 from DNCR2-VPR is similar to that obtained on these same genes for a direct dCas9-VPR fusion and two other inducible dCas9/VPR systems employing the gibberellin and abscisic acid CIDs.[11] To the best of our knowledge, inducible repression using dCas9 on endogenous promoters has not previously been demonstrated.

To enable temporal switching or graded control of gene expression from repression to overexpression, we utilized a scaffold RNA/RNA-binding protein (RBP) system with NS3a fused to the RBP MS2, GNCR1 fused to VPR, and DNCR2 fused to KRAB-MeCP2, a repressor with enhanced activity over KRAB.[12] While the transcriptional activation and repression observed with the scaffold RNA/RBP system was more modest than with the direct dCas9-NS3a fusion, this switchable system also demonstrated statistically significant overexpression (from grazoprevir treatment) or repression (from danoprevir treatment) of CXCR4 and CD95 (Supplementary Fig. 10e,f). Notably, this was using guides that were previously published as optimal for inducing overexpression of these genes and that anneal 5' to the transcription start site for each gene. Optimization of guide positions, or utilization of multiple guides that tile before and after the transcription start site could be explored in the future to improve the dynamic range of this switchable VPR/KRAB-MeCP2 system.

Finally, in a demonstration of the multi-state transcriptional outputs that can be achieved with PROCISiR, we combined GNCR1, DNCR2, and ANR with three orthogonal scRNA/RBP pairs (com/com, PP7/PCP, and MS2/MCP) to control the expression of CXCR4, CD95, and GFP, respectively, in a GFP-report HEK293 cell line (Supplementary Fig. 10g). This system exhibited four distinct transcriptional output states under four input states: DMSO (GFP expression under control of ANR), 10 μM danoprevir (CD95 expression under control of DNCR2), 1 μM grazoprevir (CXCR4 expression under control of GNCR1), and 1 μM asunaprevir (no gene expression, as asunaprevir disrupts ANR's interaction with NS3a-VPR but does not promote complex formation with DNCR2 or GNCR1). This demonstrates that all 3 readers can be used orthogonally to control multiple output states.

Membrane colocalization in HeLa and NIH3T3 cells

We performed single-drug titrations of membrane colocalization in HeLa cells co-expressing EGFP-DNCR2, BFP-GNCR1, and mCherry-NS3a-CAAX. The dose-responses, quantified by Pearson's r of EGFP/mCherry or BFP/mCherry correlation, are shown in Supplementary Fig. 11a,b. Neither DNCR2 nor GNCR1 colocalizes with NS3a in response to the non-target inducer, grazoprevir or danoprevir, respectively. One-site, total binding curves fit to the DNCR2:danoprevir and GNCR1:grazoprevir response gave EC_{50} values ~50-fold higher than the K_i values for those drugs and NS3a, which is in contrast to the close agreement between drug:NS3a K_i values and EC_{50} values for transcriptional activation we observed (Supplementary Fig. 8c,d). This disparity may be due to what is likely the high expression levels of NS3a-CAAX in HeLa cells. The EC_{50} for DNCR2:danoprevir:NS3a colocalization was 51 ± 16 nM and the EC_{50} for GNCR1:grazoprevir:NS3a colocalization was 7.3 ± 3.6 nM (mean, standard deviation), which accurately reflects the seven-fold difference in affinity for NS3a of the two drugs. Therefore, in order to identify drug concentrations that would achieve a range of intermediate levels of DNCR2:NS3a and GNCR1:NS3a colocalization, we used the drug:NS3a K_i values (1.0 and 0.14 nM for danoprevir and grazoprevir, respectively) to model the predicted fraction of NS3a:drug complexes formed in response to different combinations of danoprevir and grazoprevir (Supplementary Notes, "Modeling of NS3a drug complex binding"). We quantified colocalization from these drug concentrations in HeLa cells (Fig. 4b), and NIH3T3 cells (Supplementary Fig. 11c) co-expressing EGFP-DNCR2, BFP-GNCR1, and membrane-localized NS3a with confocal microscopy. NIH3T3 cells showed the predicted graded and proportional membrane colocalization of DNCR2:NS3a and GNCR1:NS3a (Supplementary Fig. 9 and Supplementary Fig. 11c). HeLa cells showed the expected graded membrane colocalization of

GNCR1:NS3a, with more modest gradation of DNCR2:NS3a membrane colocalization at higher grazoprevir concentrations (Fig. 4b). Future models could be further parameterized to improve accuracy, but our simple steady-state modeling based on drug:NS3a K_i values was sufficient to predict a useful regime for achieving intermediate response levels.

Cell morphology changes in single-effector versus dual-effector HeLa cells

The distributions of morphology statistics for the three HeLa cell lines (DNCR2-TIAM/GNCR1-LARG co-expressing and single-effector versions thereof: DNCR2-TIAM (in the presence of GNCR1 that is not fused to an effector) and GNCR1-LARG (in the presence of DNCR2 that is not fused to an effector)) after 60 minutes of drug treatment are shown in Supplementary Fig. 12e-g. Interestingly, the area and perimeter changes appear graded on the single-cell level, while solidity changes appear more binary. This trend of cells partitioning between two extremes of solidity defined by the single-drug conditions is more obvious in the dual-effector cells, which have a larger range of solidity changes. In the dual-effector cells, the intermediate drug combinations with low grazoprevir exhibit a bimodal or broadened solidity distribution when compared to the single-drug conditions, indicative of some cells withdrawing protrusions and achieving the high solidity state, while others retain their original morphology (Supplementary Fig. 11e). This binary cell solidity change was previously noted when modulating Rac/Rho activity indirectly with Pak inhibitors.[13] These results are suggestive of some events leading to changes in cell morphology being more abrupt (withdrawal of protrusions following Rho activation), while others (changes to cell size) exhibit more gradual behavior. The three HeLa cell lines showed no systematic differences in starting morphology (Supplementary

Fig. 11h), validating that the observed morphological changes are due to TIAM and LARG recruitment in response to danoprevir and grazoprevir, respectively.

Graded and proportional control of GTPase-driven signaling pathways in NIH3T3 cells

Plasma membrane colocalization of DNCR2-TIAM and GNCR1-LARG with NS3a-CAAX was also investigated in NIH3T3 cells using the danoprevir/grazoprevir combinations suggested from modeling. Danoprevir treatment appeared to increase membrane ruffling, which is a known result of Rac1 activation, while grazoprevir treatment caused stress fiber formation and cell contraction from RhoA activity (Supplementary Fig. 11d). The drug combinations from Supplementary Fig. 11c were applied to NIH3T3 cells transiently co-expressing DNCR2-TIAM, GNCR1-LARG, and NS3a-CAAX, and the area, perimeter, solidity, and circularity were tracked with wide-field microscopy over time (Supplementary Fig. 11e). Although danoprevir treatment and subsequent Rac1 activation led to the formation of observable lamellipodia, it did not induce measurable changes in morphology. This suggests that Rac1 activity may have different effects in NIH3T3 cells than in HeLa cells. NIH3T3 cells are fibroblasts, and therefore start with a highly adherent, flat, and elongated morphology, while HeLa cells are an epithelial line and start with a more rounded morphology. Visually observed membrane ruffling from Rac1 activity in NIH3T3 cells may not be captured by the gross cell size and shape parameters quantified, and as NIH3T3 cells are already fairly flat and spread out, there is little further spreading from Rac1 activation. In HeLa cells expressing DNCR2-TIAM, danoprevir treatment caused significant cell spreading, as indicated by increases in area and perimeter (Fig. 4, Supplementary Fig. 12). In NIH3T3 cells, grazoprevir treatment (LARG/RhoA activation) caused significant contraction of cell length and protrusions as indicated by increases in circularity and solidity, respectively,

which was consistent between the cell lines (Supplementary Fig. 11e, Fig. 4). Gradations in RhoA effect on cell morphology were observable at the intermediate danoprevir/grazoprevir concentrations. The NIH3T3 data is from approximately an order of magnitude fewer cells ($n \geq 22$) than the HeLa datasets ($n \geq 201$) and is therefore considerably noisier than the HeLa data, including a spike at t=0 min due to focusing and segmentation issues when drug was added. Nevertheless, these data illustrate that graded and proportional control of signaling pathways can be performed with PROCISiR in cells of different types and uncover differences in cell response to the same stimuli.

Supplementary Table 1 | Apparent dissociation constants for yeast-displayed design variants to NS3a:drug complexes

Clone	Drug	K_D (nM) ± standard deviation or relative binding	Fold drug specificity
D5	danoprevir	++	-
	grazoprevir	+++	none
	asunaprevir	+	modest
DNCR1	danoprevir	190 ± 10 nM	-
	grazoprevir	2900 ± 100 nM	15
	asunaprevir	6300 ± 2600 nM	33
DNCR2	danoprevir	0.036 ± 0.0002 nM	-
	grazoprevir	2000 ± 100 nM	56,000
	asunaprevir	770 ± 50 nM	21,000
G3	grazoprevir	++	-
	danoprevir	no binding	high
	asunaprevir	+	modest
GNCR1	grazoprevir	140 ± 20 nM	-
	danoprevir	>10,000 nM	>71
	asunaprevir	>10,000 nM	>71

Data are from three technical replicates. Relative binding of different NS3a:drug complexes is given for conditions where binding was too weak to achieve full titration curves on yeast, indicating binding in the low-to-mid micromolar-range, or weaker. Curves for DNCR1, DNCR2, and GNCR1 are shown in Supplementary Fig. 14. See Supplementary Fig. 2A, 3C for single concentration point data for D5 and G3.

Supplementary Table 2 | Crystallography data collection and refinement statistics

	DNCR2:NS3a:danoprevir
Data collection	
Space group	$P2_1$
Cell dimensions	
a, *b*, *c* (Å)	70.84, 69.26, 99.34
α, β, γ (°)	90, 108.59, 90
Resolution (Å)	50.0 - 2.30 (2.37 - 2.30) *
R_{sym}	0.102 (0.340)
$I / \sigma I$	14.4 (2.6)
Completeness (%)	99.3 (93.6)
Redundancy	4.1 (3.0)
Refinement	
Resolution (Å)	50.0 - 2.30
No. reflections	38559
R_{work} / R_{free}	0.203 / 0.240
No. atoms	
Protein	5818
Ligand/ion	134
Water	209
B-factors	
Protein	29.9
Ligand/ion	33.4
Water	37.4
R.m.s. deviations	
Bond lengths (Å)	0.012
Bond angles (°)	1.545

This diffraction data set was collected from a single crystal.
*Values in parentheses are for highest-resolution shell.

Supplementary Table 3 | Statistics and reproducibility
Values are from one-way ANOVA with significance for each comparison (P <0.05) determined by Tukey's multiple comparisons test, except where noted.

Figure	Condition	Condition 1	Condition 2	Number of cells (1,2)	Number of wells (1,2)	ANOVA results	
						Mean difference	Signif-cant
Fig. 2B		One-way ANOVA P value				<0.0001	
		DMSO	10 μM danoprevir	26, 26	3, 3	-0.6277	Yes
		DMSO	10 μM asunaprevir	26, 32	3, 4	0.004479	No
		DMSO	10 μM grazoprevir	26, 34	3, 4	0.08568	No
		10 μM danoprevir	10 μM asunaprevir	26, 32	3, 4	0.6321	Yes
		10 μM danoprevir	10 μM grazoprevir	26, 34	3, 4	0.7133	Yes
Fig. 2C	GNCR1/NS3a	One-way ANOVA P value				<0.0001	
		DMSO	5 μM danoprevir	37, 30	3, 3	0.04179	No
		DMSO	5 μM grazoprevir	37, 35	3, 3	-0.6140	Yes
		5 μM danoprevir	5 μM grazoprevir	30, 35	3, 3	-0.6558	Yes
	DNCR2/NS3a	One-way ANOVA P value				<0.0001	
		DMSO	5 μM danoprevir	37, 30	3, 3	-0.6409	Yes
		DMSO	5 μM grazoprevir	37, 35	3, 3	0.2358	Yes
		5 μM danoprevir	5 μM grazoprevir	30, 35	3, 3	0.8767	Yes
Fig. 2D	ANR/NS3a	One-way ANOVA P value				<0.0001	
		DMSO	5 μM danoprevir	29, 25	3, 3	0.4612	Yes
		DMSO	5 μM grazoprevir	29, 26	3, 3	0.3235	Yes
		5 μM danoprevir	5 μM grazoprevir	25, 26	3, 3	-0.1377	Yes
	DNCR2/NS3a	One-way ANOVA P value				<0.0001	
		DMSO	5 μM danoprevir	29, 25	3, 3	-0.6039	Yes
		DMSO	5 μM grazoprevir	29, 26	3, 3	-0.4252	Yes
		5 μM danoprevir	5 μM grazoprevir	25, 26	3, 3	0.1786	Yes
Fig. 4b		DMSO		18	1		
		100 nM danoprevir		18	1		
		100 nM danoprevir, 3.5 nM grazoprevir		17	1		

		100 nM danoprevir, 9.4 nM grazoprevir		14	1	
		100 nM danoprevir, 21 nM grazoprevir		20	1	
		100 nM danoprevir, 57 nM grazoprevir		16	1	
		57 nM grazoprevir		20	1	
Fig. 4d-g and Supp. Fig 12	DNCR2-TIAM/GNCR1-LARG	DMSO		385	4	
		100 nM danoprevir		340	4	
		100 nM danoprevir, 3.5 nM grazoprevir		328	4	
		100 nM danoprevir, 9.4 nM grazoprevir		201	4	
		100 nM danoprevir, 21 nM grazoprevir		248	4	
		100 nM danoprevir, 57 nM grazoprevir		260	4	
		57 nM grazoprevir		266	4	
	DNCR2-TIAM	DMSO		374	4	
		100 nM danoprevir		273	4	
		100 nM danoprevir, 3.5 nM grazoprevir		292	4	
		100 nM danoprevir, 9.4 nM grazoprevir		387	4	
		100 nM danoprevir, 21 nM grazoprevir		309	4	
		100 nM danoprevir, 57 nM grazoprevir		274	4	
		57 nM grazoprevir		323	4	
	GNCR1-LARG	DMSO		307	4	
		100 nM danoprevir		313	4	
		100 nM danoprevir, 3.5 nM grazoprevir		328	4	
		100 nM danoprevir, 9.4 nM grazoprevir		237	4	
		100 nM danoprevir, 21 nM grazoprevir		286	4	
		100 nM danoprevir, 57 nM grazoprevir		247	4	
		57 nM grazoprevir		298	4	
Supp. Fig. 6C		One-way ANOVA P value				<0.0001
		DMSO	10 μM danoprevir	25, 42	3, 5	-0.4154	Yes
		DMSO	10 μM asunaprevir	25, 27	3, 3	-0.1721	No
		DMSO	10 μM grazoprevir	25, 27	3, 3	-0.1751	No
		10 μM danoprevir	10 μM asunaprevir	42, 27	5, 3	0.2433	Yes
		10 μM danoprevir	10 μM grazoprevir	42, 27	5, 3	0.2402	Yes
Supp. Fig.6D		One-way ANOVA P value				<0.0001	
		DMSO	10 μM danoprevir	33, 45	3, 5	-0.6159	Yes

		DMSO	10 μM asunaprevir	33, 37	3, 3	-0.2954	Yes
		DMSO	10 μM grazoprevir	33, 32	3, 3	-0.2641	Yes
		10 μM danoprevir	10 μM asunaprevir	45, 37	5, 3	0.3205	Yes
		10 μM danoprevir	10 μM grazoprevir	45, 32	5, 3	0.3519	Yes
Supp. Fig. 7C	GNCR1/NS3a	One-way ANOVA P value				<0.0001	
		DMSO	10 μM danoprevir	26, 27	2, 2	-0.2066	Yes
		DMSO	10 μM grazoprevir	26, 29	2, 2	-0.7921	Yes
		10 μM danoprevir	10 μM grazoprevir	27, 29	2, 2	-0.5855	Yes
	DNCR2/NS3a	One-way ANOVA P value				<0.0001	
		DMSO	10 μM danoprevir	26, 27	2, 2	-0.7846	Yes
		DMSO	10 μM grazoprevir	26, 29	2, 2	-0.0729	No
		10 μM danoprevir	10 μM grazoprevir	27, 29	2, 2	0.7117	Yes
Supp. Fig. 7D	ANR/NS3a	One-way ANOVA P value				<0.0001	
		DMSO	5 μM danoprevir	39, 33	3, 5	0.1010	Yes
		DMSO	5 μM grazoprevir	39, 41	3, 4	0.3764	Yes
		5 μM danoprevir	5 μM grazoprevir	33, 41	5, 4	0.2754	Yes
	DNCR2/NS3a	One-way ANOVA P value				<0.0001	
		DMSO	5 μM danoprevir	39, 33	3, 5	-0.4278	Yes
		DMSO	5 μM grazoprevir	39, 41	3, 4	0.1308	Yes
		5 μM danoprevir	5 μM grazoprevir	33, 41	5, 4	0.5587	Yes
Supp. Fig. 8B	CXCR4	One-way ANOVA P value				<0.0001	
		DMSO	danoprevir	NA	3, 3	-11.67	No
		DMSO	grazoprevir	NA	3, 3	-5458	Yes
		danoprevir	grazoprevir	NA	3, 3	-5447	Yes
	GFP	One-way ANOVA P value				<0.0001	
		DMSO	danoprevir	NA	3, 3	-388.2	Yes
		DMSO	grazoprevir	NA	3, 3	-16.70	No
		danoprevir	grazoprevir	NA	3, 3	371.5	Yes
Supp. Fig. 10A	No CXCR4 guide	DMSO	danoprevir	NA	3, 3	0.8382[a]	
	CXCR4 guide	DMSO	danoprevir	NA	3, 3	<0.0001[a]	
Supp. Fig. 10B	No CXCR4 guide	DMSO	danoprevir	NA	3, 3	0.3309[a]	
	CXCR4 guide	DMSO	danoprevir	NA	3, 3	0.0008[a]	
Supp. Fig. 10C	No CD95 guide	DMSO	danoprevir	NA	3, 3	0.0049[a]	
	CD95 guide	DMSO	danoprevir	NA	3, 3	<0.0001[a]	

Supp. Fig. 10D	No CD95 guide	DMSO	danoprevir	NA	3, 3	0.01[a]	
	CD95 guide	DMSO	danoprevir	NA	3, 3	0.0006[a]	
Supp. Fig. 10E		One-way ANOVA P value				<0.0001	
		DMSO	danoprevir	NA	3, 3	33.67	No
		DMSO	grazoprevir	NA	3, 3	-677.7	Yes
		DMSO	Control guide	NA	3, 3	-15.00	No
Supp. Fig. 10F		One-way ANOVA P value				0.0002	
		DMSO	danoprevir	NA	3, 3	718.0	No
		DMSO	grazoprevir	NA	3, 3	-1499	Yes
		DMSO	Control guide	NA	3, 3	358.3	No
Supp. Fig. 10G	GFP	One-way ANOVA P value				<0.0001	
		DMSO	10 μM danoprevir	NA	3, 3	4.949	Yes
		DMSO	1 μM grazoprevir	NA	3, 3	4.937	Yes
		DMSO	1 μM asunaprevir	NA	3, 3	5.105	Yes
		10 μM danoprevir	1 μM grazoprevir	NA	3, 3	-0.0118	No
		10 μM danoprevir	1 μM asunaprevir	NA	3, 3	0.1562	No
		1 μM grazoprevir	1 μM asunaprevir	NA	3, 3	0.1680	No
	CXCR4	One-way ANOVA P value				<0.0001	
		DMSO	10 μM danoprevir	NA	3, 3	0.06206	No
		DMSO	1 μM grazoprevir	NA	3, 3	-2.691	Yes
		DMSO	1 μM asunaprevir	NA	3, 3	0.03393	No
		10 μM danoprevir	1 μM grazoprevir	NA	3, 3	-2.753	Yes
		10 μM danoprevir	1 μM asunaprevir	NA	3, 3	-0.0281	No
		1 μM grazoprevir	1 μM asunaprevir	NA	3, 3	2.725	Yes
	CD95	One-way ANOVA P value				0.0003	
		DMSO	10 μM danoprevir	NA	3, 3	-5.006	Yes
		DMSO	1 μM grazoprevir	NA	3, 3	-0.6903	No
		DMSO	1 μM asunaprevir	NA	3, 3	-1.180	No
		10 μM danoprevir	1 μM grazoprevir	NA	3, 3	4.316	Yes
		10 μM danoprevir	1 μM asunaprevir	NA	3, 3	3.826	Yes
		1 μM grazoprevir	1 μM asunaprevir	NA	3, 3	-0.4897	No
Supp. Fig 11a		1600.0 nM		25	1		
		400.0 nM		28	1		
		100.0 nM		18	1		
		25.0 nM		20	1		

		6.3 nM	21	1		
		1.6 nM	20	1		
		0.4 nM	19	1		
		0.1 nM	19	1		
Supp. Fig 11b		1600.0 nM	25	1		
		400.0 nM	22	1		
		100.0 nM	23	1		
		25.0 nM	21	1		
		6.3 nM	26	1		
		1.6 nM	22	1		
		0.4 nM	19	1		
		0.1 nM	25	1		
Supp. Fig 11c		DMSO	15	1		
		100 nM danoprevir	15	1		
		100 nM danoprevir, 3.5 nM grazoprevir	15	1		
		100 nM danoprevir, 9.4 nM grazoprevir	15	1		
		100 nM danoprevir, 21 nM grazoprevir	14	1		
		100 nM danoprevir, 57 nM grazoprevir	18	1		
		57 nM grazoprevir	14	1		
Supp. Fig 11e		100 nM danoprevir	22	1		
		100 nM danoprevir, 3.5 nM grazoprevir	30	1		
		100 nM danoprevir, 9.4 nM grazoprevir	39	1		
		100 nM danoprevir, 21 nM grazoprevir	57	1		
		100 nM danoprevir, 57 nM grazoprevir	33	1		
		57 nM grazoprevir	30	1		

[a]P values from unpaired, two-sided t-test.

Supplementary Table 4 | Sequences of constructs and primers and usage in figures

Sequence ID	Plasmid ID	Description	Figures	Sequence (Reader/NS3a component in bold, fusions/tags/linkers in regular font)
NS3a_1	GWF020	Tagless NS3a/4a-solubility optimized-S139A (His-SMT3 removed by ULP1 cleavage) (*E. coli*)	Fig. 1D,E; Supp. Fig. 2C-F	MGHHHHHHHHHHGSLQDSEVNQEA KPEVKPEVKPETHINLKVSDGSSEIFF KIKKTTPLRRLMEAFAKRQGKEMDSL RFLYDGIRIQADQAPEDLDMEDNDIIE AHREQIGG**MKKKGSVVIVGRINLSG DTAYAQQTRGEEGCQETSQTGRDK NQVEGEVQIVSTATQTFLATSINGVL WTVYHGAGTRTIASPKGPVTQMYTN VDKDLVGWQAPQGSRSLTPCTCGS SDLYLVTRHADVIPVRRRGDSRGSL LSPRPISYLKGSAGGPLLCPAGHAV GIFRAAVSTRGVAKAVDFIPVESLET TMRSP**
DNCR2_1	GWF017	Tagless DNCR2 (His-SMT3 removed by ULP1 cleavage) (*E. coli*)	Fig. 1D,E; Supp. Fig. 2C-F	MGHHHHHHHHHHGSLQDSEVNQEA KPEVKPEVKPETHINLKVSDGSSEIFF KIKKTTPLRRLMEAFAKRQGKEMDSL RFLYDGIRIQADQAPEDLDMEDNDIIE AHREQIGG**SSDEEEARELIERAKEA AERAQEAAERTGDPRVRELARELK RLAQEAAEEVKRDPSSSDVNEALKL IVEAIEAAVDALEAAERTGDPEVREL ARELVRLAVEAAEEVQRNPSSSDVN EALHSIVYAIEAAIFALEAAERTGDPE VRELARELVRLAVEAAEEVQRNPSS RNVEHALMRIVLAIYLAEENLREAEE SGDPEKREKARERVREAVERAEEV QRDPSGWLNH**
NS3a_2	GWF016	Avi-His$_6$-NS3a/4a-solubility optimized S139A (*E. coli*)	Library sorting;	MAGGLNDIFEAQKIEWHEDTGGSSH HHHHHGSGSGS**MKKKGSVVIVGRIN LSGDTAYAQQTRGEEGCQETSQTG RDKNQVEGEVQIVSTATQTFLATSIN GVLWTVYHGAGTRTIASPKGPVTQM YTNVDKDLVGWQAPQGSRSLTPCT CGSSDLYLVTRHADVIPVRRRGDSR GSLLSPRPISYLKGSAGGPLLCPAG HAVGIFRAAVSTRGVAKAVDFIPVES LETTMRSP**
NS3a_3	GWF005	Avi-His$_6$-NS3a/4a-solubility optimized catalytically active (*E. coli*)	Fig. 1C; Fig. 2A; Supp. Fig. 2A,B; Supp. Fig. 3C; Supp. Table 1	MAGGLNDIFEAQKIEWHEDTGGSSH HHHHHGSGSGS**MKKKGSVVIVGRIN LSGDTAYAQQTRGEEGCQETSQTG RDKNQVEGEVQIVSTATQTFLATSIN GVLWTVYHGAGTRTIASPKGPVTQM YTNVDKDLVGWQAPQGSRSLTPCT CGSSDLYLVTRHADVIPVRRRGDSR GSLLSPRPISYLKGSSGGPLLCPAG HAVGIFRAAVSTRGVAKAVDFIPVES LETTMRSP**
G3	GWF041	Yeast surface display G3, C-terminal	Fig. 1A; Supp. Fig.	...KDNSSTIEGRYPYDVPDYALQASG GGGSGGGGSGGGGSASHM**DIEKLC KKAEEEAKEAQEKADELRQRHPDS**

		fusion to Aga2	3C; Supp. Table 1	**QAAEDAEDLANEAEAAVLAACSLA QEHPNADIAKLCIKAASEAAEAASK AAELAQRHPDSQAARDAIKLASQAA RAVILAIMLAAENPNADIAKLCIKAAS EAAEAASKAAELAQRHPDSQAARD AIKLASQAAEAVERAIWLAAENPNA DIAKKCIKAASEAAEEASKAAEEAQ RHPDSQKARDEIKEASQKAEEVKER CKS**LEGGGSEQKLISEEDL
GNCR1	GWF351	Yeast surface display GNCR1, C-terminal fusion to Aga2	Supp. Fig. 3C; Supp. Table 1	...KDNSSTIEGRYPYDVPDYALQASG GGGSGGGGSGGGGSASHM**DIEKLC KKAEEEAKEAQEKADELRQRHPDS QAAEDAEDLANLAVAAVLTACLLAQ EHPNADIAKLCIKAASEAAEAASKA AELAQRHPDSQAARDAIKLASQAAR AVILAIMLAAENPNADIAKLCIKAASE AAEAASKAAELAQRHPDSQAARDAI KLASQAAEAVERAIWLAAENPNADI AKKCIKAASEAAEEASKAAEEAQRH PDSQKARDEIKEASQKAEEVKERCK S**LEGGGSEQKLISEEDL
D5	GWF036	Yeast surface display D5, C-terminal fusion to Aga2	Fig. 1C; Supp. Fig. 2A	...KDNSSTIEGRYPYDVPDYALQASG GGGSGGGGSGGGGSASHM**SSDEE EARELIERAKEAAERAQEAAERTGD PRVRELARELKRLAQEAAEEVKRDP SSSDVNEALKLIVEAIEAAVDALEAA ERTGDPEVRELARELVRLAVEAAEE VQRNPSSSDVNEALLTIVIAIEAAVNA LEAAERTGDPEVRELARELVRLAVE AAEEVQRNPSSREVNIALWKIVLAIQ EAVESLREAEESGDPEKREKARERV REAVERAEEVQRDPSGWLNH**LEGG GSEQKLISEEDL
DNCR1	GWF040	Yeast surface display DNCR1, C-terminal fusion to Aga2	Supp. Fig. 2A	...KDNSSTIEGRYPYDVPDYALQASG GGGSGGGGSGGGGSASHM**SSDEE EARELIERAKEAAERAQEAAERTGD PRVRELARELKRLAQEAAEEVKRDP SSSDVNEALKLIVEAIEAAVDALEAA ERTGDPEVRELARELVRLAVEAAEE VQRNPSSSDVNEALLSIVIAIEAAVH ALEAAERTGDPEVRELARELVRLAV EAAEEVQRNPSSREVEHALMKIVLAI YEAEESLREAEESGDPEKREKARER VREAVERAEEVQRDPSGWLNH**LEG GGSEQKLISEEDL
DNCR2	GWF352	Yeast surface display DNCR2, C-terminal fusion to Aga2	Supp. Fig. 2A,B	...KDNSSTIEGRYPYDVPDYALQASG GGGSGGGGSGGGGSASHM**SSDEE EARELIERAKEAAERAQEAAERTGD PRVRELARELKRLAQEAAEEVKRDP SSSDVNEALKLIVEAIEAAVDALEAA ERTGDPEVRELARELVRLAVEAAEE VQRNPSSSDVNEALHSIVYAIEAAIF ALEAAERTGDPEVRELARELVRLAV EAAEEVQRNPSSRNVEHALMRIVLAI YLAEENLREAEESGDPEKREKARER**

				VREAVERAEEVQRDPSGWLNHLEG GGSEQKLISEEDL
DNCR2-EGFP	GWF122	(in pcDNA5/FRT/TO)	Fig. 2B; Supp. Fig. 4A; Supp. Fig. 7A,C	**MSSDEEEARELIERAKEAAERAQEA AERTGDPRVRELARELKRLAQEAAE EVKRDPSSSDVNEALKLIVEAIEAAV DALEAAERTGDPEVRELARELVRLA VEAAEEVQRNPSSSDVNEALHSIVY AIEAAIFALEAAERTGDPEVRELARE LVRLAVEAAEEVQRNPSSRNVEHAL MRIVLAIYLAEENLREAEESGDPEKR EKARERVREAVERAEEVQRDPSGW LNH**EQKLISEEDLGSGTGSGTMVSK GEELFTGVVPILVELDGDVNGHKFSV SGEGEGDATYGKLTLKFICTTGKLPV PWPTLVTTLTYGVQCFSRYPDHMKQ HDFFKSAMPEGYVQERTIFFKDDGN YKTRAEVKFEGDTLVNRIELKGIDFKE DGNILGHKLEYNYNSHNVYIMADKQK NGIKVNFKIRHNIEDGSVQLADHYQQ NTPIGDGPVLLPDNHYLSTQSALSKD PNEKRDHMVLLEFVTAAGITLGMDEL YK
Tom20-DNCR1-EGFP	GWF115	(in pcDNA5/FRT/TO)	Supp. Fig. 6B,D	MVGRNSAIAAGVCGALFIGYCIYFDR KRRSDPNF**SSDEEEARELIERAKEA AERAQEAAERTGDPRVRELARELK RLAQEAAEEVKRDPSSSDVNEALKL IVEAIEAAVDALEAAERTGDPEVREL ARELVRLAVEAAEEVQRNPSSSDVN EALLSIVIAIEAAVHALEAAERTGDPE VRELARELVRLAVEAAEEVQRNPSS REVEHALMKIVLAIYEAEESLREAEE SGDPEKREKARERVREAVERAEEV QRDPSGWLNH**EQKLISEEDLGSGTG SGTMVSKGEELFTGVVPILVELDGDV NGHKFSVSGEGEGDATYGKLTLKFIC TTGKLPVPWPTLVTTLTYGVQCFSRY PDHMKQHDFFKSAMPEGYVQERTIF FKDDGNYKTRAEVKFEGDTLVNRIEL KGIDFKEDGNILGHKLEYNYNSHNVYI MADKQKNGIKVNFKIRHNIEDGSVQL ADHYQQNTPIGDGPVLLPDNHYLST QSALSKDPNEKRDHMVLLEFVTAAGI TLGMDELYK
DNCR1-EGFP-Giantin	GWF114	(in pcDNA5/FRT/TO)	Supp. Fig. 6B,C	**MSSDEEEARELIERAKEAAERAQEA AERTGDPRVRELARELKRLAQEAAE EVKRDPSSSDVNEALKLIVEAIEAAV DALEAAERTGDPEVRELARELVRLA VEAAEEVQRNPSSSDVNEALLSIVIAI EAAVHALEAAERTGDPEVRELAREL VRLAVEAAEEVQRNPSSREVEHALM KIVLAIYEAEESLREAEESGDPEKRE KARERVREAVERAEEVQRDPSGWL NH**EQKLISEEDLGSGTGSGTMVSKG EELFTGVVPILVELDGDVNGHKFSVS GEGEGDATYGKLTLKFICTTGKLPVP WPTLVTTLTYGVQCFSRYPDHMKQH

				DFFKSAMPEGYVQERTIFFKDDGNY KTRAEVKFEGDTLVNRIELKGIDFKED GNILGHKLEYNYNSHNVYIMADKQKN GIKVNFKIRHNIEDGSVQLADHYQQN TPIGDGPVLLPDNHYLSTQSALSKDP NEKRDHMVLLEFVTAAGITLGMDELY KGSGTGSGSGEPQQSFSEAQQQLC NTRQEVNELRKLLEEERDQRVAAEN ALSVAEEQIRRLEHSEWDSSRTPIIGS CGTQEQALLIDLTSNSCRRTRSGVG WKRVLRSLCHSRTRVPLLAAIYFLMI HVLLILCFTGHL
3xNLS-DNCR1-EGFP	GWF111	(in pcDNA5/FRT/TO)	Supp. Fig. 6B	MDPKKKRKVDPKKKRKVDPKKKRKV **SSDEEEARELIERAKEAAERAQEAA ERTGDPRVRELARELKRLAQEAAEE VKRDPSSSDVNEALKLIVEAIEAAVD ALEAAERTGDPEVRELARELVRLAV EAAEEVQRNPSSSDVNEALLSIVIAIE AAVHALEAAERTGDPEVRELARELV RLAVEAAEEVQRNPSSREVEHALM KIVLAIYEAEESLREAEESGDPEKRE KARERVREAVERAEEVQRDPSGWL NH**EQKLISEEDLGSGTGSGTMVSKG EELFTGVVPILVELDGDVNGHKFSVS GEGEGDATYGKLTLKFICTTGKLPVP WPTLVTTLTYGVQCFSRYPDHMKQH DFFKSAMPEGYVQERTIFFKDDGNY KTRAEVKFEGDTLVNRIELKGIDFKED GNILGHKLEYNYNSHNVYIMADKQKN GIKVNFKIRHNIEDGSVQLADHYQQN TPIGDGPVLLPDNHYLSTQSALSKDP NEKRDHMVLLEFVTAAGITLGMDELY K
DNCR1-EGFP	GWF112	(in pcDNA5/FRT/TO)	Supp. Fig. 6A	**MSSDEEEARELIERAKEAAERAQEA AERTGDPRVRELARELKRLAQEAAE EVKRDPSSSDVNEALKLIVEAIEAAV DALEAAERTGDPEVRELARELVRLA VEAAEEVQRNPSSSDVNEALLSIVIAI EAAVHALEAAERTGDPEVRELAREL VRLAVEAAEEVQRNPSSREVEHALM KIVLAIYEAEESLREAEESGDPEKRE KARERVREAVERAEEVQRDPSGWL NH**EQKLISEEDLGSGTGSGTMVSKG EELFTGVVPILVELDGDVNGHKFSVS GEGEGDATYGKLTLKFICTTGKLPVP WPTLVTTLTYGVQCFSRYPDHMKQH DFFKSAMPEGYVQERTIFFKDDGNY KTRAEVKFEGDTLVNRIELKGIDFKED GNILGHKLEYNYNSHNVYIMADKQKN GIKVNFKIRHNIEDGSVQLADHYQQN TPIGDGPVLLPDNHYLSTQSALSKDP NEKRDHMVLLEFVTAAGITLGMDELY K
mCherry-NS3a	GWF104	NS3a solubility	Supp. Fig. 6B,C,D	MVSKGEEDNMAIIKEFMRFKVHMEG SVNGHEFEIEGEGEGRPYEGTQTAK LKVTKGGPLPFAWDILSPQFMYGSK

		optimized, S139A (in pcDNA5/FRT /TO)		AYVKHPADIPDYLKLSFPEGFKWERV MNFEDGGVVTVTQDSSLQDGEFIYK VKLRGTNFPSDGPVMQKKTMGWEA SSERMYPEDGALKGEIKQRLKLKDG GHYDAEVKTTYKAKKPVQLPGAYNV NIKLDITSHNEDYTIVEQYERAEGRHS TGGMDELYKGSGTGDYKDDDDK**KK KGSVVIVGRINLSGDTAYAQQTRGE EGCQETSQTGRDKNQVEGEVQIVST ATQTFLATSINGVLWTVYHGAGTRTI ASPKGPVTQMYTNVDKDLVGWQAP QGSRSLTPCTCGSSDLYLVTRHADV IPVRRRGDSRGSLLSPRPISYLKGSA GGPLLCPAGHAVGIFRAAVSTRGVA KAVDFIPVESLETTMRSP**
Tom20-mCherry-NS3a	GWF105	NS3a solubility optimized, S139A (in pcDNA5/FRT /TO)	Fig. 2B; Supp. Fig. 6A	MVGRNSAIAAGVCGALFIGYCIYFDR KRRSDPNFGSGMVSKGEEDNMAIIK EFMRFKVHMEGSVNGHEFEIEGEGE GRPYEGTQTAKLKVTKGGPLPFAWD ILSPQFMYGSKAYVKHPADIPDYLKL SFPEGFKWERVMNFEDGGVVTVTQ DSSLQDGEFIYKVKLRGTNFPSDGPV MQKKTMGWEASSERMYPEDGALKG EIKQRLKLKDGGHYDAEVKTTYKAKK PVQLPGAYNVNIKLDITSHNEDYTIVE QYERAEGRHSTGGMDELYKGSGTG DYKDDDDK**KKKGSVVIVGRINLSGD TAYAQQTRGEEGCQETSQTGRDKN QVEGEVQIVSTATQTFLATSINGVLW TVYHGAGTRTIASPKGPVTQMYTNV DKDLVGWQAPQGSRSLTPCTCGSS DLYLVTRHADVIPVRRRGDSRGSLL SPRPISYLKGSAGGPLLCPAGHAVGI FRAAVSTRGVAKAVDFIPVESLETTM RSP**
mCherry-NS3a-Giantin	GWF107	NS3a solubility optimized, S139A (in pcDNA5/FRT /TO)	Supp. Fig. 6A	MVSKGEEDNMAIIKEFMRFKVHMEG SVNGHEFEIEGEGEGRPYEGTQTAK LKVTKGGPLPFAWDILSPQFMYGSK AYVKHPADIPDYLKLSFPEGFKWERV MNFEDGGVVTVTQDSSLQDGEFIYK VKLRGTNFPSDGPVMQKKTMGWEA SSERMYPEDGALKGEIKQRLKLKDG GHYDAEVKTTYKAKKPVQLPGAYNV NIKLDITSHNEDYTIVEQYERAEGRHS TGGMDELYKGSGTGDYKDDDDK**KK KGSVVIVGRINLSGDTAYAQQTRGE EGCQETSQTGRDKNQVEGEVQIVST ATQTFLATSINGVLWTVYHGAGTRTI ASPKGPVTQMYTNVDKDLVGWQAP QGSRSLTPCTCGSSDLYLVTRHADV IPVRRRGDSRGSLLSPRPISYLKGSA GGPLLCPAGHAVGIFRAAVSTRGVA KAVDFIPVESLETTMRSP**GSGTGSG SGEPQQSFSEAQQQLCNTRQEVNEL RKLLEEERDQRVAAENALSVAEEQIR RLEHSEWDSSRTPIIGSCGTQEQALL

				IDLTSNSCRRTRSGVGWKRVLRSLC HSRTRVPLLAAIYFLMIHVLLILCFTGH L
3xNLS-mCherry-NS3a	GWF106	NS3a solubility optimized, S139A (in pcDNA5/FRT/TO)	Supp. Fig. 6A	MDPKKKRKVDPKKKRKVDPKKKRKV GSGMVSKGEEDNMAIIKEFMRFKVH MEGSVNGHEFEIEGEGEGRPYEGTQ TAKLKVTKGGPLPFAWDILSPQFMYG SKAYVKHPADIPDYLKLSFPEGFKWE RVMNFEDGGVVTVTQDSSLQDGEFI YKVKLRGTNFPSDGPVMQKKTMGW EASSERMYPEDGALKGEIKQRLKLKD GGHYDAEVKTTYKAKKPVQLPGAYN VNIKLDITSHNEDYTIVEQYERAEGRH STGGMDELYKGSGTGDYKDDDDK**K KKGSVVIVGRINLSGDTAYAQQTRG EEGCQETSQTGRDKNQVEGEVQIVS TATQTFLATSINGVLWTVYHGAGTR TIASPKGPVTQMYTNVDKDLVGWQA PQGSRSLTPCTCGSSDLYLVTRHAD VIPVRRRGDSRGSLLSPRPISYLKGS AGGPLLCPAGHAVGIFRAAVSTRGV AKAVDFIPVESLETTMRSP**
Myristoyl-tag-mCherry-NS3a	GWF100	NS3a solubility optimized, S139A (in pcDNA5/FRT/TO)	Supp. Fig. 4A; Supp. Fig. 6A; Supp. Fig. 4B	MGCGCSSHPEDDGSGTGSGMVSKG EEDNMAIIKEFMRFKVHMEGSVNGH EFEIEGEGEGRPYEGTQTAKLKVTKG GPLPFAWDILSPQFMYGSKAYVKHP ADIPDYLKLSFPEGFKWERVMNFED GGVVTVTQDSSLQDGEFIYKVKLRGT NFPSDGPVMQKKTMGWEASSERMY PEDGALKGEIKQRLKLKDGGHYDAE VKTTYKAKKPVQLPGAYNVNIKLDITS HNEDYTIVEQYERAEGRHSTGGMDE LYKGSGTGDYKDDDDK**KKKGSVVIV GRINLSGDTAYAQQTRGEEGCQETS QTGRDKNQVEGEVQIVSTATQTFLA TSINGVLWTVYHGAGTRTIASPKGPV TQMYTNVDKDLVGWQAPQGSRSLT PCTCGSSDLYLVTRHADVIPVRRRG DSRGSLLSPRPISYLKGSAGGPLLC PAGHAVGIFRAAVSTRGVAKAVDFIP VESLETTMRSP**
NS3aH1-mCherry	GWF094	ANR-binding-competent NS3a, catalytically active (in pcDNA5/FRT/TO)	Fig. 2C,D; Supp. Fig. 5	**MKKKGSVVIVGRINLSGDTAYSQQT RGLEGCQETSQTGRDKNQVEGEVQ VVSTATQSFLATSINGVLWTVYHGA GTRTIASPKGPVTQMYTNVDKDLVG WQAPQGSRSLTPCTCGSSDLYLVT RHADVIPVRRRGDSRGSLLSPRPISY LKGSSGGPLLCPAGHAVGIFRAAVS TRGVAKAVDFIPVESLETTMRSP**GS GTGSGMVSKGEEDNMAIIKEFMRFK VHMEGSVNGHEFEIEGEGEGRPYEG TQTAKLKVTKGGPLPFAWDILSPQFM YGSKAYVKHPADIPDYLKLSFPEGFK WERVMNFEDGGVVTVTQDSSLQDG EFIYKVKLRGTNFPSDGPVMQKKTM GWEASSERMYPEDGALKGEIKQRLK

				LKDGGHYDAEVKTTYKAKKPVQLPG AYNVNIKLDITSHNEDYTIVEQYERAE GRHSTGGMDELYKGSGTGDYKDDD DK
3xNLS-DNCR2-EGFP	GWF124	(in pcDNA5/FRT/TO)	Fig. 2D; Supp. Fig. 5B	MDPKKKRKVDPKKKRKVDPKKKRKV GSG**SSDEEEARELIERAKEAAERAQ** **EAAERTGDPRVRELARELKRLAQEA** **AEEVKRDPSSSDVNEALKLIVEAIEA** **AVDALEAAERTGDPEVRELARELVR** **LAVEAAEEVQRNPSSSDVNEALHSI** **VYAIEAAIFALEAAERTGDPEVRELA** **RELVRLAVEAAEEVQRNPSSRNVEH** **ALMRIVLAIYLAEENLREAEESGDPE** **KREKARERVREAVERAEEVQRDPS** **GWLNH**EQKLISEEDLGSGTGSGTMV SKGEELFTGVVPILVELDGDVNGHKF SVSGEGEGDATYGKLTLKFICTTGKL PVPWPTLVTTLTYGVQCFSRYPDHM KQHDFFKSAMPEGYVQERTIFFKDD GNYKTRAEVKFEGDTLVNRIELKGID FKEDGNILGHKLEYNYNSHNVYIMAD KQKNGIKVNFKIRHNIEDGSVQLADH YQQNTPIGDGPVLLPDNHYLSTQSAL SKDPNEKRDHMVLLEFVTAAGITLGM DELYK
ANR-ANR-BFP-CAAX	GWF135	(in pcDNA5/FRT/TO)	Fig. 2D; Supp. Fig. 5B	M**GELDELVYLLDGPGYDPIHSD**GSG TGSGTGSGTGTTSGTGTGGSTG**GE** **LDELVYLLDGPGYDPIHSD**GSGTGS GTGSGTGTTSGTGTGGSTGEQKLIS EEDLGSGSSELIKENMHMKLYMEGT VDNHHFKCTSEGEGKPYEGTQTMRI KVVEGGPLPFAFDILATSFLYGSKTFI NHTQGIPDFFKQSFPEGFTWERVTT YEDGGVLTATQDTSLQDGCLIYNVKI RGVNFTSNGPVMQKKTLGWEAFTET LYPADGGLEGRNDMALKLVGGSHLI ANIKTTYRSKKPAKNLKMPGVYYVDY RLERIKEANNETYVEQHEVAVARYCD LPSKLGHKLNRKHKEKMSKDGKKKK KKSKTKCVIM
Tom20-BFP-ANR-ANR-P2a-DNCR2-EGFP-CAAX	GWF143	(in pcDNA5/FRT/TO)	Supp. Fig. 7B,D	MVGRNSAIAAGVCGALFIGYCIYFDR KRRSDPNFMSELIKENMHMKLYMEG TVDNHHFKCTSEGEGKPYEGTQTMR IKVVEGGPLPFAFDILATSFLYGSKTFI NHTQGIPDFFKQSFPEGFTWERVTT YEDGGVLTATQDTSLQDGCLIYNVKI RGVNFTSNGPVMQKKTLGWEAFTET LYPADGGLEGRNDMALKLVGGSHLI ANIKTTYRSKKPAKNLKMPGVYYVDY RLERIKEANNETYVEQHEVAVARYCD LPSKLGHKLNSGSGEQKLISEEDLGS GTGSGTGSGTGTTSGTGTGGSTG**G** **ELDELVYLLDGPGYDPIHSD**GSGTG SGTGSGTGTTSGTGTGGSTG**GELD** **ELVYLLDGPGYDPIHSD**GSGATNFSL LKQAGDVEENPGPM**SSDEEEARELI**

				ERAKEAAERAQEAAERTGDPRVRE LARELKRLAQEAAEEVKRDPSSSDV NEALKLIVEAIEAAVDALEAAERTGD PEVRELARELVRLAVEAAEEVQRNP SSSDVNEALHSIVYAIEAAIFALEAAE RTGDPEVRELARELVRLAVEAAEEV QRNPSSRNVEHALMRIVLAIYLAEEN LREAEESGDPEKREKARERVREAVE RAEEVQRDPSGWLNHEQKLISEEDL GSGTGSGTMVSKGEELFTGVVPILVE LDGDVNGHKFSVSGEGEGDATYGKL TLKFICTTGKLPVPWPTLVTTLTYGV QCFSRYPDHMKQHDFFKSAMPEGY VQERTIFFKDDGNYKTRAEVKFEGDT LVNRIELKGIDFKEDGNILGHKLEYNY NSHNVYIMADKQKNGIKVNFKIRHNIE DGSVQLADHYQQNTPIGDGPVLLPD NHYLSTQSALSKDPNEKRDHMVLLE FVTAAGITLGMDELYKRKHKEKMSKD GKKKKKKSKTKCVIM
Tom20-DNCR2-EGFP	GWF125	(in pcDNA5/FRT/TO)	Fig. 2C; Supp. Fig. 5A	MVGRNSAIAAGVCGALFIGYCIYFDR KRRSDPNF**SSDEEEARELIERAKEA AERAQEAAERTGDPRVRELARELK RLAQEAAEEVKRDPSSSDVNEALKL IVEAIEAAVDALEAAERTGDPEVREL ARELVRLAVEAAEEVQRNPSSSDVN EALHSIVYAIEAAIFALEAAERTGDPE VRELARELVRLAVEAAEEVQRNPSS RNVEHALMRIVLAIYLAEENLREAEE SGDPEKREKARERVREAVERAEEV QRDPSGWLNH**EQKLISEEDLGSGTG SGTMVSKGEELFTGVVPILVELDGDV NGHKFSVSGEGEGDATYGKLTLKFIC TTGKLPVPWPTLVTTLTYGVQCFSRY PDHMKQHDFFKSAMPEGYVQERTIF FKDDGNYKTRAEVKFEGDTLVNRIEL KGIDFKEDGNILGHKLEYNYNSHNVYI MADKQKNGIKVNFKIRHNIEDGSVQL ADHYQQNTPIGDGPVLLPDNHYLST QSALSKDPNEKRDHMVLLEFVTAAGI TLGMDELYK
GNCR1-BFP-CAAX	GWF148	(in pcDNA5/FRT/TO)	Fig. 2C; Supp. Fig. 5A	**MDIEKLCKKAEEEAKEAQEKADELR QRHPDSQAAEDAEDLANLAVAAVL TACLLAQEHPNADIAKLCIKAASEAA EAASKAAELAQRHPDSQAARDAIKL ASQAARAVILAIMLAAENPNADIAKL CIKAASEAAEAASKAAELAQRHPDS QAARDAIKLASQAAEAVERAIWLAA ENPNADIAKKCIKAASEAAEEASKA AEEAQRHPDSQKARDEIKEASQKAE EVKERCKS**EQKLISEEDLGSGSSELI KENMHMKLYMEGTVDNHHFKCTSE GEGKPYEGTQTMRIKVVEGGPLPFA FDILATSFLYGSKTFINHTQGIPDFFK QSFPEGFTWERVTTYEDGGVLTATQ DTSLQDGCLIYNVKIRGVNFTSNGPV

				MQKKTLGWEAFTETLYPADGGLEGR NDMALKLVGGSHLIANIKTTYRSKKP AKNLKMPGVYYVDYRLERIKEANNET YVEQHEVAVARYCDLPSKLGHKLNR KHKEKMSKDGKKKKKKSKTKCVIM
NS3aH1-mCherry-CAAX	GWF096	ANR-binding-competent NS3a, catalytically active (in pcDNA5/FRT/TO)	Supp. Fig. 7A,C	**MKKKGSVVIVGRINLSGDTAYSQQT RGLEGCQETSQTGRDKNQVEGEVQ VVSTATQSFLATSINGVLWTVYHGA GTRTIASPKGPVTQMYTNVDKDLVG WQAPQGSRSLTPCTCGSSDLYLVT RHADVIPVRRRGDSRGSLLSPRPISY LKGSSGGPLLCPAGHAVGIFRAAVS TRGVAKAVDFIPVESLETTMRSP**GS GTGSGMVSKGEEDNMAIIKEFMRFK VHMEGSVNGHEFEIEGEGEGRPYEG TQTAKLKVTKGGPLPFAWDILSPQFM YGSKAYVKHPADIPDYLKLSFPEGFK WERVMNFEDGGVVTVTQDSSLQDG EFIYKVKLRGTNFPSDGPVMQKKTM GWEASSERMYPEDGALKGEIKQRLK LKDGGHYDAEVKTTYKAKKPVQLPG AYNVNIKLDITSHNEDYTIVEQYERAE GRHSTGGMDELYKGSGTGDYKDDD DKQHKLRKLNPPDESGPGCMSCKC VLS
GNCR1-BFP	GWF146	(in pcDNA5/FRT/TO)	Supp. Fig. 7A,C	**MDIEKLCKKAEEEAKEAQEKADELR QRHPDSQAAEDAEDLANLAVAAVL TACLLAQEHPNADIAKLCIKAASEAA EAASKAAELAQRHPDSQAARDAIKL ASQAARAVILAIMLAAENPNADIAKL CIKAASEAAEAASKAAELAQRHPDS QAARDAIKLASQAAEAVERAIWLAA ENPNADIAKKCIKAASEAAEEASKA AEEAQRHPDSQKARDEIKEASQKAE EVKERCKS**EQKLISEEDLGSGSSELI KENMHMKLYMEGTVDNHHFKCTSE GEGKPYEGTQTMRIKVVEGGPLPFA FDILATSFLYGSKTFINHTQGIPDFFK QSFPEGFTWERVTTYEDGGVLTATQ DTSLQDGCLIYNVKIRGVNFTSNGPV MQKKTLGWEAFTETLYPADGGLEGR NDMALKLVGGSHLIANIKTTYRSKKP AKNLKMPGVYYVDYRLERIKEANNET YVEQHEVAVARYCDLPSKLGHKLN
DNCR2-iSH2	GWF129	Inter-SH2 domain of human PIP3K fused to C-term of DNCR2 (in pcDNA5/FRT/TO)	Supp. Fig. 4B	**MSSDEEEARELIERAKEAAERAQEA AERTGDPRVRELARELKRLAQEAAE EVKRDPSSSDVNEALKLIVEAIEAAV DALEAAERTGDPEVRELARELVRLA VEAAEEVQRNPSSSDVNEALHSIVY AIEAAIFALEAAERTGDPEVRELARE LVRLAVEAAEEVQRNPSSRNVEHAL MRIVLAIYLAEENLREAEESGDPEKR EKARERVREAVERAEEVQRDPSGW LNH**EQKLISEEDLGSGTGSGTRLLYP VSKYQQDQIVKEDSVEAVGAQLKVY HQQYQDKSREYDQLYEEYTRTSQEL

				QMKRTAIEAFNETIKIFEEQGQTQEK CSKEYLERFRREGNEKEMQRILLNSE RLKSRIAEIHESRTKLEQQLRAQASD NREIDKRMNSLKPDLMQLRKIRDQYL VWLTQKGARQKKINEWLGIKNETED QYALMEDEDDLP
DNCR2-VPR	GWF180	In pB-CAG-DNCR2-VPR-IRES-Puro-WPRE-SV40PA-PGK-NS3aH1-tagBFP-SpdCas9	Fig. 2A,B,C; Supp. Fig. 10A,C	**MSSDEEEARELIERAKEAAERAQEA AERTGDPRVRELARELKRLAQEAAE EVKRDPSSSDVNEALKLIVEAIEAAV DALEAAERTGDPEVRELARELVRLA VEAAEEVQRNPSSSDVNEALHSIVY AIEAAIFALEAAERTGDPEVRELARE LVRLAVEAAEEVQRNPSSRNVEHAL MRIVLAIYLAEENLREAEESGDPEKR EKARERVREAVERAEEVQRDPSGW LNH**EQKLISEEDLEFSSAAGTSDALD DFDLDMLGSDALDDFDLDMLGSDAL DDFDLDMLGSDALDDFDLDMLGSPK KKRKVGSQYLPDTDDRHRIEEKRKR TYETFKSIMKKSPFSGPTDPRPPPRR IAVPSRSSASVPKPAPQPYPFTSSLS TINYDEFPTMVFPSGQISQASALAPA PPQVLPQAPAPAPAPAMVSALAQAP APVPVLAPGPPQAVAPPAPKPTQAG EGTLSEALLQLQFDDEDLGALLGNST DPAVFTDLASVDNSEFQQLLNQGIPV APHTTEPMLMEYPEAITRLVTGAQRP PDPAPAPLGAPGLPNGLLSGDEDFS SIADMDFSALLSQISSGSGSGSRDSR EGMFLPKPEAGSAISDVFEGREVCQ PKRIRPFHPPGSPWANRPLPASLAPT PTGPVHEPVGSLTPAPVPQPLDPAP AVTPEASHLLEDPDEETSQAVKALRE MADTVIPQKEEAAICGQMDLSHPPPR GHLDELTTTLESMTEDLNLDSPLTPE LNEILDTFLNDECLLHAMHISTGLSIFD TSLF
DNCR2-KRAB	GWF181	In pB-CAG-DNCR2-KRAB-IRES-Puro-WPRE-SV40PA-PGK-NS3aH1-tagBFP-SpdCas9	Supp. Fig. 10B,D	**MSSDEEEARELIERAKEAAERAQEA AERTGDPRVRELARELKRLAQEAAE EVKRDPSSSDVNEALKLIVEAIEAAV DALEAAERTGDPEVRELARELVRLA VEAAEEVQRNPSSSDVNEALHSIVY AIEAAIFALEAAERTGDPEVRELARE LVRLAVEAAEEVQRNPSSRNVEHAL MRIVLAIYLAEENLREAEESGDPEKR EKARERVREAVERAEEVQRDPSGW LNH**EQKLISEEDLEFSSAAGTSGGG GGMDAKSLTAWSRTLVTFKDVFVDF TREEWKLLDTAQQIVYRNVMLENYK NLVSLGYQLTKPDVILRLEKGEEP
NS3aH1-tagBFP-SpdCas9	GWF180,181	ANR-binding-competent NS3a, catalytically active,	Fig. 2A,B,C; Supp. Fig. 10A-D	**MKKKGSVVIVGRINLSGDTAYSQQT RGLEGCQETSQTGRDKNQVEGEVQ VVSTATQSFLATSINGVLWTVYHGA GTRTIASPKGPVTQMYTNVDKDLVG WQAPQGSRSLTPCTCGSSDLYLVT RHADVIPVRRRGDSRGSLLSPRPISY**

		In pB-CAG-DNCR2-VPR/KRAB-IRES-Puro-WPRE-SV40PA-PGK-NS3aH1-tagBFP-SpdCas9		**LKGSSGGPLLCPAGHAVGIFRAAVS** **TRGVAKAVDFIPVESLETTMRSP**HM SSAAGATMSELIKENMHMKLYMEGT VDNHHFKCTSEGEGKPYEGTQTMRI KVVEGGPLPFAFDILATSFLYGSKTFI NHTQGIPDFFKQSFPEGFTWERVTT YEDGGVLTATQDTSLQDGCLIYNVKI RGVNFTSNGPVMQKKTLGWEAFTET LYPADGGLEGRNDMALKLVGGSHLI ANIKTTYRSKKPAKNLKMPGVYYVDY RLERIKEANNETYVEQHEVAVARYCD LPSKLGHKLNSSAAGATMDKKYSIGL AIGTNSVGWAVITDEYKVPSKKFKVL GNTDRHSIKKNLIGALLFDSGETAEAT RLKRTARRRYTRRKNRICYLQEIFSN EMAKVDDSFFHRLEESFLVEEDKKH ERHPIFGNIVDEVAYHEKYPTIYHLRK KLVDSTDKADLRLIYLALAHMIKFRGH FLIEGDLNPDNSDVDKLFIQLVQTYN QLFEENPINASGVDAKAILSARLSKSR RLENLIAQLPGEKKNGLFGNLIALSLG LTPNFKSNFDLAEDAKLQLSKDTYDD DLDNLLAQIGDQYADLFLAAKNLSDAI LLSDILRVNTEITKAPLSASMIKRYDE HHQDLTLLKALVRQQLPEKYKEIFFD QSKNGYAGYIDGGASQEEFYKFIKPI LEKMDGTEELLVKLNREDLLRKQRTF DNGSIPHQIHLGELHAILRRQEDFYPF LKDNREKIEKILTFRIPYYVGPLARGN SRFAWMTRKSEETITPWNFEEVVDK GASAQSFIERMTNFDKNLPNEKVLPK HSLLYEYFTVYNELTKVKYVTEGMRK PAFLSGEQKKAIVDLLFKTNRKVTVK QLKEDYFKKIECFDSVEISGVEDRFN ASLGTYHDLLKIIKDKDFLDNEENEDI LEDIVLTLTLFEDREMIEERLKTYAHL FDDKVMKQLKRRRYTGWGRLSRKLI NGIRDKQSGKTILDFLKSDGFANRNF MQLIHDDSLTFKEDIQKAQVSGQGDS LHEHIANLAGSPAIKKGILQTVKVVDE LVKVMGRHKPENIVIEMARENQTTQK GQKNSRERMKRIEEGIKELGSQILKE HPVENTQLQNEKLYLYYLQNGRDMY VDQELDINRLSDYDVDAIVPQSFLKD DSIDNKVLTRSDKNRGKSDNVPSEE VVKKMKNYWRQLLNAKLITQRKFDN LTKAERGGLSELDKAGFIKRQLVETR QITKHVAQILDSRMNTKYDENDKLIRE VKVITLKSKLVSDFRKDFQFYKVREIN NYHHAHDAYLNAVVGTALIKKYPKLE SEFVYGDYKVYDVRKMIAKSEQEIGK ATAKYFFYSNIMNFFKTEITLANGEIR KRPLIETNGETGEIVWDKGRDFATVR KVLSMPQVNIVKKTEVQTGGFSKESI LPKRNSDKLIARKKDWDPKKYGGFD SPTVAYSVLVVAKVEKGKSKKLKSVK

				ELLGITIMERSSFEKNPIDFLEAKGYK EVKKDLIIKLPKYSLFELENGRKRMLA SAGELQKGNELALPSKYVNFLYLASH YEKLKGSPEDNEQKQLFVEQHKHYL DEIIEQISEFSKRVILADANLDKVLSAY NKHRDKPIREQAENIIHLFTLTNLGAP AAFKYFDTTIDRKRYTSTKEVLDATLI HQSITGLYETRIDLSQLGGDAYPYDV PDYASLGSGSPKKKRKVEDPKKKRK VDGIGSGSNG
CXCR4-C1	GWF271	C1 guide in gRNA_Cloning Vector	Fig. 2A,B; Supp. Fig. 10A,B	GCGGGTGGTCGGTAGTGAGTC
CXCR4-C2	GWF272	C2 guide in gRNA_Cloning Vector	Fig. 2A,B; Supp. Fig. 10A,B	GCAGACGCGAGGAAGGAGGGCGC
CXCR4-C3	GWF273	C3 guide in gRNA_Cloning Vector	Fig. 2A,B; Supp. Fig. 10A,B	GCCTCTGGGAGGTCCTGTCCGGCTC
CD95-1	GWF279	CD95-1 guide in gRNA_Cloning Vector	Fig. 2C; Supp. Fig. 10C,D	GTACAGCAGAAGCCTTTAGAA
CD95-2	GWF280	CD95-2 guide in gRNA_Cloning Vector	Fig. 2C; Supp. Fig. 10C,D	GTGGCATGCTCACTTCAGGTG
CD95-3	GWF281	CD95-3 guide in gRNA_Cloning Vector	Fig. 2C; Supp. Fig. 10C,D	GAAGCCTCGCTGGGGAACGCC
CXCR4-C1-2xMS2	GWF310	scRNA, wt + f6 MS2 expressed with NLS-MCP-GNCR1-P2a-BFP	Fig. 2D,E,F; Supp. Fig. 8B,C,D	**GCGGGTGGTCGGTAGTGAGTC**GTT TAAGAGCTATGCTGGAAACAGCATA GCAAGTTTAAATAAGGCTAGTCCGT TATCAACTTGAAAAAGTGGCACCGA GTCGGTGCGGGAGCACATGAGGAT CACCCATGTGCGACTCCCACAGTC ACTGGGGAGTCTTCCCTTTTTTTGT TTTTTATGTCT
CXCR4-C2-2xMS2	GWF311	scRNA, 2x wt MS2 expressed with NLS-MCP-GNCR1-P2a-BFP	Fig. 2D,E,F; Supp. Fig. 8B,C,D	**GCAGACGCGAGGAAGGAGGGCGC** GTTTAAGAGCTATGCTGGAAACAGC ATAGCAAGTTTAAATAAGGCTAGTC CGTTATCAACTTGAAAAAGTGGCAC CGAGTCGGTGCGGGAGCACATGAG GATCACCCATGTGCCACGAGCGAC ATGAGGATCACCCATGTCGCTCGT GTTCCCTTTTTTTGTTTTTTATGTCT
CXCR4-C3-2xMS2	GWF312	scRNA, wt + f6 expressed with NLS-MCP-	Fig. 2D,E,F; Supp. Fig. 8B,C,D	**GCCTCTGGGAGGTCCTGTCCGGCT C**GTTTAAGAGCTATGCTGGAAACAG CATAGCAAGTTTAAATAAGGCTAGT CCGTTATCAACTTGAAAAAGTGGCA CCGAGTCGGTGCGGGAGCACATGA

		GNCR1-P2a-BFP		GGATCACCCATGTGCGACTCCCAC AGTCACTGGGGAGTCTTCCCTTTTT TTGTTTTTTATGTCT
NLS-MCP-GNCR1-P2a-BFP	GWF310-2	Expressed with CXCR4-2xMS2 scRNAs	Fig. 2D,E,F; Supp. Fig. 8B,C,D	MPKKKRKVGSMASNFTQFVLVDNG GTGDVTVAPSNFANGIAEWISSNSRS QAYKVTCSVRQSSAQNRKYTIKVEV PKGAWRSYLNMELTIPIFATNSDCELI VKAMQGLLKDGNPIPSAIAANSGIYG SGGSG**DIEKLCKKAEEEAKEAQEKA DELRQRHPDSQAAEDAEDLANLAV AAVLTACLLAQEHPNADIAKLCIKAA SEAAEAASKAAELAQRHPDSQAAR DAIKLASQAARAVILAIMLAAENPNA DIAKLCIKAASEAAEAASKAAELAQ RHPDSQAARDAIKLASQAAEAVERA IWLAAENPNADIAKKCIKAASEAAEE ASKAAEEAQRHPDSQKARDEIKEAS QKAEEVKERCKS**EQKLISEEDLGSG ATNFSLLKQAGDVEENPGPSELIKEN MHMKLYMEGTVDNHHFKCTSEGEG KPYEGTQTMRIKVVEGGPLPFAFDIL ATSFLYGSKTFINHTQGIPDFFKQSFP EGFTWERVTTYEDGGVLTATQDTSL QDGCLIYNVKIRGVNFTSNGPVMQK KTLGWEAFTETLYPADGGLEGRNDM ALKLVGGSHLIANIKTTYRSKKPAKNL KMPGVYYVDYRLERIKEANNETYVE QHEVAVARYCDLPSKLGHKLN
CXCR4-C1-com	GWF313	scRNA expressed with NLS-com-GNCR1-P2a-BFP	Supp. Fig. 10G	**GCGGGTGGTCGGTAGTGAGTC**GTT TAAGAGCTATGCTGGAAACAGCATA GCAAGTTTAAATAAGGCTAGTCCGT TATCAACTTGAAAAAGTGGCACCGA GTCGGTGCCTGAATGCCTGCGAGC ATCTTTTTTTGTTTTTTATGTCT
CXCR4-C2-com	GWF314	scRNA expressed with NLS-com-GNCR1-P2a-BFP	Supp. Fig. 10G	**GCAGACGCGAGGAAGGAGGGCGC** GTTTAAGAGCTATGCTGGAAACAGC ATAGCAAGTTTAAATAAGGCTAGTC CGTTATCAACTTGAAAAAGTGGCAC CGAGTCGGTGCCTGAATGCCTGCG AGCATCTTTTTTTGTTTTTTATGTCT
CXCR4-C3-com	GWF315	scRNA expressed with NLS-com-GNCR1-P2a-BFP	Supp. Fig. 10G	**GCCTCTGGGAGGTCCTGTCCGGCT C**GTTTAAGAGCTATGCTGGAAACAG CATAGCAAGTTTAAATAAGGCTAGT CCGTTATCAACTTGAAAAAGTGGCA CCGAGTCGGTGCCTGAATGCCTGC GAGCATCTTTTTTTGTTTTTTATGTC T
NLS-com-GNCR1-P2a-BFP	GWF313-5	Expressed with CXCR4-com scRNAs	Supp. Fig. 10G	MPKKKRKVGSMKSIRCKNCNKLLFK ADSFDHIEIRCPRCKRHIIMLNACEHP TEKHCGKREKITHSDETVRYGSGSG SG**DIEKLCKKAEEEAKEAQEKADEL RQRHPDSQAAEDAEDLANLAVAAV LTACLLAQEHPNADIAKLCIKAASEA AEAASKAAELAQRHPDSQAARDAIK LASQAARAVILAIMLAAENPNADIAK LCIKAASEAAEAASKAAELAQRHPD**

				SQAARDAIKLASQAAEAVERAIWLA AENPNADIAKKCIKAASEAAEEASK AAEEAQRHPDSQKARDEIKEASQK AEEVKERCKSEQKLISEEDLGSGAT NFSLLKQAGDVEENPGPSELIKENMH MKLYMEGTVDNHHFKCTSEGEGKPY EGTQTMRIKVVEGGPLPFAFDILATS FLYGSKTFINHTQGIPDFFKQSFPEG FTWERVTTYEDGGVLTATQDTSLQD GCLIYNVKIRGVNFTSNGPVMQKKTL GWEAFTETLYPADGGLEGRNDMALK LVGGSHLIANIKTTYRSKKPAKNLKM PGVYYVDYRLERIKEANNETYVEQHE VAVARYCDLPSKLGHKLN
CD95-1-2xPP7	GWF303	scRNA expressed with NLS-PCP-DNCR2-P2a-BFP	Supp. Fig. 10G	**GTACAGCAGAAGCCTTTAGAA**GTT TAAGAGCTATGCTGGAAACAGCATA GCAAGTTTAAATAAGGCTAGTCCGT TATCAACTTGAAAAAGTGGCACCGA GTCGGTGCGGGAGCTAAGGAGTTT ATATGGAAACCCTTAGCCTGCTGC GTAAGGAGTTTATATGGAAACCCTT ACGCAGCAGTTCCCTTTTTTTGTTT TTTATGTCT
CD95-2-2xPP7	GWF304	scRNA expressed with NLS-PCP-DNCR2-P2a-BFP	Supp. Fig. 10G	**GTGGCATGCTCACTTCAGGTG**GTT TAAGAGCTATGCTGGAAACAGCATA GCAAGTTTAAATAAGGCTAGTCCGT TATCAACTTGAAAAAGTGGCACCGA GTCGGTGCGGGAGCTAAGGAGTTT ATATGGAAACCCTTAGCCTGCTGC GTAAGGAGTTTATATGGAAACCCTT ACGCAGCAGTTCCCTTTTTTTGTTT TTTATGTCT
CD95-3-2xPP7	GWF305	scRNA expressed with NLS-PCP-DNCR2-P2a-BFP	Supp. Fig. 10G	**GAAGCCTCGCTGGGGAACGCC**GT TTAAGAGCTATGCTGGAAACAGCAT AGCAAGTTTAAATAAGGCTAGTCCG TTATCAACTTGAAAAAGTGGCACCG AGTCGGTGCGGGAGCTAAGGAGTT TATATGGAAACCCTTAGCCTGCTGC GTAAGGAGTTTATATGGAAACCCTT ACGCAGCAGTTCCCTTTTTTTGTTT TTTATGTCT
TRE3G-2xPP7	GWF306	scRNA expressed with NLS-PCP-DNCR2-P2a-BFP	Fig. 2D,E,F; Supp. Fig. 8B,C,D	**GTACGTTCTCTATCACTGATA**GTTT AAGAGCTATGCTGGAAACAGCATA GCAAGTTTAAATAAGGCTAGTCCGT TATCAACTTGAAAAAGTGGCACCGA GTCGGTGCGGGAGCTAAGGAGTTT ATATGGAAACCCTTAGCCTGCTGC GTAAGGAGTTTATATGGAAACCCTT ACGCAGCAGTTCCCTTTTTTTGTTT TTTATGTCT
NLS-PCP-DNCR2-P2a-BFP	GWF303-6	Expressed with TRE3G-2xPP7 or CD95-2xPP7 scRNAs	Fig. 2D,E,F; Supp. Fig. 8B,C,D; Supp. Fig. 10G	MPKKKRKVGSMSKTIVLSVGEATRTL TEIQSTADRQIFEEKVGPLVGRLRLTA SLRQNGAKTAYRVNLKLDQADVVDS GLPKVRYTQVWSHDVTIVANSTEAS RKSLYDLTKSLVATSQVEDLVVNLVP LGRGSGSG**SSDEEEARELIERAKEA**

				AERAQEAAERTGDPRVRELARELK RLAQEAAEEVKRDPSSSDVNEALKL IVEAIEAAVDALEAAERTGDPEVREL ARELVRLAVEAAEEVQRNPSSSDVN EALHSIVYAIEAAIFALEAAERTGDPE VRELARELVRLAVEAAEEVQRNPSS RNVEHALMRIVLAIYLAEENLREAEE SGDPEKREKARERVREAVERAEEV QRDPSGWLNHEQKLISEEDLGSGAT NFSLLKQAGDVEENPGPSELIKENMH MKLYMEGTVDNHHFKCTSEGEGKPY EGTQTMRIKVVEGGPLPFAFDILATS FLYGSKTFINHTQGIPDFFKQSFPEG FTWERVTTYEDGGVLTATQDTSLQD GCLIYNVKIRGVNFTSNGPVMQKKTL GWEAFTETLYPADGGLEGRNDMALK LVGGSHLIANIKTTYRSKKPAKNLKM PGVYYVDYRLERIKEANNETYVEQHE VAVARYCDLPSKLGHKLN
TRE3G-2xMS2	GWF297	scRNA, wt+f6 MS2 expressed with NLS-MCP-ANR-ANR-P2a-BFP	Supp. Fig. 10G	**GTACGTTCTCTATCACTGATA**GTTT AAGAGCTATGCTGGAAACAGCATA GCAAGTTTAAATAAGGCTAGTCCGT TATCAACTTGAAAAAGTGGCACCGA GTCGGTGCGGGAGCACATGAGGAT CACCCATGTGCGACTCCCACAGTC ACTGGGGAGTCTTCCCTTTTTTTGT TTTTTATGTCT
NLS-MCP-ANR-ANR-P2a-BFP	GWF297	Expressed with TRE3G-2xMS2	Supp. Fig. 10G	MPKKKRKVGSMASNFTQFVLVDNG GTGDVTVAPSNFANGIAEWISSNSRS QAYKVTCSVRQSSAQNRKYTIKVEV PKGAWRSYLNMELTIPIFATNSDCELI VKAMQGLLKDGNPIPSAIAANSGIYG SGGSGTGSGTGSGTGTTSGTGTGG STG**GELDELVYLLDGPGYDPIHSD**G SGTGSGTGSGTGTTSGTGTGGSTG **GELDELVYLLDGPGYDPIHSD**GSGA TNFSLLKQAGDVEENPGPSELIKENM HMKLYMEGTVDNHHFKCTSEGEGK PYEGTQTMRIKVVEGGPLPFAFDILA TSFLYGSKTFINHTQGIPDFFKQSFPE GFTWERVTTYEDGGVLTATQDTSLQ DGCLIYNVKIRGVNFTSNGPVMQKKT LGWEAFTETLYPADGGLEGRNDMAL KLVGGSHLIANIKTTYRSKKPAKNLK MPGVYYVDYRLERIKEANNETYVEQ HEVAVARYCDLPSKLGHKLN
NS3aH1-VPR	GWF196	ANR-binding-competent NS3a, catalytically active, In pcDNA5/FRT/TO	Fig. 2D,E,F; Supp. Fig. 8B,C,D; Supp. Fig. 10G	**MKKKGSVVIVGRINLSGDTAYSQQT RGLEGCQETSQTGRDKNQVEGEVQ VVSTATQSFLATSINGVLWTVYHGA GTRTIASPKGPVTQMYTNVDKDLVG WQAPQGSRSLTPCTCGSSDLYLVT RHADVIPVRRRGDSRGSLLSPRPISY LKGSSGGPLLCPAGHAVGIFRAAVS TRGVAKAVDFIPVESLETTMRSP**GS GTGSGEQKLISEEDLEFSSAAGTSDA LDDFDLDMLGSDALDDFDLDMLGSD

				ALDDFDLDMLGSDALDDFDLDMLGS PKKKRKVGSQYLPDTDDRHRIEEKR KRTYETFKSIMKKSPFSGPTDPRPPP RRIAVPSRSSASVPKPAPQPYPFTSS LSTINYDEFPTMVFPSGQISQASALA PAPPQVLPQAPAPAPAPAMVSALAQ APAPVPVLAPGPPQAVAPPAPKPTQ AGEGTLSEALLQLQFDDEDLGALLGN STDPAVFTDLASVDNSEFQQLLNQGI PVAPHTTEPMLMEYPEAITRLVTGAQ RPPDPAPAPLGAPGLPNGLLSGDED FSSIADMDFSALLSQISSGSGSGSRD SREGMFLPKPEAGSAISDVFEGREV CQPKRIRPFHPPGSPWANRPLPASL APTPTGPVHEPVGSLTPAPVPQPLD PAPAVTPEASHLLEDPDEETSQAVKA LREMADTVIPQKEEAAICGQMDLSHP PPRGHLDELTTTLESMTEDLNLDSPL TPELNEILDTFLNDECLLHAMHISTGL SIFDTSLF
dCas9	GWF198	N-terminal FLAG-Sp-dCas9-SV40-NLS in pCDNA5/FRT/TO	Fig. 2D,E,F; Supp. Fig. 8B,C,D	MDYKDDDDKDKKYSIGLAIGTNSVG WAVITDEYKVPSKKFKVLGNTDRHSI KKNLIGALLFDSGETAEATRLKRTAR RRYTRRKNRICYLQEIFSNEMAKVDD SFFHRLEESFLVEEDKKHERHPIFGNI VDEVAYHEKYPTIYHLRKKLVDSTDK ADLRLIYLALAHMIKFRGHFLIEGDLN PDNSDVDKLFIQLVQTYNQLFEENPI NASGVDAKAILSARLSKSRRLENLIAQ LPGEKKNGLFGNLIALSLGLTPNFKS NFDLAEDAKLQLSKDTYDDDLDNLLA QIGDQYADLFLAAKNLSDAILLSDILR VNTEITKAPLSASMIKRYDEHHQDLTL LKALVRQQLPEKYKEIFFDQSKNGYA GYIDGGASQEEFYKFIKPILEKMDGT EELLVKLNREDLLRKQRTFDNGSIPH QIHLGELHAILRRQEDFYPFLKDNRE KIEKILTFRIPYYVGPLARGNSRFAWM TRKSEETITPWNFEEVVDKGASAQSF IERMTNFDKNLPNEKVLPKHSLLYEY FTVYNELTKVKYVTEGMRKPAFLSGE QKKAIVDLLFKTNRKVTVKQLKEDYF KKIECFDSVEISGVEDRFNASLGTYH DLLKIIKDKDFLDNEENEDILEDIVLTL TLFEDREMIEERLKTYAHLFDDKVMK QLKRRRYTGWGRLSRKLINGIRDKQ SGKTILDFLKSDGFANRNFMQLIHDD SLTFKEDIQKAQVSGQGDSLHEHIAN LAGSPAIKKGILQTVKVVDELVKVMG RHKPENIVIEMARENQTTQKGQKNS RERMKRIEEGIKELGSQILKEHPVENT QLQNEKLYLYYLQNGRDMYVDQELD INRLSDYDVDAIVPQSFLKDDSIDNKV LTRSDKNRGKSDNVPSEEVVKKMKN YWRQLLNAKLITQRKFDNLTKAERG GLSELDKAGFIKRQLVETRQITKHVA

				QILDSRMNTKYDENDKLIREVKVITLK SKLVSDFRKDFQFYKVREINNYHHAH DAYLNAVVGTALIKKYPKLESEFVYG DYKVYDVRKMIAKSEQEIGKATAKYF FYSNIMNFFKTEITLANGEIRKRPLIET NGETGEIVWDKGRDFATVRKVLSMP QVNIVKKTEVQTGGFSKESILPKRNS DKLIARKKDWDPKKYGGFDSPTVAY SVLVVAKVEKGKSKKLKSVKELLGITI MERSSFEKNPIDFLEAKGYKEVKKDL IIKLPKYSLFELENGRKRMLASAGELQ KGNELALPSKYVNFLYLASHYEKLKG SPEDNEQKQLFVEQHKHYLDEIIEQIS EFSKRVILADANLDKVLSAYNKHRDK PIREQAENIIHLFTLTNLGAPAAFKYF DTTIDRKRYTSTKEVLDATLIHQSITG LYETRIDLSQLGGDSRADPKKKRKV
CXCR4-C1-2xMS2	GWF324	pU6-guide-2xMS2(wt+f6)/CMV-BFP	Supp. Fig. 10E	**GCGGGTGGTCGGTAGTGAGTC**GTT TAAGAGCTATGCTGGAAACAGCATA GCAAGTTTAAATAAGGCTAGTCCGT TATCAACTTGAAAAAGTGGCACCGA GTCGGTGCGGGAGCACATGAGGAT CACCCATGTGCGACTCCCACAGTC ACTGGGGAGTCTTCCCTTTTTTTGT TTTTTATGTCT
CXCR4-C2-2xMS2	GWF325	pU6-guide-2xMS2(wt+f6)/CMV-BFP	Supp. Fig. 10E	**GCAGACGCGAGGAAGGAGGGCGC** GTTTAAGAGCTATGCTGGAAACAGC ATAGCAAGTTTAAATAAGGCTAGTC CGTTATCAACTTGAAAAAGTGGCAC CGAGTCGGTGCGGGAGCACATGAG GATCACCCATGTGCGACTCCCACA GTCACTGGGGAGTCTTCCCTTTTTT TGTTTTTTATGTCT
CXCR4-C3-2xMS2	GWF326	pU6-guide-2xMS2(wt+f6)/CMV-BFP	Supp. Fig. 10E	**GCCTCTGGGAGGTCCTGTCCGGCT C**GTTTAAGAGCTATGCTGGAAACAG CATAGCAAGTTTAAATAAGGCTAGT CCGTTATCAACTTGAAAAAGTGGCA CCGAGTCGGTGCGGGAGCACATGA GGATCACCCATGTGCGACTCCCAC AGTCACTGGGGAGTCTTCCCTTTTT TTGTTTTTTATGTCT
CD95-1-2xMS2	GWF321	pU6-guide-2xMS2(wt+f6)/CMV-BFP	Supp. Fig. 10F	**GTACAGCAGAAGCCTTTAGAA**GTT TAAGAGCTATGCTGGAAACAGCATA GCAAGTTTAAATAAGGCTAGTCCGT TATCAACTTGAAAAAGTGGCACCGA GTCGGTGCGGGAGCACATGAGGAT CACCCATGTGCGACTCCCACAGTC ACTGGGGAGTCTTCCCTTTTTTTGT TTTTTATGTCT
CD95-2-2xMS2	GWF322	pU6-guide-2xMS2(wt+f6)/CMV-BFP	Supp. Fig. 10F	**GTGGCATGCTCACTTCAGGTG**GTT TAAGAGCTATGCTGGAAACAGCATA GCAAGTTTAAATAAGGCTAGTCCGT

				TATCAACTTGAAAAAGTGGCACCGA GTCGGTGCGGGAGCACATGAGGAT CACCCATGTGCGACTCCCACAGTC ACTGGGGAGTCTTCCCTTTTTTTGT TTTTTATGTCT
CD95-3-2xMS2	GWF323	pU6-guide-2xMS2(wt+f6)/CMV-BFP	Supp. Fig. 10F	**GAAGCCTCGCTGGGGAACGCC**GT TTAAGAGCTATGCTGGAAACAGCAT AGCAAGTTTAAATAAGGCTAGTCCG TTATCAACTTGAAAAAGTGGCACCG AGTCGGTGCGGGAGCACATGAGGA TCACCCATGTGCGACTCCCACAGT CACTGGGGAGTCTTCCCTTTTTTTG TTTTTTATGTCT
MCP-NS3a-P2a-DNCR2-KRAB-MeCP2-P2a-GNCR1-VPR-(IRES-BFP)	GWF169	NS3a solubility optimized S139A, DNCR2, and GNCR1 all in bold (in pCDNA5/FRT/TO)	Supp. Fig. 10E,F	MPKKKRKVGSMASNFTQFVLVDNG GTGDVTVAPSNFANGIAEWISSNSRS QAYKVTCSVRQSSAQNRKYTIKVEV PKGAWRSYLNMELTIPIFATNSDCELI VKAMQGLLKDGNPIPSAIAANSGIYG SGGSGTGEQKLISEEDLGG**KKKGSV VIVGRINLSGDTAYAQQTRGEEGCQ ETSQTGRDKNQVEGEVQIVSTATQT FLATSINGVLWTVYHGAGTRTIASPK GPVTQMYTNVDKDLVGWQAPQGSR SLTPCTCGSSDLYLVTRHADVIPVRR RGDSRGSLLSPRPISYLKGSAGGPL LCPAGHAVGIFRAAVSTRGVAKAVD FIPVESLETTMRSP**GSGATNFSLLKQ AGDVEENPGP**MSSDEEEARELIERA KEAAERAQEAAERTGDPRVRELAR ELKRLAQEAAEEVKRDPSSSDVNEA LKLIVEAIEAAVDALEAAERTGDPEV RELARELVRLAVEAAEEVQRNPSSS DVNEALHSIVYAIEAAIFALEAAERTG DPEVRELARELVRLAVEAAEEVQRN PSSRNVEHALMRIVLAIYLAEENLRE AEESGDPEKREKARERVREAVERA EEVQRDPSGWLNH**EQKLISEEDLSG GGSGGSGSMDAKSLTAWSRTLVTFK DVFVDFTREEWKLLDTAQQIVYRNV MLENYKNLVSLGYQLTKPDVILRLEK GEEPWLVSGGGSGGSGSSPKKKRK VEASVQVKRVLEKSPGKLLVKMPFQ ASPGGKGEGGGATTSAQVMVIKRPG RKRKAEADPQAIPKKRGRKPGSVVA AAAAEAKKKAVKESSIRSVQETVLPIK KRKTRETVSIEVKEVVKPLLVSTLGEK SGKGLKTCKSPGRKSKESSPKGRSS SASSPPKKEHHHHHHHAESPKAPMP LLPPPPPPEPQSSEDPISPPEPQDLS SSICKEEKMPRAGSLESDGCPKEPA KTQPMVAAAATTTTTTTTTVAEKYKH RGEGERKDIVSSSMPRPNREEPVDS RTPVTERVSGSGATNFSLLKQAGDV EENPGP**DIEKLCKKAEEEAKEAQEK ADELRQRHPDSQAAEDAEDLANLA VAAVLTACLLAQEHPNADIAKLCIKA**

				ASEAAEAASKAAELAQRHPDSQAA RDAIKLASQAARAVILAIMLAAENPN ADIAKLCIKAASEAAEAASKAAELA QRHPDSQAARDAIKLASQAAEAVER AIWLAAENPNADIAKKCIKAASEAAE EASKAAEEAQRHPDSQKARDEIKEA SQKAEEVKERCKSEQKLISEEDLEFS SAAGTSDALDDFDLDMLGSDALDDF DLDMLGSDALDDFDLDMLGSDALDD FDLDMLGSPKKKRKVGSQYLPDTDD RHRIEEKRKRTYETFKSIMKKSPFSG PTDPRPPPRRIAVPSRSSASVPKPAP QPYPFTSSLSTINYDEFPTMVFPSGQ ISQASALAPAPPQVLPQAPAPAPAPA MVSALAQAPAPVPVLAPGPPQAVAP PAPKPTQAGEGTLSEALLQLQFDDE DLGALLGNSTDPAVFTDLASVDNSEF QQLLNQGIPVAPHTTEPMLMEYPEAI TRLVTGAQRPPDPAPAPLGAPGLPN GLLSGDEDFSSIADMDFSALLSQISS GSGSGSRDSREGMFLPKPEAGSAIS DVFEGREVCQPKRIRPFHPPGSPWA NRPLPASLAPTPTGPVHEPVGSLTPA PVPQPLDPAPAVTPEASHLLEDPDEE TSQAVKALREMADTVIPQKEEAAICG QMDLSHPPPRGHLDELTTTLESMTE DLNLDSPLTPELNEILDTFLNDECLLH AMHISTGLSIFDTSLF
LifeAct-mCherry	GWF214	(in pCDNA5/FRT/TO)	Fig. 4C-G, Supp. Fig. 11, Supp. Fig. 12C-E	MGVADLIKKFESISKEEGDPPVATMV SKGEEDNMAIIKEFMRFKVHMEGSV NGHEFEIEGEGEGRPYEGTQTAKLK VTKGGPLPFAWDILSPQFMYGSKAY VKHPADIPDYLKLSFPEGFKWERVM NFEDGGVVTVTQDSSLQDGEFIYKV KLRGTNFPSDGPVMQKKTMGWEAS SERMYPEDGALKGEIKQRLKLKDGG HYDAEVKTTYKAKKPVQLPGAYNVNI KLDITSHNEDYTIVEQYERAEGRHST GGMDELYK
mCherry-NS3a-CAAX-(IRES)-EGFP-DNCR2-P2a-BFP-GNCR1	GWF223	NS3a solubility optimized S139A. CAAX from KRAS4b. IRES not shown. NS3a, DNCR1, and GNCR1 in bold (in pEF5-FRT)	Fig. 4B; Supp. Fig. 12A-C	MVSKGEEDNMAIIKEFMRFKVHMEG SVNGHEFEIEGEGEGRPYEGTQTAK LKVTKGGPLPFAWDILSPQFMYGSK AYVKHPADIPDYLKLSFPEGFKWERV MNFEDGGVVTVTQDSSLQDGEFIYK VKLRGTNFPSDGPVMQKKTMGWEA SSERMYPEDGALKGEIKQRLKLKDG GHYDAEVKTTYKAKKPVQLPGAYNV NIKLDITSHNEDYTIVEQYERAEGRHS TGGMDELYKGSGTGEQKLISEEDLG G**KKKGSVVIVGRINLSGDTAYAQQT RGEEGCQETSQTGRDKNQVEGEVQ IVSTATQTFLATSINGVLWTVYHGAG TRTIASPKGPVTQMYTNVDKDLVGW QAPQGSRSLTPCTCGSSDLYLVTRH ADVIPVRRRGDSRGSLLSPRPISYLK GSAGGPLLCPAGHAVGIFRAAVSTR**

				GVAKAVDFIPVESLETTMRSPSAGG SAGGEKMSKDGKKKKKKSKTKCVIM – (IRES) – MVSKGEELFTGVVPILVELDGDVNGH KFSVSGEGEGDATYGKLTLKFICTTG KLPVPWPTLVTTLTYGVQCFSRYPD HMKQHDFFKSAMPEGYVQERTIFFK DDGNYKTRAEVKFEGDTLVNRIELKG IDFKEDGNILGHKLEYNYNSHNVYIM ADKQKNGIKVNFKIRHNIEDGSVQLA DHYQQNTPIGDGPVLLPDNHYLSTQ SALSKDPNEKRDHMVLLEFVTAAGIT LGMDELYKSGSGEQKLISEEDLGSG **SSDEEEARELIERAKEAAERAQEAA ERTGDPRVRELARELKRLAQEAAEE VKRDPSSSDVNEALKLIVEAIEAAVD ALEAAERTGDPEVRELARELVRLAV EAAEEVQRNPSSSDVNEALHSIVYAI EAAIFALEAAERTGDPEVRELARELV RLAVEAAEEVQRNPSSRNVEHALM RIVLAIYLAEENLREAEESGDPEKRE KARERVREAVERAEEVQRDPSGWL NH**SAGGSAGGSAGGSAGGSGASGS GATNFSLLKQAGDVEENPGPSELIKE NMHMKLYMEGTVDNHHFKCTSEGE GKPYEGTQTMRIKVVEGGPLPFAFDI LATSFLYGSKTFINHTQGIPDFFKQSF PEGFTWERVTTYEDGGVLTATQDTS LQDGCLIYNVKIRGVNFTSNGPVMQK KTLGWEAFTETLYPADGGLEGRNDM ALKLVGGSHLIANIKTTYRSKKPAKNL KMPGVYYVDYRLERIKEANNETYVE QHEVAVARYCDLPSKLGHKLNSGSG EQKLISEEDLGSGTGSGTGSGTGTT SGTGTGGSTG**MDIEKLCKKAEEEAK EAQEKADELRQRHPDSQAAEDAED LANLAVAAVLTACLLAQEHPNADIA KLCIKAASEAAEAASKAAELAQRHP DSQAARDAIKLASQAARAVILAIMLA AENPNADIAKLCIKAASEAAEAASK AAELAQRHPDSQAARDAIKLASQAA EAVERAIWLAAENPNADIAKKCIKAA SEAAEEASKAAEEAQRHPDSQKAR DEIKEASQKAEEVKERCKS**SAGGSA GGSAGGSAGGSAG
NS3a-CAAX-(IRES)-EGFP-DNCR2-TIAM-P2a-BFP-GNCR1-LARG	GWF243, GWF228	NS3a solubility optimized S139A. CAAX from KRAS4b. IRES not shown. NS3a, DNCR1, and GNCR1 in	Fig. 4C-G; Supp. Fig. 11A-E,H; Supp. Fig. 12D,E	MEQKLISEEDLGG**KKKGSVVIVGRIN LSGDTAYAQQTRGEEGCQETSQTG RDKNQVEGEVQIVSTATQTFLATSIN GVLWTVYHGAGTRTIASPKGPVTQM YTNVDKDLVGWQAPQGSRSLTPCT CGSSDLYLVTRHADVIPVRRRGDSR GSLLSPRPISYLKGSAGGPLLCPAG HAVGIFRAAVSTRGVAKAVDFIPVES LETTMRSP**SAGGSAGGEKMSKDGK KKKKKSKTKCVIM – (IRES) – MVSKGEELFTGVVPILVELDGDVNGH

		bold. TIAM and LARG underlined (in PB501B or pEF5-FRT)		KFSVSGEGEGDATYGKLTLKFICTTG KLPVPWPTLVTTLTYGVQCFSRYPD HMKQHDFFKSAMPEGYVQERTIFFK DDGNYKTRAEVKFEGDTLVNRIELKG IDFKEDGNILGHKLEYNYNSHNVYIM ADKQKNGIKVNFKIRHNIEDGSVQLA DHYQQNTPIGDGPVLLPDNHYLSTQ SALSKDPNEKRDHMVLLEFVTAAGIT LGMDELYKSGSGEQKLISEEDLGSG **SSDEEEARELIERAKEAAERAQEAA ERTGDPRVRELARELKRLAQEAAEE VKRDPSSSDVNEALKLIVEAIEAAVD ALEAAERTGDPEVRELARELVRLAV EAAEEVQRNPSSSDVNEALHSIVYAI EAAIFALEAAERTGDPEVRELARELV RLAVEAAEEVQRNPSSRNVEHALM RIVLAIYLAEENLREAEESGDPEKRE KARERVREAVERAEEVQRDPSGWL NH**SAGGSAGGSAGGSAGGSGASRQ LSDADKLRKVICELLETERTYVKDLN CLMERYLKPLQKETFLTQDELDVLFG NLTEMVEFQVEFLKTLEDGVRLVPDL EKLEKVDQFKKVLFSLGGSFLYYADR FKLYSAFCASHTKVPKVLVKAKTDTA FKAFLDAQNPKQQHSSTLESYLIKPIQ RILKYPLLLRELFALTDAESEEHYHLD VAIKTMNKVASHINEMQKIHEEGSGA TNFSLLKQAGDVEENPGPSELIKENM HMKLYMEGTVDNHHFKCTSEGEGK PYEGTQTMRIKVVEGGPLPFAFDILA TSFLYGSKTFINHTQGIPDFFKQSFPE GFTWERVTTYEDGGVLTATQDTSLQ DGCLIYNVKIRGVNFTSNGPVMQKKT LGWEAFTETLYPADGGLEGRNDMAL KLVGGSHLIANIKTTYRSKKPAKNLK MPGVYYVDYRLERIKEANNETYVEQ HEVAVARYCDLPSKLGHKLNSGSGE QKLISEEDLGSGTGSGTGSGTGTTS GTGTGGSTG**MDIEKLCKKAEEEAKE AQEKADELRQRHPDSQAAEDAEDL ANLAVAAVLTACLLAQEHPNADIAK LCIKAASEAAEAASKAAELAQRHPD SQAARDAIKLASQAARAVILAIMLAA ENPNADIAKLCIKAASEAAEAASKA AELAQRHPDSQAARDAIKLASQAAE AVERAIWLAAENPNADIAKKCIKAAS EAAEEASKAAEEAQRHPDSQKARD EIKEASQKAEEVKERCKS**SAGGSAG GSAGGSAGGSAGTPPNWQQLVSRE VLLGLKPCEIKRQEVINELFYTERAHV RTLKVLDQVFYQRVSREGILSPSELR KIFSNLEDILQLHIGLNEQMKAVRKRN ETSVIDQIGEDLLTWFSGPGEEKLKH AAATFCSNQPFALEMIKSRQKKDSRF QTFVQDAESNPLCRRLQLKDIIPTQM QRLTKYPLLLDNIAKYTEWPTEREKV

				KKAADHCRQILNYVNQAVKEAENKQR
NS3a-CAAX-(IRES)-EGFP-DNCR2-TIAM-P2a-BFP-GNCR1	GWF246	NS3a solubility optimized S139A. CAAX from KRAS4b. IRES not shown. NS3a, DNCR1, and GNCR1 in bold. TIAM underlined (in PB501B)	Fig. 4D-G; Supp. Fig. 12A-D,F,H	MEQKLISEEDLGG**KKKGSVVIVGRIN LSGDTAYAQQTRGEEGCQETSQTG RDKNQVEGEVQIVSTATQTFLATSIN GVLWTVYHGAGTRTIASPKGPVTQM YTNVDKDLVGWQAPQGSRSLTPCT CGSSDLYLVTRHADVIPVRRRGDSR GSLLSPRPISYLKGSAGGPLLCPAG HAVGIFRAAVSTRGVAKAVDFIPVES LETTMRSP**SAGGSAGGEKMSKDGK KKKKKSKTKCVIM – (IRES) – MVSKGEELFTGVVPILVELDGDVNGH KFSVSGEGEGDATYGKLTLKFICTTG KLPVPWPTLVTTLTYGVQCFSRYPD HMKQHDFFKSAMPEGYVQERTIFFK DDGNYKTRAEVKFEGDTLVNRIELKG IDFKEDGNILGHKLEYNYNSHNVYIM ADKQKNGIKVNFKIRHNIEDGSVQLA DHYQQNTPIGDGPVLLPDNHYLSTQ SALSKDPNEKRDHMVLLEFVTAAGIT LGMDELYKSGSGEQKLISEEDLGSG **SSDEEEARELIERAKEAAERAQEAA ERTGDPRVRELARELKRLAQEAAEE VKRDPSSSDVNEALKLIVEAIEAAVD ALEAAERTGDPEVRELARELVRLAV EAAEEVQRNPSSSDVNEALHSIVYAI EAAIFALEAAERTGDPEVRELARELV RLAVEAAEEVQRNPSSRNVEHALM RIVLAIYLAEENLREAEESGDPEKRE KARERVREAVERAEEVQRDPSGWL NH**SAGGSAGGSAGGSAGGSGASRQ LSDADKLRKVICELLETERTYVKDLN CLMERYLKPLQKETFLTQDELDVLFG NLTEMVEFQVEFLKTLEDGVRLVPDL EKLEKVDQFKKVLFSLGGSFLYYADR FKLYSAFCASHTKVPKVLVKAKTDTA FKAFLDAQNPKQQHSSTLESYLIKPIQ RILKYPLLLRELFALTDAESEEHYHLD VAIKTMNKVASHINEMQKIHEEGSGA TNFSLLKQAGDVEENPGPSELIKENM HMKLYMEGTVDNHHFKCTSEGEGK PYEGTQTMRIKVVEGGPLPFAFDILA TSFLYGSKTFINHTQGIPDFFKQSFPE GFTWERVTTYEDGGVLTATQDTSLQ DGCLIYNVKIRGVNFTSNGPVMQKKT LGWEAFTETLYPADGGLEGRNDMAL KLVGGSHLIANIKTTYRSKKPAKNLK MPGVYYVDYRLERIKEANNETYVEQ HEVAVARYCDLPSKLGHKLNSGSGE QKLISEEDLGSGTGSGTGSGTGTTS GTGTGGSTG**MDIEKLCKKAEEEAKE AQEKADELRQRHPDSQAAEDAEDL ANLAVAAVLTACLLAQEHPNADIAK LCIKAASEAAEAASKAAELAQRHPD SQAARDAIKLASQAARAVILAIMLAA**

				ENPNADIAKLCIKAASEAAEAASKA AELAQRHPDSQAARDAIKLASQAAE AVERAIWLAAENPNADIAKKCIKAAS EAAEEASKAAEEAQRHPDSQKARD EIKEASQKAEEVKERCKSSAGGSAG GSAGGSAGGSAG
NS3a-CAAX-(IRES)-EGFP-DNCR2-P2a-BFP-GNCR1-LARG	GWF248	NS3a solubility optimized S139A. CAAX from KRAS4b. IRES not shown. NS3a, DNCR1, and GNCR1 in bold. LARG underlined (in PB501B)	Fig. 4D-G; Supp. Fig. 12A-D,G,H	MEQKLISEEDLGG**KKKGSVVIVGRIN LSGDTAYAQQTRGEEGCQETSQTG RDKNQVEGEVQIVSTATQTFLATSIN GVLWTVYHGAGTRTIASPKGPVTQM YTNVDKDLVGWQAPQGSRSLTPCT CGSSDLYLVTRHADVIPVRRRGDSR GSLLSPRPISYLKGSAGGPLLCPAG HAVGIFRAAVSTRGVAKAVDFIPVES LETTMRSP**SAGGSAGGEKMSKDGK KKKKKSKTKCVIM – (IRES) – MVSKGEELFTGVVPILVELDGDVNGH KFSVSGEGEGDATYGKLTLKFICTTG KLPVPWPTLVTTLTYGVQCFSRYPD HMKQHDFFKSAMPEGYVQERTIFFK DDGNYKTRAEVKFEGDTLVNRIELKG IDFKEDGNILGHKLEYNYNSHNVYIM ADKQKNGIKVNFKIRHNIEDGSVQLA DHYQQNTPIGDGPVLLPDNHYLSTQ SALSKDPNEKRDHMVLLEFVTAAGIT LGMDELYKSGSGEQKLISEEDLGSG **SSDEEEARELIERAKEAAERAQEAA ERTGDPRVRELARELKRLAQEAAEE VKRDPSSSDVNEALKLIVEAIEAAVD ALEAAERTGDPEVRELARELVRLAV EAAEEVQRNPSSSDVNEALHSIVYAI EAAIFALEAAERTGDPEVRELARELV RLAVEAAEEVQRNPSSRNVEHALM RIVLAIYLAEENLREAEESGDPEKRE KARERVREAVERAEEVQRDPSGWL NH**SAGGSAGGSAGGSAGGSGASGS GATNFSLLKQAGDVEENPGPSELIKE NMHMKLYMEGTVDNHHFKCTSEGE GKPYEGTQTMRIKVVEGGPLPFAFDI LATSFLYGSKTFINHTQGIPDFFKQSF PEGFTWERVTTYEDGGVLTATQDTS LQDGCLIYNVKIRGVNFTSNGPVMQK KTLGWEAFTETLYPADGGLEGRNDM ALKLVGGSHLIANIKTTYRSKKPAKNL KMPGVYYVDYRLERIKEANNETYVE QHEVAVARYCDLPSKLGHKLNSGSG EQKLISEEDLGSGTGSGTGSGTGTT SGTGTGGSTG**MDIEKLCKKAEEEAK EAQEKADELRQRHPDSQAAEDAED LANLAVAAVLTACLLAQEHPNADIA KLCIKAASEAAEAASKAAELAQRHP DSQAARDAIKLASQAARAVILAIMLA AENPNADIAKLCIKAASEAAEAASK AAELAQRHPDSQAARDAIKLASQAA EAVERAIWLAAENPNADIAKKCIKAA SEAAEEASKAAEEAQRHPDSQKAR

				DEIKEASQKAEEVKERCKSSAGGSA GGSAGGSAGGSAGTPPNWQQLVSR EVLLGLKPCEIKRQEVINELFYTERAH VRTLKVLDQVFYQRVSREGILSPSEL RKIFSNLEDILQLHIGLNEQMKAVRKR NETSVIDQIGEDLLTWFSGPGEEKLK HAAATFCSNQPFALEMIKSRQKKDS RFQTFVQDAESNPLCRRLQLKDIIPT QMQRLTKYPLLLDNIAKYTEWPTERE KVKKAADHCRQILNYVNQAVKEAEN KQR
Gal4DBD-NS3a-P2a-DNCR2-VPR	GWF058	From pLenti-UAS-minCMV-mCherry/CMV-Gal4DBD-NS3a-P2a-DNCR2-VPR, with NS3a and DNCR2 in bold	Supp. Fig. 8A	MKLLSSIEQACDICRLKKLKCSKEKPK CAKCLKNNWECRYSPKTKRSPLTRA HLTEVESRLERLEQLFLLIFPREDLDM ILKMDSLQDIKALLGTPAAASTLEGG GSAGSGG**KKKGSVVIVGRINLSGDT** **AYAQQTRGEEGCQETSQTGRDKNQ** **VEGEVQIVSTATQTFLATSINGVLWT** **VYHGAGTRTIASPKGPVTQMYTNVD** **KDLVGWQAPQGSRSLTPCTCGSSD** **LYLVTRHADVIPVRRRGDSRGSLLS** **PRPISYLKGSAGGPLLCPAGHAVGIF** **RAAVSTRGVAKAVDFIPVESLETTM** **RSP**GSGATNFSLLKQAGDVEENPGP **MSSDEEEARELIERAKEAAERAQEA** **AERTGDPRVRELARELKRLAQEAAE** **EVKRDPSSSDVNEALKLIVEAIEAAV** **DALEAAERTGDPEVRELARELVRLA** **VEAAEEVQRNPSSSDVNEALHSIVY** **AIEAAIFALEAAERTGDPEVRELARE** **LVRLAVEAAEEVQRNPSSRNVEHAL** **MRIVLAIYLAEENLREAEESGDPEKR** **EKARERVREAVERAEEVQRDPSGW** **LNH**EQKLISEEDLDALDDFDLDMLGS DALDDFDLDMLGSDALDDFDLDMLG SDALDDFDLDMLGSPKKKRKVGSQY LPDTDDRHRIEEKRKRTYETFKSIMK KSPFSGPTDPRPPPRRIAVPSRSSAS VPKPAPQPYPFTSSLSTINYDEFPTM VFPSGQISQASALAPAPPQVLPQAPA PAPAPAMVSALAQAPAPVPVLAPGP PQAVAPPAPKPTQAGEGTLSEALLQL QFDDEDLGALLGNSTDPAVFTDLASV DNSEFQQLLNQGIPVAPHTTEPMLM EYPEAITRLVTGAQRPPDPAPAPLGA PGLPNGLLSGDEDFSSIADMDFSALL SQISSGSGSGSRDSREGMFLPKPEA GSAISDVFEGREVCQPKRIRPFHPPG SPWANRPLPASLAPTPTGPVHEPVG SLTPAPVPQPLDPAPAVTPEASHLLE DPDEETSQAVKALREMADTVIPQKEE AAICGQMDLSHPPPRGHLDELTTTLE SMTEDLNLDSPLTPELNEILDTFLNDE CLLHAMHISTGLSIFDTSLF

CXCR4_fwd		qPCR primer	Fig. 4A; Supp. Fig. 10G	GAAGCTGTTGGCTGAAAAGG
CXCR4_rev		qPCR primer	Fig. 4A; Supp. Fig. 10G	CTCACTGACGTTGGCAAAGA
GAPDH_fwd		qPCR primer	Supp. Fig. 10G	ACAGTCAGCCGCATCTTCTT
GAPDH_rev		qPCR primer	Supp. Fig. 10G	ACGACCAAATCCGTTGACTC
GFP_fwd		qPCR primer	Supp. Fig. 10G	AGCAGAAGAACGGCATCAAG
GFP_rev		qPCR primer	Supp. Fig. 10G	GGGGTGTTCTGCTGGTAGTG
CD95_fwd		qPCR primer	Supp. Fig. 10G	ATGGTGTCAATGAAGCCAAA
CD95_rev		qPCR primer	Supp. Fig. 10G	TGATGCCAATTACGAAGCAG

Supplementary Table 5 | Drug concentrations used for Figure 3b,c

	grazoprevir (nM)		
	low proportion grazoprevir	medium proportion grazoprevir	high proportion grazoprevir
danoprevir (nM)	2-fold serial dilutions	1.5-fold serial dilutions	1.25-fold serial dilutions
1000.00	10.00	10.00	10.00
400.00	5.00	6.67	8.00
160.00	2.50	4.44	6.40
64.00	1.25	2.96	5.12
25.60	0.63	1.98	4.10
10.24	0.31	1.32	3.28
4.10	0.16	0.88	2.62
1.64	0.08	0.59	2.10
0.66	0.04	0.39	1.68
0.26	0.02	0.26	1.34
0.10	0.01	0.17	1.07
0.04	0.005	0.12	0.86

Design scripts

ROSETTA Script cid_design.xml:

```
<dock_design>

 <SCOREFXNS>
  <sfxn_hard weights=talaris2014/>
  <sfxn_soft weights=soft_rep/>

  <sfxn_hard_cst weights=talaris2014>
   <Reweight scoretype=coordinate_constraint weight=1 />
  </sfxn_hard_cst>

  ### score function that contains the full atom attractive forces only
  <VDW weights="empty" >
            <Reweight scoretype="fa_atr" weight=1.0/>
  </VDW>
 </SCOREFXNS>

 <RESIDUE_SELECTORS>
  In the setup below, chain A is target (NS3a)  and chain B is scaffold, X is ligand.
  In the input pdb, chain B should be 1st, followed by chain A and chain X.
  <Chain name=chA chains=A,X/>
  <Chain name=chX chains=X/>
  <Chain name=chB chains=B/>
  <InterfaceByVector name=intf cb_dist_cut=10 nearby_atom_cut=5.5 vector_angle_cut=75.0 vector_dist_cut=9.0
grp1_selector=chA grp2_selector=chB/>
  <InterfaceByVector name=ligand_intf cb_dist_cut=10 nearby_atom_cut=5.5 vector_angle_cut=75.0
vector_dist_cut=9.0 grp1_selector=chX grp2_selector=chB/>
  <ResidueName name=hp residue_name3="VAL,PHE,TYR,ILE,LEU,TRP,MET" />
  <And name=hp_in_A selectors=intf,hp,chA/>        hydrophobic residues on target
  <Or name=hp_in_A_and_X selectors=hp_in_A,chX/> union: hydrophobic residues on target + Ligand +
contacting residues on scaffold
  <Neighborhood name=hp_neighbor selector=hp_in_A_and_X distance=10.0/>
  <And name=hp_contact_in_B selectors=chB,hp_neighbor/>contacting residues on scaffold
  <Or name=hpA_contactB selectors=hp_in_A,hp_contact_in_B/> union: hydrophobic residues on target +
contacting residues on scaffold
  <Not name=not_hpA_contactB selector=hpA_contactB/>    negation of hpA_contactB for restriction
  <Not name=not_ligand_intf selector=ligand_intf/> negation of hpA_contactB for restriction

  # hp_revert
  <Neighborhood name=hp_revert selector=chX distance=10.0/>
  <And name=hp_rvt selectors=hp_revert/>


 </RESIDUE_SELECTORS>

 <TASKOPERATIONS>
  <ProteinLigandInterfaceUpweighter name=up interface_weight=1.5/>
  <DesignAround name=da design_shell=10 resnums=1X repack_shell=10.0 allow_design=1
resnums_allow_design=0/>
  <IncludeCurrent name=inclcur/>
  <PreventChainFromRepacking chain=2 name=pctr2/>
  <PreventChainFromRepacking chain=3 name=pctr3/>
  <ExtraRotamersGeneric name=exrot ex1=1 ex2=1 extrachi_cutoff=1/>
```

```
    <InitializeFromCommandline name=init/>
    <LimitAromaChi2 name=arochi2 chi2max=110 chi2min=70 />
    <RestrictAbsentCanonicalAAS name=nohis keep_aas="ACDEFGIKLMNPQRSTVWY"/>
    <RestrictAbsentCanonicalAAS name=nocys keep_aas="ADEFIKLMNPQRSTVWYH"/>
    #noCys & noGly
    # this allows PRO, GLY, CYS in the interface it seems that CYS is overfavoured so restrict this might be
necessary
    <ProteinInterfaceDesign name=dzn_inter design_chain1=1 design_chain2=0 repack_chain1=1 repack_chain2=0
jump=1 interface_distance_cutoff=11.0 allow_all_aas=1/>


    Design ONLY near the hydrophobic residues on target
    <OperateOnResidueSubset name=hp_task selector=not_hpA_contactB >
      <PreventRepackingRLT/>
    </OperateOnResidueSubset>
    <OperateOnResidueSubset name=ligand_interface selector=not_ligand_intf >
      <PreventRepackingRLT/>
    </OperateOnResidueSubset>

    <DisallowIfNonnative name=dis_charge resnum=0 disallow_aas=RQKDEG/>

    <DesignAround name=da10 design_shell=12 resnums=1X repack_shell=14.0 allow_design=1
resnums_allow_design=0/>
    # Selector hp_revert contains all residues within the ligand
    # these are set to prevent repacking
    <OperateOnResidueSubset name=nodesignaroundligand
       selector=hp_revert >
      <PreventRepackingRLT/>
    </OperateOnResidueSubset>

    ### this task operation defines an extended generous interface for minimization
    <ProteinInterfaceDesign name="pack_long" design_chain1="0" design_chain2="0" jump="1"
interface_distance_cutoff="15"/> //


  </TASKOPERATIONS>

  <MOVERS>

    <MinMover name=min_rb chi=1 bb=0 jump=1>
      <MoveMap>
        <Chain number=1 chi=1 bb=0/>          only chi for LRR
        <Chain number=2 chi=1 bb=0/>          only chi for target
        <Chain number=3 chi=0 bb=0/>          not chi for Ligand fixed as in crystal structure
      </MoveMap>
    </MinMover>

    <MinMover name=min_init chi=1 bb=0 jump=0>
      <MoveMap>
        <Chain number=1 chi=1 bb=0/>          only chi for LRR
        <Chain number=2 chi=0 bb=0/>          only chi for target
        <Chain number=3 chi=0 bb=0/>          only chi for Ligand
      </MoveMap>
    </MinMover>
```

```
   <TaskAwareMinMover name=min_chi bb=0 chi=1 jump=0 scorefxn=sfxn_hard
task_operations=init,arochi2,inclcur,exrot,dzn_inter/>
   <AtomTree name=simple_ft docking_ft=0 simple_ft=1/>

    # Design based on ligand task_operation
    <PackRotamersMover name=dzn_packrot_layer_soft_ligand scorefxn=sfxn_soft
task_operations=init,exrot,inclcur,arochi2,nohis,pctr2,da,up,nocys,dis_charge/>
    <PackRotamersMover name=dzn_packrot_layer_hard_ligand scorefxn=sfxn_hard
task_operations=init,exrot,inclcur,arochi2,nohis,pctr2,da,up,nocys,dis_charge/>

    # Normal design
    <PackRotamersMover name=dzn_packrot_soft scorefxn=sfxn_soft
task_operations=init,exrot,inclcur,arochi2,nohis,dzn_inter,pctr2,pctr3,up,nocys/>
    <PackRotamersMover name=dzn_packrot_hard scorefxn=sfxn_hard
task_operations=init,exrot,inclcur,arochi2,nohis,dzn_inter,pctr2,pctr3,nocys/>

    <DumpPdb name=d1 fname=dump1.pdb scorefxn=sfxn_hard_cst />
    <DumpPdb name=d2 fname=dump2.pdb scorefxn=sfxn_hard_cst />
    <DumpPdb name=d3 fname=dump3.pdb scorefxn=sfxn_hard_cst />
    <DumpPdb name=d4 fname=dump4.pdb scorefxn=sfxn_hard_cst />
    <DumpPdb name=d5 fname=dump5.pdb scorefxn=sfxn_hard_cst />

    # Normal design
    <PackRotamersMover name=dzn_packrot_soft_last scorefxn=sfxn_soft
task_operations=init,exrot,inclcur,arochi2,nohis,dzn_inter,nocys,pctr2,pctr3,up,nodesignaroundligand/>
    <PackRotamersMover name=dzn_packrot_hard_last scorefxn=sfxn_hard
task_operations=init,exrot,inclcur,arochi2,nohis,dzn_inter,nocys,pctr2,pctr3,nodesignaroundligand/>

   ### minimization of the extended PPI
    <TaskAwareMinMover name=min scorefxn=sfxn_hard bb=0 chi=1 task_operations=pack_long/>

  </MOVERS>


 <FILTERS>
   <Sasa name=sasa_jump1 threshold=1100 confidence=1 jump=1/> # scaffold. Confidence=1 used for grazoprevir
CID design, but not danoprevir CID design
   <Sasa name=sasa_jump2 confidence=0 jump=2/>  # ligand
   <Sasa name="interface_hydrophobic_sasa" confidence=0 hydrophobic=True/>
   <Sasa name="interface_polar_sasa" confidence=0 polar=True/>
   <Ddg name=ddg_jump1 threshold=-10 scorefxn=sfxn_hard jump=1 repack=1 relax_mover=min_chi repeats=1
confidence=0/>    # ligand
   <Ddg name=ddg_jump2 threshold=-10 scorefxn=sfxn_hard jump=2 repack=1 relax_mover=min_chi repeats=1
confidence=0/>    # ligand
   <Ddg name="ddg_fa_atr"  threshold=-10 jump=1 repeats=5 repack=1 relax_mover=min confidence=0
scorefxn=VDW />
   <Ddg name="ddg_fa_atr_norepack"  threshold=-10 jump=1 repeats=1 repack=0 confidence=0 scorefxn=VDW/>
   <ScoreType name=total_score scorefxn=sfxn_hard score_type=total_score threshold=0 confidence=0/>
   <AverageDegree name=deg threshold=8.6 distance_threshold=8 task_operations=dzn_inter confidence=0/>

   <CalculatorFilter name="ddg_fa_atr_per_1000sasa" equation="1000 * ddg / (sasa+0.01)" threshold="1"
confidence="0">
      <VAR name="ddg" filter="ddg_fa_atr"/>
      <VAR name="sasa" filter=sasa_jump1/>
   </CalculatorFilter>
```

```
   <CalculatorFilter name="ddg_fa_atr_norepack_per_1000sasa" equation="1000 * ddg / (sasa+0.01)"
threshold="1" confidence="0">
       <VAR name="ddg" filter="ddg_fa_atr_norepack"/>
            <VAR name="sasa" filter=sasa_jump1/>
   </CalculatorFilter>

   <ShapeComplementarity name=sc_jump1 jump=1 verbose=1 min_sc=0.6 confidence=0/>          #scaffold
   <ShapeComplementarity name=sc_jump2 jump=2 verbose=1 min_sc=0.6 confidence=0/>          #ligand
   <LigInterfaceEnergy name=interfE  scorefxn=sfxn_hard jump_number=2 energy_cutoff=-5 confidence=0/>

   <DesignableResidues name=dr task_operations=init,exrot,inclcur,arochi2,nohis,dzn_inter,pctr3 designable=1
packable=1/>
   <InterfaceHoles name="interface_holes" confidence=0/>
   <Sasa name="hydrophobic_sasa" confidence=0 jump=1 hydrophobic=True/>
   <BuriedUnsatHbonds2 name="interface_unsat_hbond" confidence=0/>
   <Rmsd name=rmsdB chains="B" threshold=2.0 superimpose=0 confidence=0/>
  </FILTERS>

  <APPLY_TO_POSE>
  </APPLY_TO_POSE>


  <PROTOCOLS>

   # Setting up atomtree with simple foldtree
   <Add mover=simple_ft/>
   # Movemaps to minimize scaffold
   <Add mover=min_init/>
   # PackRotamer with soft score function
   <Add mover=dzn_packrot_soft/>
   <Add mover=min_chi/>
   <Add mover=dzn_packrot_hard/>
   <Add mover=min_chi/>

   <Add mover=dzn_packrot_soft/>
   <Add mover=min_chi/>
   <Add mover=dzn_packrot_hard/>
   <Add mover=min_chi/>

   #Design around the ligand
   <Add mover=dzn_packrot_layer_soft_ligand/>
   <Add mover=min_chi/>
   <Add mover=dzn_packrot_layer_hard_ligand/>
   <Add mover=min_chi/>

   <Add mover=min_rb/>

   <Add mover=dzn_packrot_layer_soft_ligand/>
   <Add mover=min_chi/>
   <Add mover=dzn_packrot_layer_hard_ligand/>
   <Add mover=min_chi/>

   <Add mover=dzn_packrot_soft_last/>
   <Add mover=dzn_packrot_hard_last/>

   <Add filter=sasa_jump1/>
```

```
   <Add filter=sasa_jump2/>
   <Add filter=deg/>
   <Add filter=total_score/>
   <Add filter=sc_jump1/>
   <Add filter=sc_jump2/>
   <Add filter=ddg_jump1/>
   <Add filter=ddg_jump2/>
   <Add filter=interfE/>
   <Add filter=dr/>
   <Add filter="interface_holes"/>
   <Add filter="hydrophobic_sasa"/>
   <Add filter="rmsdB"/>
   <Add filter="interface_unsat_hbond"/>
   <Add filter="interface_hydrophobic_sasa"/>
   <Add filter="interface_polar_sasa"/>
   <Add filter="ddg_fa_atr"/>
   <Add filter="ddg_fa_atr_norepack"/>
   <Add filter="ddg_fa_atr_per_1000sasa"/>
   <Add filter="ddg_fa_atr_norepack_per_1000sasa"/>
  </PROTOCOLS>
</dock_design>
```

ROSETTA Script cid_roll_design.xml:

```
<dock_roll_design>

  <SCOREFXNS>
   <sfxn_hard weights=talaris2014/>
   <sfxn_soft weights=soft_rep/>

   <sfxn_hard_cst weights=talaris2014>
     <Reweight scoretype=coordinate_constraint weight=1 />
   </sfxn_hard_cst>
   ### score function that contains the full atom attractive forces only
   <VDW weights="empty" >
          <Reweight scoretype="fa_atr" weight=1.0/>
   </VDW>
  </SCOREFXNS>

  <RESIDUE_SELECTORS>
   In the setup below, chain A is target and chain B is scaffold, X is ligand.
   In the input pdb, chain B should be 1st, followed by chain A and chain X.
   <Chain name=chA chains=A,X/>
   <Chain name=chX chains=X/>
   <Chain name=chB chains=B/>
   <InterfaceByVector name=intf cb_dist_cut=10 nearby_atom_cut=5.5 vector_angle_cut=75.0 vector_dist_cut=9.0
grp1_selector=chA grp2_selector=chB/>
```

```
   <InterfaceByVector name=ligand_intf cb_dist_cut=10 nearby_atom_cut=5.5 vector_angle_cut=75.0
vector_dist_cut=9.0 grp1_selector=chX grp2_selector=chB/>
   <ResidueName name=hp residue_name3="VAL,PHE,TYR,ILE,LEU,TRP,MET" />
   <And name=hp_in_A selectors=intf,hp,chA/>         hydrophobic residues on target
   <Or name=hp_in_A_and_X selectors=hp_in_A,chX/> union: hydrophobic residues on target + Ligand +
contacting residues on scaffold
   <Neighborhood name=hp_neighbor selector=hp_in_A_and_X distance=10.0/>
   <And name=hp_contact_in_B selectors=chB,hp_neighbor/>contacting residues on scaffold
   <Or name=hpA_contactB selectors=hp_in_A,hp_contact_in_B/> union: hydrophobic residues on target +
contacting residues on scaffold
   <Not name=not_hpA_contactB selector=hpA_contactB/>     negation of hpA_contactB for restriction
   <Not name=not_ligand_intf selector=ligand_intf/> negation of hpA_contactB for restriction

   # hp_revert
   <Neighborhood name=hp_revert selector=chX distance=10.0/>
   <And name=hp_rvt selectors=hp_revert/>


 </RESIDUE_SELECTORS>

 <TASKOPERATIONS>
   <ProteinLigandInterfaceUpweighter name=up interface_weight=1.5/>
   <DesignAround name=da design_shell=10 resnums=1X repack_shell=10.0 allow_design=1
resnums_allow_design=0/>
   <IncludeCurrent name=inclcur/>
   <PreventChainFromRepacking chain=2 name=pctr2/>
   <PreventChainFromRepacking chain=3 name=pctr3/>
   <ExtraRotamersGeneric name=exrot ex1=1 ex2=1 extrachi_cutoff=1/>
   <InitializeFromCommandline name=init/>
   <LimitAromaChi2 name=arochi2 chi2max=110 chi2min=70 />
   <RestrictAbsentCanonicalAAS name=nohis keep_aas="ACDEFGIKLMNPQRSTVWY"/>
   <RestrictAbsentCanonicalAAS name=nocys keep_aas="ADEFIKLMNPQRSTVWYH"/>
   #noCys & noGly
   # this allows PRO, GLY, CYS in the interface it seems that CYS is overfavoured so restrict this might be
necessary
   <ProteinInterfaceDesign name=dzn_inter design_chain1=1 design_chain2=0 repack_chain1=1 repack_chain2=0
jump=1 interface_distance_cutoff=11.0 allow_all_aas=1/>


   Design ONLY near the hydrophobic residues on target
   <OperateOnResidueSubset name=hp_task selector=not_hpA_contactB >
     <PreventRepackingRLT/>
   </OperateOnResidueSubset>
   <OperateOnResidueSubset name=ligand_interface selector=not_ligand_intf >
     <PreventRepackingRLT/>
   </OperateOnResidueSubset>

   <DisallowIfNonnative name=dis_charge resnum=0 disallow_aas=RQKHDEG/>

   <DesignAround name=da10 design_shell=12 resnums=1X repack_shell=14.0 allow_design=1
resnums_allow_design=0/>
   # Selector hp_revert contains all residues within the ligand
   # these are set to prevent repacking
   <OperateOnResidueSubset name=nodesignaroundligand
      selector=hp_revert >
     <PreventRepackingRLT/>
```

```
   </OperateOnResidueSubset>


   ### this task operation defines an extended generous interface for minimization
   <ProteinInterfaceDesign name="pack_long" design_chain1="0" design_chain2="0" jump="1"
interface_distance_cutoff="15"/> //

  </TASKOPERATIONS>

  <MOVERS>
   <RollMover name="randomroll" chain=1 random_roll=1 random_roll_angle_mag=4.0
random_roll_trans_mag=3.0 />

   <MinMover name=min_rb chi=1 bb=0 jump=1>
    <MoveMap>
     <Chain number=1 chi=1 bb=0/>          only chi for scaffold
     <Chain number=2 chi=1 bb=0/>          only chi for target
     <Chain number=3 chi=0 bb=0/>          not chi for Ligand fixed as in crystal structure
    </MoveMap>
   </MinMover>

   <MinMover name=min_init chi=1 bb=0 jump=0>
    <MoveMap>
     <Chain number=1 chi=1 bb=0/>          only chi for scaffold
     <Chain number=2 chi=0 bb=0/>
     <Chain number=3 chi=0 bb=0/>
    </MoveMap>
   </MinMover>

   <TaskAwareMinMover name=min_chi bb=0 chi=1 jump=0 scorefxn=sfxn_hard
task_operations=init,arochi2,inclcur,exrot,dzn_inter/>
   <AtomTree name=simple_ft docking_ft=0 simple_ft=1/>

    # Design based on ligand task_operation
    <PackRotamersMover name=dzn_packrot_layer_soft_ligand scorefxn=sfxn_soft
task_operations=init,exrot,inclcur,arochi2,nohis,pctr2,da,up,nocys,dis_charge/>
    <PackRotamersMover name=dzn_packrot_layer_hard_ligand scorefxn=sfxn_hard
task_operations=init,exrot,inclcur,arochi2,nohis,pctr2,da,up,nocys,dis_charge/>

    # Normal design
    <PackRotamersMover name=dzn_packrot_soft scorefxn=sfxn_soft
task_operations=init,exrot,inclcur,arochi2,nohis,dzn_inter,pctr2,pctr3,up,nocys/>
    <PackRotamersMover name=dzn_packrot_hard scorefxn=sfxn_hard
task_operations=init,exrot,inclcur,arochi2,nohis,dzn_inter,pctr2,pctr3,nocys/>

    <DumpPdb name=d1 fname=dump1.pdb scorefxn=sfxn_hard_cst />
    <DumpPdb name=d2 fname=dump2.pdb scorefxn=sfxn_hard_cst />
    <DumpPdb name=d3 fname=dump3.pdb scorefxn=sfxn_hard_cst />
    <DumpPdb name=d4 fname=dump4.pdb scorefxn=sfxn_hard_cst />
    <DumpPdb name=d5 fname=dump5.pdb scorefxn=sfxn_hard_cst />

    # Normal design
    <PackRotamersMover name=dzn_packrot_soft_last scorefxn=sfxn_soft
task_operations=init,exrot,inclcur,arochi2,nohis,dzn_inter,nocys,pctr2,pctr3,up,nodesignaroundligand/>
    <PackRotamersMover name=dzn_packrot_hard_last scorefxn=sfxn_hard
task_operations=init,exrot,inclcur,arochi2,nohis,dzn_inter,nocys,pctr2,pctr3,nodesignaroundligand/>
```

```
   ### minimization of the extended PPI
   <TaskAwareMinMover name=min scorefxn=sfxn_hard bb=0 chi=1 task_operations=pack_long/>

  </MOVERS>


 <FILTERS>
   <Sasa name=sasa_jump1 confidence=0 jump=1/> # scaffold
   <Sasa name=sasa_jump2 confidence=0 jump=2/>  # ligand
   <Ddg name=ddg_jump1 threshold=-10 scorefxn=sfxn_hard jump=1 repack=1 relax_mover=min_chi repeats=1
confidence=0/>    # ligand
   <Ddg name=ddg_jump2 threshold=-10 scorefxn=sfxn_hard jump=2 repack=1 relax_mover=min_chi repeats=1
confidence=0/>    # ligand
   <ScoreType name=total_score scorefxn=sfxn_hard score_type=total_score threshold=0 confidence=0/>
   <AverageDegree name=deg threshold=8.6 distance_threshold=8 task_operations=dzn_inter confidence=0/>

   <ShapeComplementarity name=sc_jump1 jump=1 verbose=1 min_sc=0.6 confidence=0/>          #scaffold
   <ShapeComplementarity name=sc_jump2 jump=2 verbose=1 min_sc=0.6 confidence=0/>          #ligand
   <LigInterfaceEnergy name=interfE  scorefxn=sfxn_hard jump_number=2 energy_cutoff=-5 confidence=0/>

   <DesignableResidues name=dr task_operations=init,exrot,inclcur,arochi2,nohis,dzn_inter,pctr3 designable=1
packable=1/>
   <InterfaceHoles name="interface_holes" confidence=0/>
   <Sasa name="hydrophobic_sasa" confidence=0 jump=1 hydrophobic=True/>
   <BuriedUnsatHbonds2 name="interface_unsat_hbond" confidence=0/>
   <Rmsd name=rmsdB chains="B" threshold=2.0 superimpose=0 confidence=0/>

   <Sasa name="interface_hydrophobic_sasa" confidence=0 hydrophobic=True/>
   <Sasa name="interface_polar_sasa" confidence=0 polar=True/>

   <Ddg name="ddg_fa_atr"  threshold=-10 jump=1 repeats=5 repack=1 relax_mover=min confidence=0
scorefxn=VDW />
   <Ddg name="ddg_fa_atr_norepack"  threshold=-10 jump=1 repeats=1 repack=0 confidence=0 scorefxn=VDW/>

   <CalculatorFilter name="ddg_fa_atr_per_1000sasa" equation="1000 * ddg / (sasa+0.01)" threshold="1"
confidence="0">
           <VAR name="ddg" filter="ddg_fa_atr"/>
           <VAR name="sasa" filter=sasa_jump1/>
   </CalculatorFilter>

   <CalculatorFilter name="ddg_fa_atr_norepack_per_1000sasa" equation="1000 * ddg / (sasa+0.01)"
threshold="1" confidence="0">
           <VAR name="ddg" filter="ddg_fa_atr_norepack"/>
           <VAR name="sasa" filter=sasa_jump1/>
   </CalculatorFilter>



  </FILTERS>

  <APPLY_TO_POSE>
  </APPLY_TO_POSE>


  <PROTOCOLS>
```

```
    # Setting up atomtree with simple foldtree
    <Add mover=simple_ft/>
    #RollMover to perturb scaffold
    <Add mover_name="randomroll"/>
    # PackRotamer with soft score function
    <Add mover=dzn_packrot_soft/>
    <Add mover=min_chi/>
    <Add mover=dzn_packrot_hard/>
    <Add mover=min_chi/>

    <Add mover=dzn_packrot_soft/>
    <Add mover=min_chi/>
    <Add mover=dzn_packrot_hard/>
    <Add mover=min_chi/>

    #Design around the ligand
    <Add mover=dzn_packrot_layer_soft_ligand/>
    <Add mover=min_chi/>
    <Add mover=dzn_packrot_layer_hard_ligand/>
    <Add mover=min_chi/>

    <Add mover=min_rb/>

    <Add mover=dzn_packrot_layer_soft_ligand/>
    <Add mover=min_chi/>
    <Add mover=dzn_packrot_layer_hard_ligand/>
    <Add mover=min_chi/>

    <Add mover=dzn_packrot_soft_last/>
    <Add mover=dzn_packrot_hard_last/>

    <Add filter=sasa_jump1/>
    <Add filter=sasa_jump2/>
    <Add filter=deg/>
    <Add filter=total_score/>
    <Add filter=sc_jump1/>
    <Add filter=sc_jump2/>
    <Add filter=ddg_jump1/>
    <Add filter=ddg_jump2/>
    <Add filter=interfE/>
    <Add filter=dr/>
    <Add filter="interface_holes"/>
    <Add filter="hydrophobic_sasa"/>
    <Add filter="rmsdB"/>
    <Add filter="interface_unsat_hbond"/>
    <Add filter="interface_hydrophobic_sasa"/>
    <Add filter="interface_polar_sasa"/>
    <Add filter="ddg_fa_atr"/>
    <Add filter="ddg_fa_atr_norepack"/>
    <Add filter="ddg_fa_atr_per_1000sasa"/>
    <Add filter="ddg_fa_atr_norepack_per_1000sasa"/>
  </PROTOCOLS>
</dock_roll_design>
```

RIF generation flags, rifgen_grazo.flags:

```
-rifgen::rif_type RotScore64
-rifgen:extra_rotamers false
-rifgen:extra_rif_rotamers true
-rif_accum_scratch_size_M 24000
-rifgen:target          input_files/3SUD_SUE.prelax.pdb
-rifgen:target_res      input_files/3SUD_SUE_target.txt
-extra_res_fa input_files/SUE.fa.params
-renumber_pdb
-hash_cart_resl             0.7
-hash_angle_resl            14.0
-rifgen::rosetta_field_resl 0.25
-rifgen::search_resolutions 3.0 1.5 0.75
-rifgen:score_threshold -0.5
-rifgen:hbond_weight 1.0          # max score per-hbond
-rifgen:upweight_multi_hbond 1.0   # extra score factor for bidentate hbonds
-rifgen:data_cache_dir    ~directorypath/data/scheme_data_exrots2
-rifgen:outdir           output_rifgen
-rifgen:outfile          3SUD_SUE.rif.gz
-rifgen:score_cut_adjust 0.7
-rifgen:apores VAL ILE LEU MET PHE TRP
-rifgen:donres SER THR TYR     GLN     ASN HIS HIS_D TRP
-rifgen:accres SER THR TYR GLU GLN ASP ASN HIS HIS_D
-hbond_cart_sample_hack_range 0.33
-hbond_cart_sample_hack_resl  0.33
-rifgen:tip_tol_deg        60.0 # for now, do either 60 or 36
-rifgen:rot_samp_resl       6.0
-rifgen:rif_hbond_dump_fraction  0.000001
-rifgen:rif_apo_dump_fraction    0.000001
-add_orbitals
-rifgen:beam_size_M 10000.0
-rifgen:hash_preallocate_mult 0.125
-rifgen:max_rf_bounding_ratio 4.0
-rifgen:hash_cart_resls   16.0   8.0   4.0   2.0   1.0
-rifgen:hash_cart_bounds   512   512   512   512   512
```

```
-rifgen:lever_bounds      16.0   8.0   4.0   2.0   1.0
-rifgen:hash_ang_resls     38.8  24.4  17.2  13.6  11.8 # yes worky worky
-rifgen:lever_radii        23.6 18.785501 13.324600  8.425850  4.855575
-database ~directorypath/rosetta/librosetta_update/database
```

RIF docking flags (rifdock_grazo.flags):

```
#### the block below comes from the bottom of the log file from rif generation
####what you need for docking ##############################################
-rif_dock:target_pdb            output_rifgen/3SUD_SUE.rif.gz_target.pdb.gz
-in:file:extra_res_fa           input_files/SUE.fa.params
-rif_dock:target_res            input_files/3SUD_SUE_target.txt
-rif_dock:target_rf_resl        0.25
-rif_dock:target_rf_cache
output_rifgen/__RF_3SUD_SUE.prelax.pdb_CEN_trhash29405780_resl0.25_osamp2_replonlybdry
-rif_dock:target_bounding_xmaps output_rifgen/3SUD_SUE.rif.gz_BOUNDING_RIF_16.xmap.gz
-rif_dock:target_bounding_xmaps output_rifgen/3SUD_SUE.rif.gz_BOUNDING_RIF_08.xmap.gz
-rif_dock:target_bounding_xmaps output_rifgen/3SUD_SUE.rif.gz_BOUNDING_RIF_04.xmap.gz
-rif_dock:target_bounding_xmaps output_rifgen/3SUD_SUE.rif.gz_BOUNDING_RIF_02.xmap.gz
-rif_dock:target_bounding_xmaps output_rifgen/3SUD_SUE.rif.gz_BOUNDING_RIF_01.xmap.gz
-rif_dock:target_rif            output_rifgen/3SUD_SUE.rif.gz
-rif_dock:extra_rotamers        0
-rif_dock:extra_rif_rotamers    1
#############################################################################################################

#### this is where the output will go, and how much
-rif_dock:outdir  rifdock_grazo_30junc
-rif_dock:dokfile all.dok
-rif_dock:n_pdb_out 20 # max number of output pdbs
-rif_dock:redundancy_filter_mag 1.0
-rif_dock:align_output_to_scaffold false
#-rif_dock:target_tag conf01 # optional tag to add to all outputs


############## overall time and resolution of search ###################
-beam_size_M 5
-hsearch_scale_factor 1.2

#### to use -beta scoring function (betaJuly16)
```

```
-beta
-score:weights beta_soft
-add_orbitals false

################ stuff related to picking designable and fixed positions #################
#### if you DO NOT supply scaffold_res files, this will attempt to pick which residues on the scaffold
#### can be mutated based on sasa, internal energy, and bb-sc hbonds
-scaffold_res_use_best_guess true

#### if scaffold_res is NOT used, this option will cause loop residues to be ignored
#### scaffold_res overrides this
-rif_dock::dont_use_scaffold_loops True

#### these cause the non-designable scaffold residues to still contribute sterically
#### and to the 1 body rotamer energies. use these flags if you have a fully-designed scaffold
-rif_dock:scaffold_to_ala false
-rif_dock:scaffold_to_ala_selonly true
-rif_dock:replace_all_with_ala_1bre false
#### if you don't have a fully designed scaffold, treat non-designable positions as alanine
# -rif_dock:scaffold_to_ala true
# -rif_dock:scaffold_to_ala_selonly false
# -rif_dock:replace_all_with_ala_1bre true

-rif_dock:hbond_weight 1.0
-rif_dock:upweight_multi_hbond 1.0 # value of 1.0 could up to double hbscore if bidentate, triple if tridentate... best in conjunction with low-ish starting hbweight

#### weight interactions with the target more than intra-scaffold interactions
#### kinda like the rosetta_score_*_weight flags, but applies to the rif calculations
-rif_dock:upweight_iface 2.0

################ rif packing options, probably don't change
-hack_pack true
-rif_dock:pack_n_iters    2
-rif_dock:pack_iter_mult  2.0
-rif_dock:hack_pack_frac  0.1
-rif_dock:packing_use_rif_rotamers        true
-rif_dock:extra_rotamers                  false
-rif_dock:always_available_rotamers_level 0

-rif_dock::rf_resl 0.5
-rif_dock::rf_oversample 2
-rif_dock:use_scaffold_bounding_grids 0

################## rosetta re-scoring / min stuff ####################

#### negative interactions are always full-weight, this is positive only
-rif_dock:rosetta_score_rifres_rifres_weight   0.6
-rif_dock:rosetta_score_rifres_scaffold_weight 0.4

#### score cut for the rosetta "score," which is kinda a ddg, but with hbond weighs highern
-rif_dock:rosetta_score_cut -15.0

-rif_dock:rosetta_score_fraction 0.006
-rif_dock:rosetta_min_fraction 0.07
-rif_dock:rosetta_min_scaffoldbb false
```

```
-rif_dock:rosetta_min_targetbb   false
-rif_dock:rosetta_hard_min false
#-rif_dock:rosetta_score_then_min_below_thresh -20.0 # this is in "rif docking score units"
#-rif_dock:rosetta_score_at_least 3000
#-rif_dock:rosetta_score_at_most  30000

#### details for how twobody rotamer energies are computed and stored, don't change
-rif_dock:rotrf_resl   0.25
-rif_dock:rotrf_spread 0.0
-rif_dock:rotrf_scale_atr 1.0
-rif_dock:rotrf_cache_dir ~directorypath/data/scheme_data_exrots2_by_structure/rot_rf_tables_025_0_atr1
-rif_dock:data_cache_dir  ./rifdock_v4_scaffdata_025_0_atr1
-rif_dock:cache_scaffold_data true




#### options to favor existing scaffold residues
-add_native_scaffold_rots_when_packing 0 # 1
-bonus_to_native_scaffold_res          0 # -0.5

-rif_dock:pdb_info_pikaa false # this is default I think

-rif_dock:global_score_cut -0.0

 # disulfides seem to cause problems... ignoring them isn't really an issue unless
 # you do bbmin where there should be disulfides
-detect_disulf 0

-database ~directorypath/rosetta/librosetta_update/database

-rif_dock:target_rf_oversample 2

-mute core.scoring.ScoreFunctionFactory
-mute core.io.pose_from_sfr.PoseFromSFRBuilder
```

Supplementary References

1. Park, K. *et al.* Control of repeat-protein curvature by computational protein design. *Nat. Struct. Mol. Biol.* **22,** 167–174 (2015).
2. Brunette, T. J. *et al.* Exploring the repeat protein universe through computational protein design. *Nature* **528,** 580–584 (2015).
3. King, I. C. *et al.* Precise assembly of complex beta sheet topologies from de novo designed building blocks. *Elife* **4,** e11012 (2015).
4. Chen, T. S., Palacios, H. & Keating, A. E. Structure-based redesign of the binding specificity of anti-apoptotic Bcl-x(L). *J. Mol. Biol.* **425,** 171–185 (2013).
5. Foight, G. W., Chen, T. S., Richman, D. & Keating, A. E. Enriching Peptide Libraries for Binding Affinity and Specificity Through Computationally Directed Library Design. *Methods Mol. Biol.* **1561,** 213–232 (2017).
6. Romano, K. P. *et al.* The molecular basis of drug resistance against hepatitis C virus NS3/4A protease inhibitors. *PLoS Pathog.* **8,** e1002832 (2012).
7. Dou, J. *et al.* De novo design of a fluorescence-activating β-barrel. *Nature* **561,** 485–491 (2018).
8. Yung-Chi, C. & Prusoff, W. H. Relationship between the inhibition constant (KI) and the concentration of inhibitor which causes 50 per cent inhibition (I50) of an enzymatic reaction. *Biochem. Pharmacol.* **22,** 3099–3108 (1973).
9. Chavez, A. *et al.* Highly efficient Cas9-mediated transcriptional programming. *Nat. Methods* **12,** 326–328 (2015).
10. Gilbert, L. A. *et al.* CRISPR-Mediated Modular RNA-Guided Regulation of Transcription in Eukaryotes. *Cell* **154,** 442–451 (2013).
11. Gao, Y. *et al.* Complex transcriptional modulation with orthogonal and inducible dCas9 regulators. *Nat. Methods* **13,** 1043 EP —1049 (2016).
12. Yeo, N. C. *et al.* An enhanced CRISPR repressor for targeted mammalian gene regulation. *Nat. Methods* **31,** 230 (2018).
13. Byrne, K. M. *et al.* Bistability in the Rac1, PAK, and RhoA Signaling Network Drives Actin Cytoskeleton Dynamics and Cell Motility Switches. *Cell Syst.* **2,** 38–48 (2016).